

Setting the Hook
for Specific Single Walled Carbon Nanotubes (SWCNT)

Inauguraldissertation

zur

Erlangung der Würde eines Doktors der Philosophie

vorgelegt der

Philosophisch-Naturwissenschaftlichen Fakultät

der Universität Basel

von

Ina Bodoky

aus Riehen (BS), Schweiz

Basel, 2018

Originaldokument gespeichert auf dem Dokumentenserver der Universität Basel

edoc.unibas.ch

Genehmigt von der Philosophisch-Naturwissenschaftlichen Fakultät
auf Antrag von

Prof. Dr. Marcel Mayor

Prof. Dr. Christof Sparr

Basel, den 17. Oktober 2017

Prof. Dr. Martin Spiess
Dekan

*Dedicated to my mum
and my grandpa*

Acknowledgement

First of all, I would like to thank **Professor Marcel Mayor** for the opportunity to work in his group, especially for the continuous support and limitless resources he provide me. Marcel, you allowed me to work almost independently on this project and allowed me to explore the field of non-covalent dispersion of single-walled carbon nanotubes, which I greatly appreciate.

I would also like to extend my thanks to **Professor Christof Sparr** for agreeing to co-refereeing my thesis and **Professor Catherine Housecraft** for chairing my defense.

The cheerful and sarcastic atmosphere in Lab 02 and Lab 06 were probably the reason for returning day by day after another reaction went to the trash. **Michel**, it's hard to put it in words, thank you - for the motivation and ongoing support you gave me during my PhD and on top of that especially for the *Boris Murphy* time we shared ;). As Güs already stated: **Manu**, *Love Lab* forever. I will especially miss to keep asking you every Monday morning what you have done during the weekend. Thanks for ...ahhh you know.

Additionally, I would like to thank **Michal Valasek** for his guidance through this work and for providing the necessary assistance. It was always a pleasure to discuss science with you. My deepest thanks to my fellow researches, many of which have become friends over these years, to the whole **Mayor group**. I would like to give special thanks for the fruitful discussions and for the good times we shared, particularly during the legendary *Inder* walks (I know Kevin, he is *Westfale* :P), which provided the needed balance to the scientific work. In particular, I would like to thank **Kevin** – *muuus* - and his beloved girlfriend **Frau Doktor Herzhaft** for always having a funny line in store. I appreciated the regular lab visits of the dream team **Lolo** and **Zwick**. **Michal**, your enthusiasm is priceless, it doesn't matter if it's for music, balcony nights, melting points, English grammar mistakes – I enjoyed them all. My Spanish lady **Almu**, I still hate climbing but that shows even more the extent to which I like you ;), thanks for teaching me the Spanish life-style. Besides my group members, I want to use this opportunity to thank a few very special girls and boys. To the 5Ts who accompanied me since the very beginning of my studies: to **Livia**, I hate you for bunking off from Switzerland, but you will never manage to disappear entirely, your unconditional friendship means a lot to me; to the passionate **Steffi**, thanks for being the force of nature you are, the stories we share are endless – *Steffi, mit dir kann ich Pferde stehlen!*; **Annika**, you are far more than a somersault in the deep snow, sharing a soul healing glass of red wine with you – happiness is guaranteed; to the concealed **Sam**, thanks for showing up in the right moments. Through my studies I appreciated the fun time and good learning atmosphere of the **Nerds** club (**Manu S.**, **Simon**, **Philipp**, **Däppe**, **Nati** and **Lukas**). **Sabse**, you got far closer than a shared run through the rain, thanks for spreading your good mood. My little princess **Dr. Corinne Ruppen** you are *my* best doctor I can ever dream of. The left overs of *musel*, especially **Zülle** and **Ambi** I would like to thank for their big supporting in no matter what. **Lulu** what would be a Tuesday lunch without you. Sporting ace **Amelie** I'm happy we can not only share the huge opportunities of *unisport* together. For the *Brandi Dog* experiences and others I want to thank Dani, I'm still sure we won ;). Moreover the *Schletti* atmosphere was the balanced to my work day, therefore I want to thank **Simi** and in particular **Noe**, your care and friendship is priceless.

Sincere thanks goes to **Michel, Šolo** and **Michal** for the care and patience with which they reviewed my thesis. To **Rahel** and **Tim** for working with me on my project. **Gin** (I cannot say it properly but I guess I can try to spell it, Guojun), it was an honor to work with you on similar projects. The help of **Samuel** in measuring polymer length was crucial for this thesis, giving his time so generously is very much appreciated. **PD Daniel Häusinger** for going above and beyond his NMR duties and to **Heinz Nadig** and **Markus Neuburger** for measuring ESI and crystal structures. Special thanks to you, **Andreas Koller, Markus Hauri, Beatrice Erismann, Brigitte Howald, Marina Mambelli-Johnson, Markus Ast, Andreas Sohler, Roy Lips, Oliver Ilg, Sylvie Mittelheisser** and **Olaf Lips** for keep this historical building alive.

I am wholeheartedly grateful for my family, **Sally, Peter, Fabian, Sandra, Seba** and **Simon (Nicolas, Katja)**– they have earned a heap of thanks for their ongoing support and the encouragement they provided me throughout all of my studies. *Ahogy az Apo mondta: mindenhol jó, de a legjobb az otthon!* Without them none of the described work would have been possible.

Abstract

The electronic properties of SWCNTs depend strongly on well-defined characteristics such as their diameter, n,m -indices and chirality.^[1-4] Traditional purification methods do not allow to selectively obtain samples of SWCNTs with precisely defined characteristics and high purity. The separation and purification of SWCNTs is an ongoing challenge as the selectivity towards traditional means of purification remains low at best.

Here, we propose a new strategy to achieve a controlled and selective debundling and separation of SWCNTs depending on their size and chirality. The focus of this thesis is the design and synthesis of a molecular hook for specific SWCNTs. Conceptually, the hook consists of a chiral building block with a concave π -system, which can be accessed using stereospecific Diels-Alder reactions as key steps. Polymerization with interlinking building blocks then leads to chiral ribbons, which are envisaged to selectively coat a specific SWCNT and disperse it. The driving force for the coating process is mainly the interaction of the SWCNT with the concave π -moiety while the size exclusion is defined by the resulting secondary structure of the polymer, the polymer backbone and the interlinking molecules. Variation of the interlinking building blocks allows altering of the properties of the polymer at a late stage in the synthesis and ultimately defines the dispersion capability of the polymer. Each of the three successfully synthesized copolymers contains an enantiomerically pure ethenoanthracene derivative as the concave π -moiety. As a reliable release of the coated SWCNT is highly desirable, we further present a diamine monomer unit designed for Schiff base linked copolymerization that will allow for acid-labile depolymerization resulting in uncoating of the dispersed SWCNTs. Each of the polymer was characterized and the dispersion capability assessed subsequently.

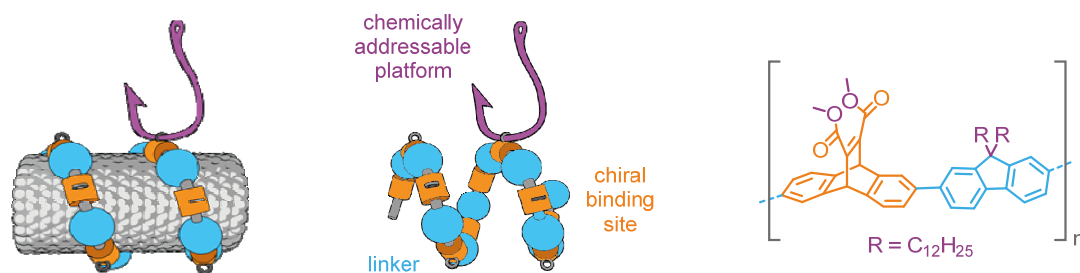


Table of Contents

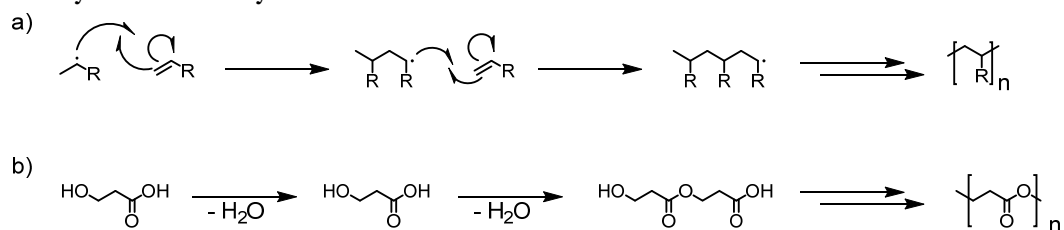
Polymers	1
Types and Synthesis of Polymers	1
Properties of Polymers	3
Polymers and their Use	6
Carbon Nanotubes	7
Carbon Nanotubes as a Promising Material	7
Classification of CNTs and their Production	8
Purification Techniques; Covalent Versus Non Covalent Functionalization	11
Postulated Sorting Mechanism of Conjugated Polymers towards SWCNTs	24
Justification for our Work	25
Molecular Design	26
Building blocks	28
Results and Discussion	29
Synthesis of dimethyl polymer P1	29
Synthesis of diisoamyl polymer P2	34
Synthesis towards imine linked polymer P3	40
Synthesis of imide polymer P4	43
Synthesis towards triptycene derivative polymer	49
Conclusion	54
Outlook	56
Experimental section	58
General Procedure	58
Experimental Section of Poly[9,10-dihydro-11,12-dicarbomethoxyethenoanthracene-2,6-diyl- <i>alt</i> -(9,9-didodecylfluorene-2,7-diyl)] (P1)	59
Experimental section of Poly[Diisopentyl-9,10-dihydro-9,10-ethenoanthracene-11,12-dicarboxylate-2,6-diyl- <i>alt</i> -(9,9-didodecylfluorene-2,7-diyl)] (P2)	62
Experimental section towards Schiff base polymer	68

Experimental section Poly[N-octyl-(2,6- bis(propargyl-1-oxy))-9,10-dihydro-9,10-maleimidoanthracene] (P4)	70
Experimental section diastereomeric resolution	75
References	83
Curriculum Vitae	87

Polymers

A polymer is a macromolecule with high molar mass that consists of repeating subunits or monomers. A key characteristic is the degree of polymerization n which relates to the number of monomers present in the polymer. The degree of polymerization has to be large enough that adding another monomeric unit does not alter the physical and chemical properties of the macromolecule. If the degree of polymerization is low ($n < 20$), the resulting macromolecule is typically called an oligomer.^[5]

Types and Synthesis of Polymers



Scheme 1. a) Molecular example of *chain-growth* polymerization of polyethylene, b) molecular example of a typical *step-growth* polymerization, a polyester condensation.

The two largest groups of synthetic polymers are called *chain-growth* and *step-growth* polymers, evidently derived from the type of polymerization used to grow the polymer chain, the chain-growth- or step-growth polymerization. The main difference between these two types is that in a *chain-growth* polymerization the reactive center is moved to the newly attached monomer unit, while in a *step-growth* polymerization the monomer unit possesses two functional groups that form a covalent bond. Therefore new monomers are added one by one in a clean *chain-growth* polymerization, while chains of monomers (oligomers or smaller polymers) can connect together to form larger polymers in a *step-growth* polymerization. In the latter, all intermediates are stable and in principle isolatable. Typical examples are polyethylene and polyesters or polyamides for *chain-growth* and the *step-growth* polymerization, respectively (scheme 1).^[6] Whereas *chain-growth* polymerization reactions typically lead to high mass polymers within seconds, the formation of long chains in *step-growth* polymerization is considerably slower.

As mentioned, polymerization reactions are usually divided into two groups, *step-* and *chain-growth* polymerization. Common ways to assemble synthetic polymers include *poly-addition*, *poly-condensation* and *ring-opening polymerization*, which are subgroups of either *step-* and *chain-growth* polymerization reactions. Clean transformations are a key feature for achieving samples with high molar mass and low dispersity (see next section for definition), as already small amounts of side reactions prevent the formation of long chains. This is especially true for *step-growth* polymerization, where all the molecules in the mixture feature the same reactivity and can take part in the reaction. For illustration, let us consider a schematic presentation of a *poly-condensation* (figure 1). In a fictional sample of 25 monomer units, where each monomer can form two bonds, a conversion of 24% would lead to 6 bond formations, mostly as dimers. Increasing the conversion to 48% can result in the formation of a sample of dimers and short oligomers. Even if the conversion would reach 80% the likelihood to form a long chain polymer is still low and the sample would contain mostly short oligomers.^[5]

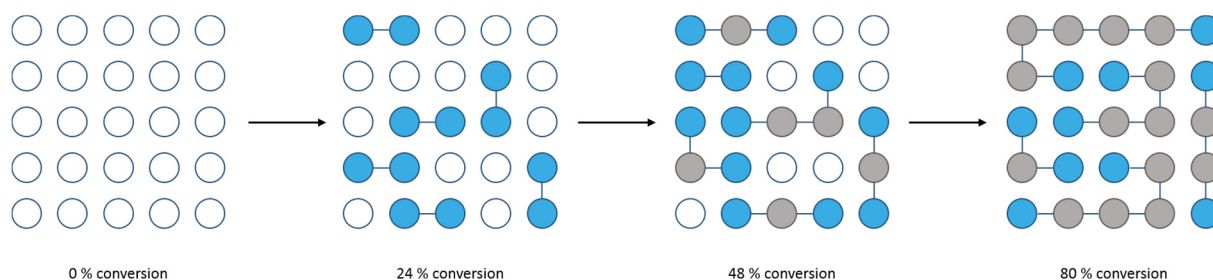


Figure 1. Schematic view of a poly condensation of a monomer with two reactive sites in relation to conversion. White: unreacted monomer; blue: subunit with one linkage; grey: subunit with two linkages

There are ample variations in polymer architecture. In the simplest case, a monomeric building block A is linearly connected (figure 2a) to give a linear polymer. If the monomer A features multiple binding sites (intersections), a branched 2D or 3D polymer may result (figure 2b). This allows for a large variety of shapes such as star, comb, brush, dendronized or ladder polymers, and dendrimers. Similar to small molecules, isomerization can occur, either during or after the product formation.

It is usually distinguished between different *structural* isomers (figure 2c), like in the case of polyvinyl alcohols and polyethylene glycols where the position of the linkage varies. The second important class are based on *stereo* isomers (figure 2d), where each monomer can theoretically adopt multiple configurations or conformations such as *cis/trans*, *R/S* or *eclipsed/staggered* isomers. It is also possible that the interlinking of monomers introduces a stereo center. If the formation of such stereo center is not stereospecific, the number of possible stereoisomers of the entire assembly can be enormous. Interestingly, the stereo centers affect the physical properties of the polymer, especially in the case of stereo regular polymers, more than it is typical in small molecules.

Polymer synthesis is not limited to a single type of monomer. A polymer formed from more than one type of monomer is called a *copolymer*. Evidently, the use of multiple building blocks greatly increases the available structural diversity. Consider the simplest case featuring two building blocks A and B. Interlinking the first two building blocks can yield four products AA, BB, AB and BA. Each can react with another monomer A or B, eventually leading to statistical copolymers with random sequential arrangements. To prevent the statistical formation of polymeric products, restrictions can be imposed upon the monomers. For instance, the functionalities can be chosen such that A exclusively reacts with B and vice versa. The formed polymer is then defined as an alternating copolymer (figure 2e, AB).^[7]

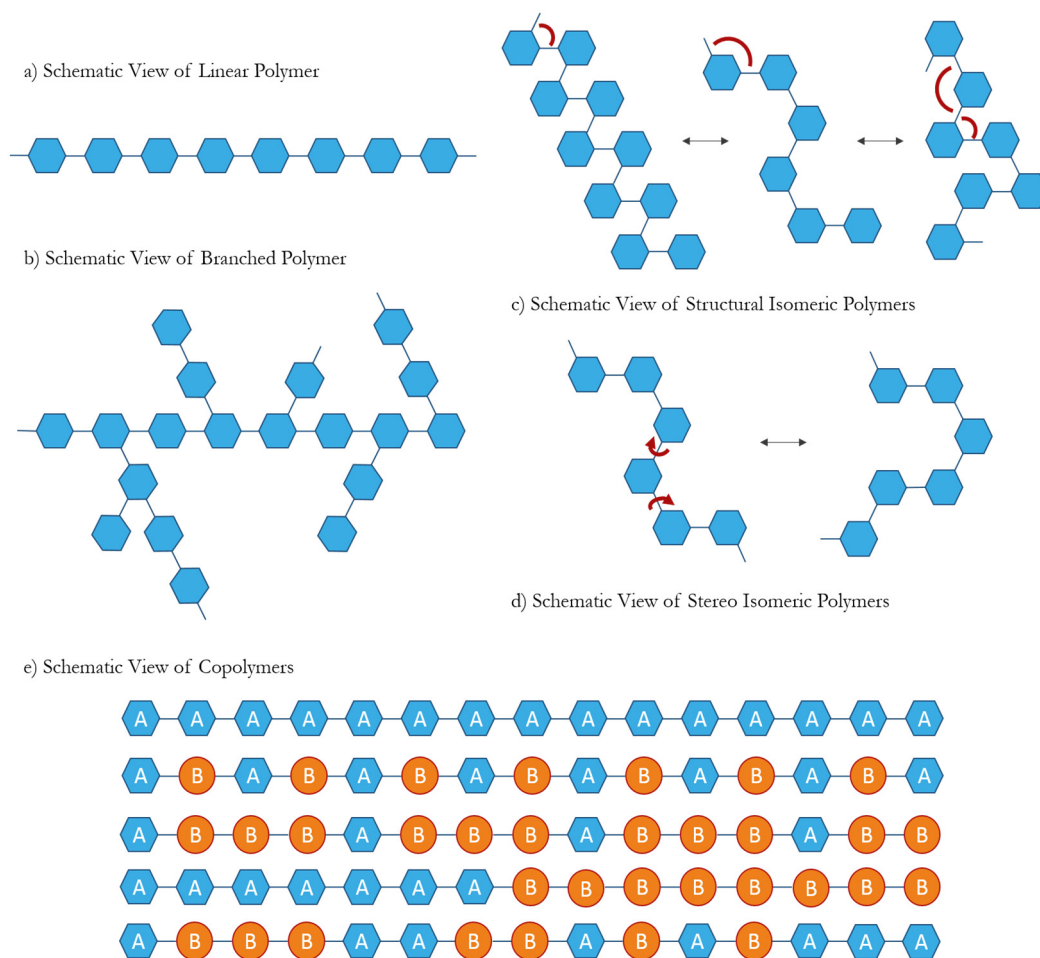


Figure 2. Schematic view of different poly architecture (upper part, a-d); variation of different copolymers: *homopolymer*, *alternating copolymer*, *periodic copolymer*, *block copolymer*, *statistical copolymer* (lower part, e)

In a *periodic* copolymer the different monomer units do not alternate with every addition but they alter in a periodic way, where a repeating pattern of the single units can be observed, e.g. AABAAB. *Block* copolymers feature domains of one monomer unit that are linked together to form a polymer (AAABBB). In the case of a *grafted* copolymer the polymer consists of a monomer backbone and side chains made from a different monomer unit.

Properties of Polymers

The physical properties of a polymer are different than that of its monomer and depend strongly on its dispersity, chain length, its architecture, level of conjugation, homogeneity and density. The monomers can, however, introduce specific functionalities that allow for molecular recognition, cross linking or solubility that can be preserved in the macroscopic polymer. Unique properties of polymers are for instance their viscoelasticity, toughness and texture, formation of glasses and semi crystalline structures. Hence it is not surprising that many polymeric structures occur in Nature, some with even vital functions for organisms.

The variety of possibilities of the final structure of a synthetic polymer has little limits. For instance, by using two sites of potential linkage in the subunit results variation of length and cross-linkage and thus its tensile strength, density and viscosity. Accordingly, increasing the complexity of the monomer leads to more complex

polymeric systems. It is therefore key to define characteristics to allow for comparability and reproducibility and ultimately to tailor the property of the polymer to the desired application.

As mentioned, polymers feature important characteristics, depending among other things on their length, weight, architecture, porosity, level of conjugation and viscosity. For example, a branched polymer can have completely different properties depending on the amount of interlinking, even though it is build up from the same number of monomer units. It is therefore essential to define typical characteristics to benchmark polymers. Two important features are: molar mass and degree of polymerization n . Over the years, several techniques were established to measure these parameters, which are divided into two groups: the *absolute methods* where the measured data can be converted directly into the molar mass and the *relative methods* where calibration to a known sample is necessary. Techniques like MALDI-TOF (*absolute*) and GPC (*relative*) are used to determine molar mass distribution. For small molecules, the molar mass is well defined. However, the synthesis of a polymer rarely provides a single defined length of the polymer chain, but instead a sample of polymers that differ in the degree of polymerization is formed. Hence, such polymer samples are polydisperse and the molar mass is defined as an average value of polymers of similar lengths contained in the sample.^[5,6]

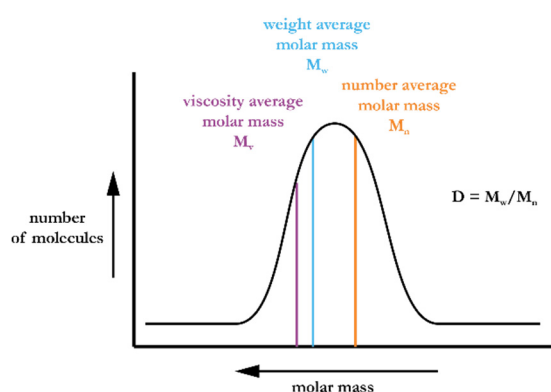


Figure 3. Schematic plot of a polymeric molar mass distribution. Along with the position of typical average molar masses M_n , M_w , M_v .

The number (M_n), the weight (M_w), the centrifugation (M_z) and the viscosity (M_v) average molar mass are the most common molar mass averages used to describe a sample of polymers (figure 3). These averaged values are equal if all the molecules in a sample have exactly the same size/chain length. Such a sample is then called monodisperse. Monodisperse polymers are rare (DNA for instance), especially for synthetic polymers. In polydisperse samples (samples containing different sizes of polymers) no single average number describes the polymer accurately. It is best to know besides an average value as well the polydispersity index ($D = M_w/M_n$) to define the polymer. A D value of 1 relates to a monodisperse sample, the larger the value gets, the broader the molar mass distribution is.^[8]

The number average molar mass (M_n) is determined by the total weight of all the polymer molecules present in a sample, divided by the total amount of polymer molecules in this sample:

$$M_n = \frac{\sum_i N_i M_i}{\sum_i N_i} \quad (1)$$

N_i = number of polymer chains in the sample with molar mass M_i
 M_i = molar mass of a polymer i with a defined chain length

All molecules are therefore weighted according to their respective amounts present in the sample. The M_n value can be determined experimentally by several methods like gel permeation chromatography (GPC), viscometry, vapor pressure osmometry, end-group determination or proton NMR.

For the weight average molar mass (M_w), the molecules in a sample are weighted according to their molar mass. Here a larger molecule contributes more to the total mass of the polymer sample than the smaller molecules do.

$$M_w = \frac{\sum_i N_i M_i^2}{\sum_i N_i M_i} \quad (2)$$

To determine M_w of a given polymer sample, static light scattering, small angle neutron scattering, X-ray scattering, sedimentation velocity and GPC are used.

Another commonly used descriptor is the centrifugation average molar mass (M_z), which is determined by the sedimentation equilibrium. M_z is calculated by the following equation (3):

$$M_z = \frac{\sum_i N_i M_i^3}{\sum_i N_i^2 M_i} \quad (3)$$

The viscosity average molar mass (M_v) is based on the idea that larger molecules induce viscosity in a sample, which scales with the size of the polymer, and therefore its mass.

$$M_v = \left[\frac{\sum_i N_i M_i^{1+\alpha}}{\sum_i N_i M_i} \right]^{\frac{1}{\alpha}} \quad (4)$$

α = exponent in the Mark-Houwink equation, which relates the intrinsic viscosity to molar mass.

In general, the molar mass values increase in the following order $M_n \leq M_v \leq M_w \leq M_z$.

Especially for an AB-copolymer, an important factor is the accuracy of stoichiometry. An excess of one of the monomer units increases the chance of having the same unit on both ends of the assembly. This prevents that two longer strands (oligomeric or even polymeric) couple together, and results in lower molar mass.

Polymers and their Use

We find many examples of polymers in nature. The main component of cell walls of green plants is a polymer – cellulose, which is likely one of the most abundant organic polymers on Earth. Other well-known examples of polymers in nature are DNA and proteins which exist in almost every living organism. Due to polymers unique physical properties, they play an essential role in various materials we now use in everyday life. Their large molar mass results in unique physical properties, including toughness, viscoelasticity, and a tendency to form glasses and semi crystalline structures rather than crystals, with tremendous implications for the electrical and electronic industry. The use of Thermoplastic, a well-known family of polymer, is widespread. On account of the material being cheap, versatile, easy to form, occurring in various degrees of stiffness and its resistance to water, it is no surprise that it is used from packing material to space shuttle construction. The use of Thermoplastics is crucial in coating electrical wires – as it is a flexible and insulating material at the same time. Even in materials applications, polymers play an important role as protecting layer, light conducting panels or dielectric medium in Microchips, solar cells and LEDs.^[5-7]

Carbon Nanotubes

Carbon Nanotubes as a Promising Material

The worldwide commercial interest in carbon nanotubes (CNTs) is reflected in its annual production exceeding several thousand tons.^[9] Two key features of CNTs are their extraordinary tensile strength, about 10-fold higher than that of any industrial fiber,^[10] and their outstanding physical properties. In particular their

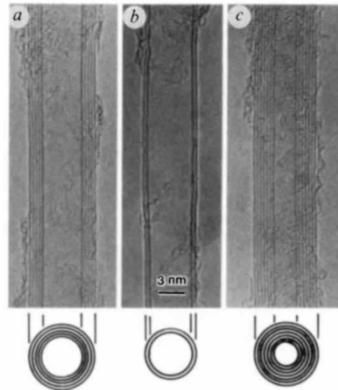


Figure 4. Electron micrographs of CNT, the parallel dark lines correspond to the (002) lattice images of graphite. The three different pictures represent a five-walled CNT (a), a two-walled CNT (b) and a seven-walled CNT (c), Reprinted with permission from S. Iijima *et al.*^[3]

thermal, electronical, mechanical and optical features make them promising functional materials in numerous applications. The thermal conductivity of individual single-walled carbon nanotubes (SWCNTs, for clarification see following chapter) exceeds the value of the thermal conductivity of diamonds (3500 W m⁻¹ K⁻¹ at room temperature based on their wall area)^[11]. Although, Oberlin *et al.* ^[12] described hollow carbon fibers obtained from vapor-growth in *Journal of Crystal Growth* (1976), Suomio Iijima is known as the first researcher to serendipitously discover the occurrence of these structures, during his attempt in 1991 to produce fullerene using arc discharge (figure 4).^[13,14] Commercial presence of CNTs has grown exponentially especially in the past decade and with it the annual number of CNT-related publications (figure 5).^[9]

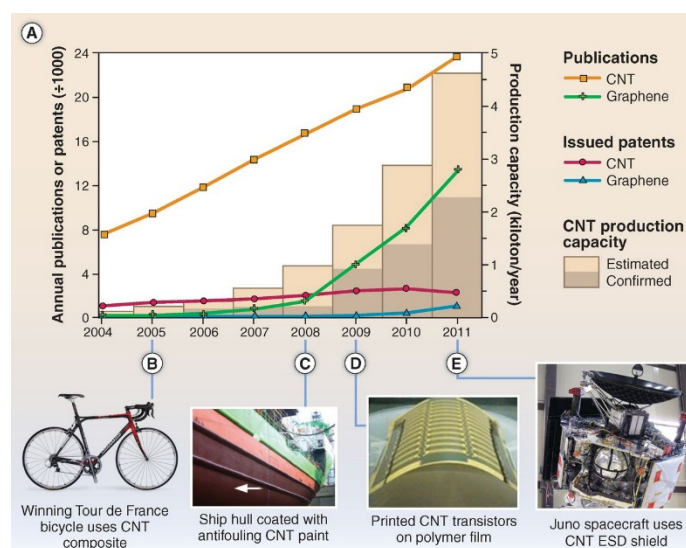


Figure 5. Trends in CNT research and commercialization. (A) Journal publications and issued worldwide patents per year, along with estimated annual production capacity (see supplementary materials). (B to E) Selected CNT-related products: composite bicycle frame [Photo courtesy of BMC Switzerland AG], antifouling coatings [Courtesy of NanoCyl], printed electronics [Photo courtesy of NEC Corporation; unauthorized use not permitted]; and electrostatic discharge shielding [Photo courtesy of NanoComp Technologies, Incorporated]. Reprinted with permission from de Volder *et al.*^[9]

As a light but extremely strong material CNTs were used in the winner's bike of Armstrong (prototype Madone SSLx, unfortunately disqualified years later) at tour the France in 2005. Not only the bicycle industry makes advantage of this material, the boat industry uses antifouling paintings made of CNTs, they are as well found in printed electronic devices and used as electrostatic discharge shields. Current applications of CNTs are mostly limited to the properties of CNTs in a bulk, which are mixtures of unorganized CNT architectures with different nanotube fragments. As of today, large scale production has yet to produce monodisperse SWCNTs. Fueled by potential promising applications of these materials, research has grown to an astonishing scale, finding new challenges and opportunities for chemistry of this material.^[15] Among others, devices such as electronic thin-film-transistors (TFT),^[16] flexible displays,^[2] flexible integrated circuits,^[17] and chemical & bio sensors^[18–21] see promising use of CNTs. The high quantum yield and the variable emission range of SWCNTs opens the opportunity for applications in photonic devices.^[22] Potential use of SWCNTs were tested for optical gain purposes as amplifier,^[23] mode-lockers for ultrafast lasers,^[24] or ultrafast optical switching.^[25] Other examples of the application potential of SWCNTs are their usage as catalytic fuel cells,^[26] as catalyst in proton exchange membrane fuel cells,^[27] as catalyst for cross coupling reactions,^[28] hydrogen storage,^[29] high strength fibers,^[1] solar cells,^[3] and transparent electrodes of solar cells.^[30] However, the fast growth of SWCNTs mass-production is hampered due to their poor solubility, which originates from their tendency to form aggregates as much as the challenges to obtain monodisperse samples of SWCNTs. The electronic properties of SWCNTs depend heavily on the integers (n, m , clarification in the next section), but in many of the above mentioned applications only a minor fraction of the SWCNTs actually possess the appropriate physical properties for the device. It can be concluded that only a small fraction of tubes contribute to the performance of the device while the rest are “silent” in the best case and dilute the active species. As SWCNTs are currently still produced as random, polydisperse mixtures, purification and targeted production of SWCNTs move increasingly into focus of interest.

Classification of CNTs and their Production

Carbon nanotubes (CNTs) are hollow cylindrical tubes of one or more layers of graphene with nanometer scale diameters and lengths up to a few micrometers.^[31] These nanostructures can be described as a strip cut of an infinite graphene sheet that is rolled up seamlessly to form a tube. Depending on number of layers of graphene in a tube they are denoted as single-walled (SWCNTs), or multiwalled (MWCNTs) carbon nanotubes.^[32] Whereas SWCNTs are made up of a single graphene sheet and closed by a hemispheric fullerene cap at its end, MWCNTs are made up of several concentric graphene cylinders. Diameters of SWCNTs are smaller than the ones of MWCNTs, typically in a range of 0.8 to 2 nm and 5 to 20 nm, respectively, although MWCNT diameters can get larger than 100 nm. Their length connects molecular and macroscopic scales, reaching from less than 100 nm up to a few centimeters.^[9]

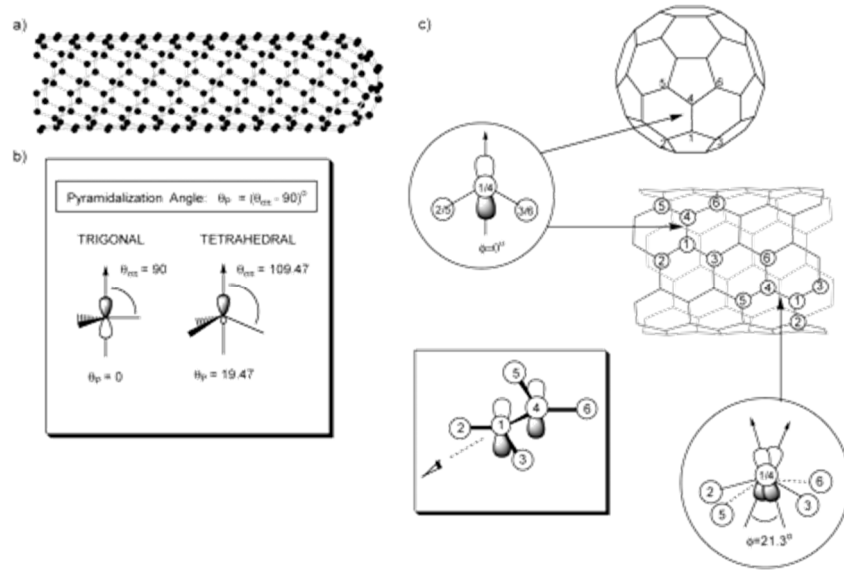


Figure 6. Diagrams of (a) metallic (5,5) SWNT, (b) pyramidalization angle (θ), and (c) the π -orbital misalignment angles (ϕ) along the C1–C4 in the (5,5) SWNT and its capping fullerene, C60. Reprinted with permission from S. Niyogi *et al.*³³

Perfect CNTs have all carbons bonded in a hexagonal lattice except at their ends and are made exclusively of sp^2 hybridized carbon atoms. Unlike in benzene, carbon atoms in a nanotube are pyramidalized because the surface of the tubes is curved. This leads to a misalignment of the π -orbitals over the carbon lattice and is more pronounced in CNT with smaller diameters (figure 6).^[33] As a result, the reactivity of CNT is higher when compared to graphene and decreases with larger diameters. The diameter and curvature of the tube and its electronic properties depend on its chirality, which is defined as the orientation of the graphene lattice with respect to the tube's axis.^[34] There are numerous distinguishable symmetry-related ways of rolling up hexagonal graphene sheets such that the edge atoms meet to form regular cylinders. To represent the diameter and the helicity of a SWCNT the chiral indices (n,m) are used. These two integers define the roll-up vector C_h of the graphene lattice of a CNT, with \vec{a}_1 and \vec{a}_2 as basis vectors (figure 7):^[35]

$$C_h = n\vec{a}_1 + m\vec{a}_2 = (n, m) \quad (5)$$

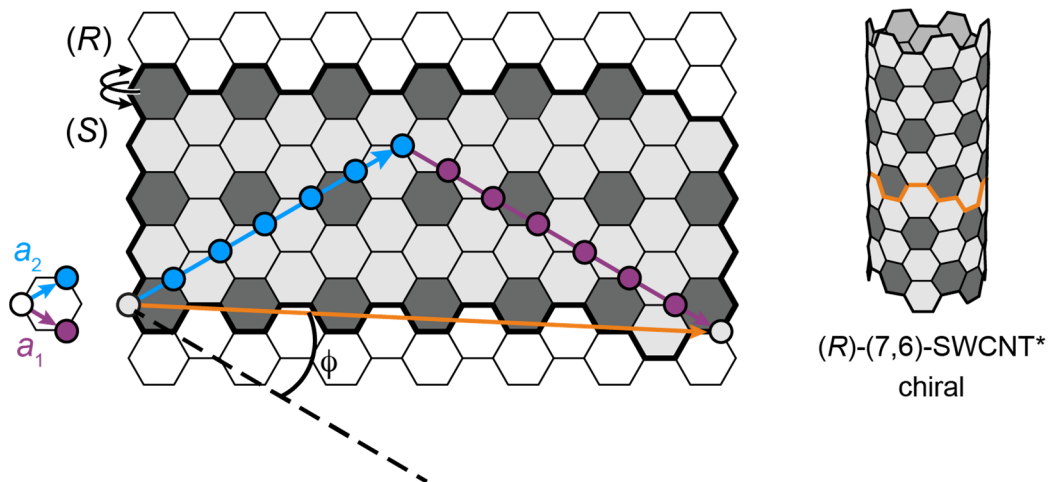


Figure 7. Principle of roll up vector of SWCNTs and example of R-(7,6) tube. n Represents the integer of the a_1 vector (purple) and m the one of the a_2 vector (blue). The roll up vector C_h (orange) defines the connecting points for a (7,6)-SWCNT and its chiral angle ϕ .

SWCNTs can be either metallic or semiconducting depending on their chiral indices. Studies have shown that for given chiral indices (n,m) , the electrical properties of the SWCNT can be predicted. If $n = m$ the tube can be referred to metallic. The quasi metallic tubes are a special case with a very small band gap; they are often defined as metallic. For these tubes $(n - m)$ is a multiple of 3 and $n \neq m$ and $n \times m \neq 0$. All other CNTs are semiconductors.^[36] This imposes that approximately one third of the SWCNT are metallic and two thirds are semiconducting. Metallic tubes have a finite value of charge carriers in the density of states at the Fermi energy while semiconducting tubes have none (figure 8). Their band gaps are inversely proportional to the tube's diameter.^[37]

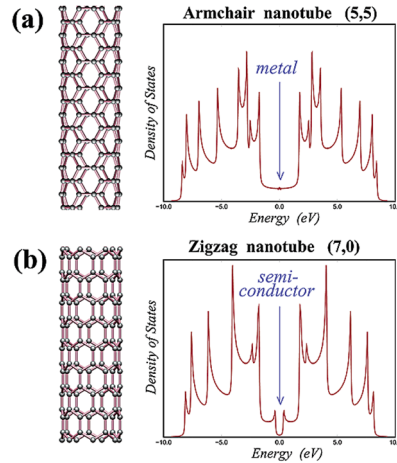


Figure 8. Electronic properties of two different CNTs and their corresponding density of states at different energies ((5,5)-metallic-armchair-SWCNT (a) and (7,0)-semiconducting-zigzag-SWCNT(b)). Reprinted with permission from J.-C. Charlier *et al.*³⁷

Not all variations of rolling up a graphene sheet end up in a helical chirality of the surface pattern on the tube. Therefore the SWCNTs are further divided into three groups according to their chirality. Achiral nanotubes are called zigzag if $m = 0$ and armchair if $n = m$. Otherwise, they possess a helical chirality with the existence of two enantiomers and are simply called chiral (figure 9).^[38]

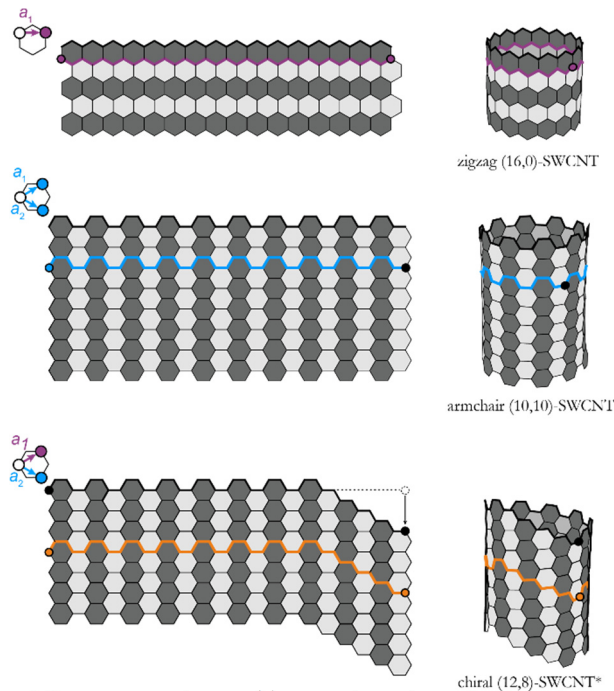


Figure 9. Illustration of the three different types of SWCNTs, zigzag ($m = 0$) armchair ($n = m$), and chiral (n,m).³⁸

Today's production of carbon nanotubes is dominated by catalytic chemical vapor deposition (CCVD), particularly with the use of the floating catalyst method^[39] using nanosized iron particles that are dispersed on the substrate or a floating reactant technique.^[12,40] The advantage of this technique is the production on large scale while maintaining the control of the multiplicity of the nanotube walls. Highly crystalline CNTs are commercially produced in combination with high-temperature thermal treatment. Other common techniques to produce CNTs are arc discharge^[41], laser ablation or high-pressure carbon monoxide disproportionation (HiPco) and high-pressure carbon monoxide disproportionation on Co-Mo catalyst (CoMoCAT) as a subcategory of the CVD method.^[42] Each method is used to produce CNTs of different range of diameters^[43]: HiPco and CoMoCAT tend to form SWCNTs with diameters between 0.7 – 1.1 nm, laser ablation 1.0 – 1.4 nm and arc discharge between 1.2 – 1.7.^[43]

Regardless of the technique used for the CNT preparation, the samples always contain undesired impurities. The outlined techniques produce powders, usually containing a small fraction of desired CNTs among other carbonaceous particles, like graphite, amorphous carbon, fullerenes, CNTs with defects, as well as metals from the catalysts. These impurities alter the properties of the CNTs in the bulk material. Additionally, these approaches do not result in monodisperse samples but mixtures of CNTs with different chiralities, diameters and lengths. Recently, the production of SWCNT samples with highly enriched single-chirality species has been described, either through controlled growth or postsynthetic separation approaches or a combination of both. Fasel and co-workers converted a molecular template into ultrashort singly capped (6,6) 'armchair' nanotube seeds to catalytically grow a well-defined SWCNT on a surface.^[44] The state-of-the-art of chiral controlled synthesis of SWCNTs is discussed in the review of Lie *et al.*^[45] in detail. The main problems of bottom up synthesis are upscaling and purity issues. Besides a targeted growth of carbon nanotubes, purification techniques to isolate CNTs with desired diameters or chirality have been investigated.

Purification Techniques; Covalent Versus Non Covalent Functionalization

Purification of SWCNTs with a specific characteristics is particularly challenging for several reasons. Two key challenges are a) the structural similarity of the side-products formed during the synthesis of the nanotubes and b) the tendency of SWCNT's to aggregate which results in their poor solubility. Strong van der Waals interactions between SWCNTs reaching up to ~500 eV per 1 μm of tube length^[46] lead to triangular, highly polarizable, smooth bundles.^[47] SWCNTs are essentially build from sp^2 hybridized carbon atoms and differ little in terms of chemical reactivity. In combination with the poor solubility the common purification methods are insufficient to obtain pure samples of SWCNTs with a specific characteristics.

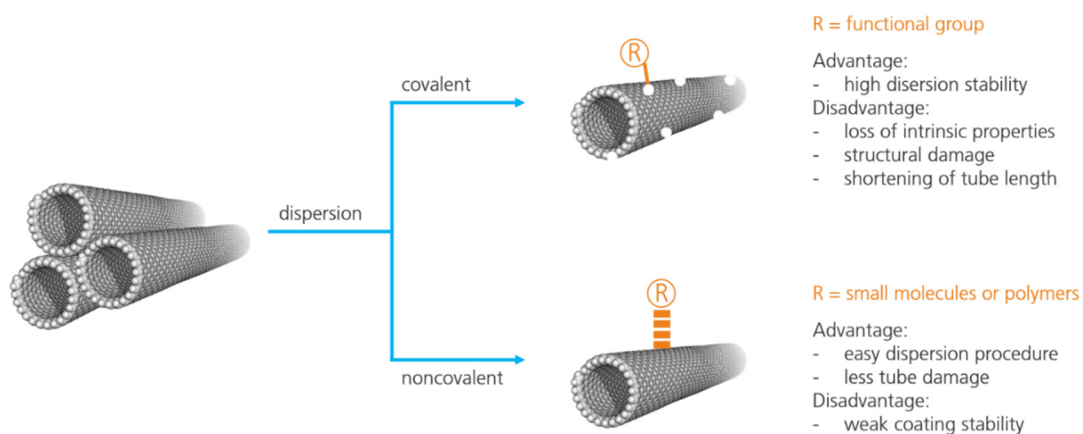


Figure 10. Advantage and disadvantage of SWCNT's dispersion methods (covalent and noncovalent)

A limited number of solvents are known to solubilize carbon nanotubes to some extent. *o*-Dichlorobenzene, *N,N*-dimethylformamide, *N*-methylpyrrolidinone and *N,N*-dimethylacetamide are among the best but the solubility is still too low to process SWCNT's samples for application use.^[48–52] Density gradient

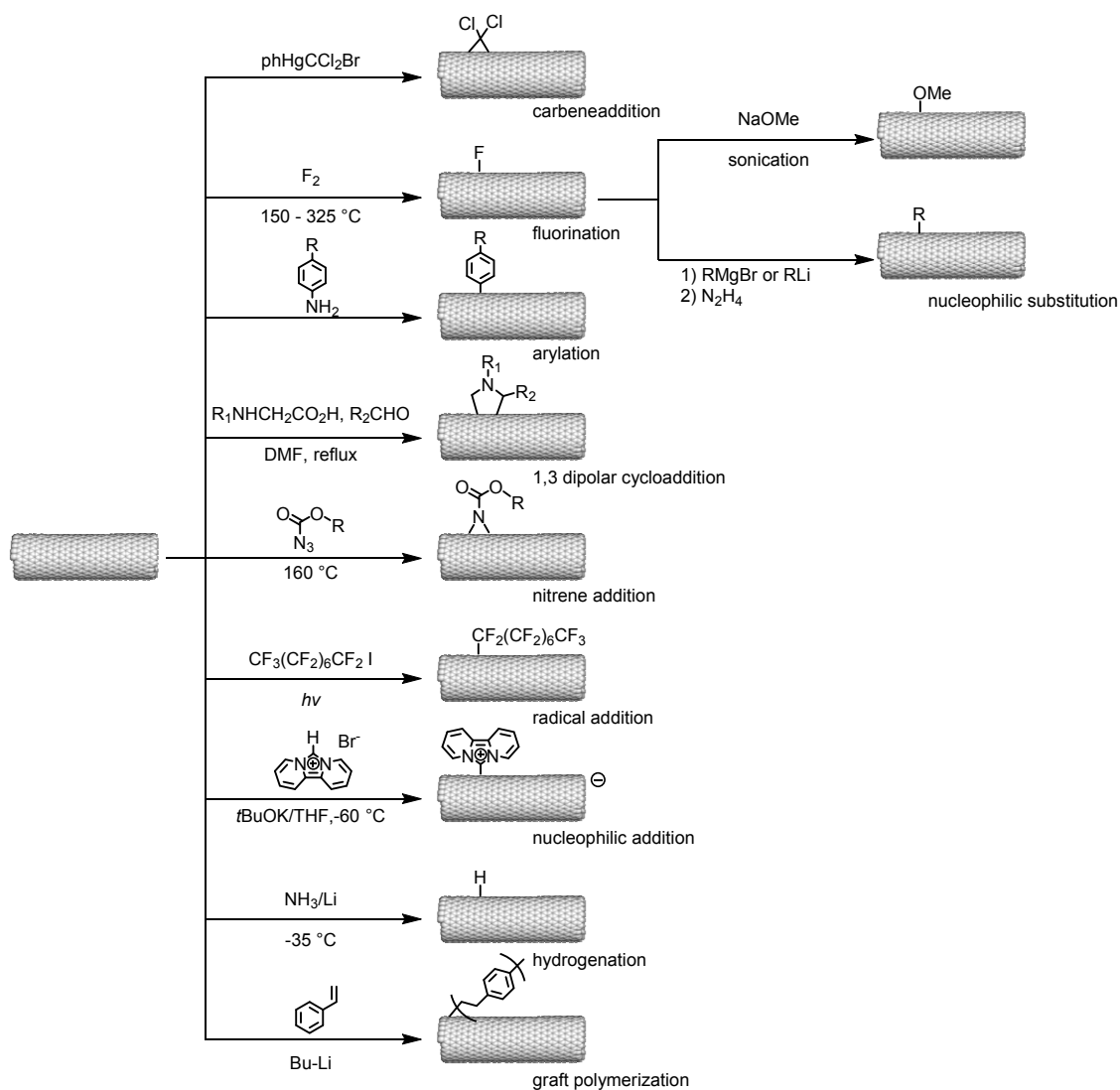


Figure 11. Summary of typical reactions used for covalent functionalization of SWCNT's for their dispersion.

ultracentrifugation^[53,54] showed promising purification results and allowed access to samples of electronically-enriched SWCNTs. Subsequently, electrophoresis,^[55] two phase extraction,^[56,57] gel^[58,59] and size–exclusion chromatography^[60] further demonstrated capability to separate metallic and semiconducting SWCNTs. Since the discovery of ultracentrifugation, two common approaches to solubilize and purify SWCNTs based on their electronic character and their chirality have been developed. Both rely on chemical modification of individual SWCNTs to break the aggregates and solubilize the tubes (figure 10).^[61] Addition of chemical groups to the tubular walls disrupts the strong interactions between the tubes and therefore helps to unbundle SWCNTs and get them into solution.^[62] Typical approaches for the covalent modification of SWCNT are summarized in figure 11. These include oxidation of CNTs end tips or sidewalls by introduction of a carboxyl group that can be further derivatized to a desired functional group,^[63–68] sidewall halogenation, hydrogenation, cycloadditions, radical additions and ozonolysis.^[69] The covalent functionalization is generally better in terms of dispersion stability when compared to the noncovalent functionalization and effective reinforcement of polymer films to the CNTs.^[70–73] However, modification of the tube’s sidewall usually influences the tube’s intrinsic properties in a permanent, uncontrollable way.^[74,75] Furthermore this technique can result in cutting the tube into shorter segments.^[74] Both the dependence of reactivity on electronic structure and the effect of chemical modification on the electrical and mechanical properties have to be well understood to use this techniques.^[76]

Noncovalent dispersion of SWCNT is a milder method less prone to damage the tube retaining its inherent properties after dispersion. It is realized by adsorption of a small molecule or a polymer to the surface of the tube, typically involving vigorous stirring (e.g. sonication followed by centrifugation). However, a common problem of this technique is a considerably weaker coating stability of the surfactant when compared to a covalent bond (figure 10).^[32,34,43,69,77] The interaction of the dispersant can take place at different sites of the tube (figure 12).

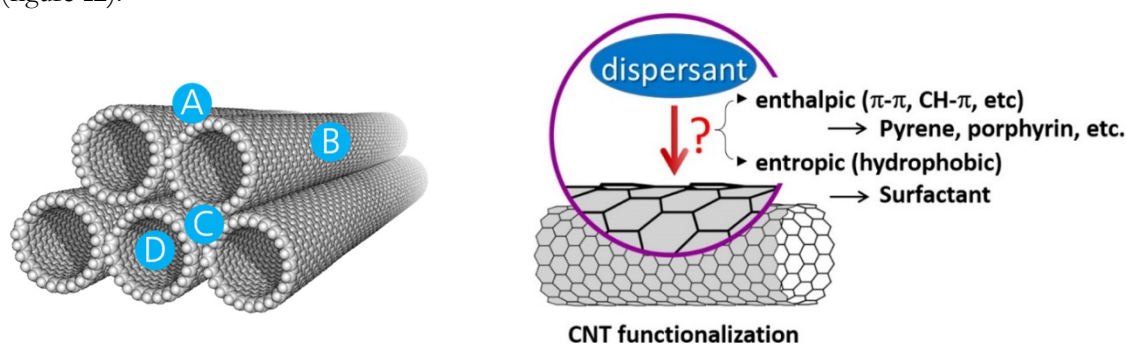


Figure 12. Different interaction sites of the tube and the surfactant: groove of two tubes (A), sidewall (B), interstitial cavity (C), individual tubes cavity (D) (left). Non covalent dispersion modes, reprinted with permission from Fujigaya *et al.*^[69](right).

It can interact with the tube at a groove of two tubes (figure 12, A), at the outer surface of a sidewall (figure 12, B), at an interstitial cavity (figure 12, C) or at the nanotube cavity (figure 12, D).^[34] In general, the interior of a SWCNT is more inert than the exterior, which is also true for covalent bonded functionalization. Dispersing SWCNTs in a noncovalent manner is either enthalpy-driven, involving π - π and van der Waals interactions etc. or an entropy-driven process, such as hydrophobic interactions using surfactants.^[78] Surfactants on the SWCNT surface are in a dynamic equilibrium with the bulk solution. This enables the

removal of the surfactants from the tube by simple filtration and dialysis to recover free aggregated tubes.^[79] Sodium dodecyl sulfate (SDS), sodium dodecylbenzene sulfonate (SDBS), sodium cholate (SC), cetyltrimethylammonium bromide (CTAB), Brij, Tween and Triton X are typically used surfactants due to their low cost and good availability.^[80] In contrast conjugated polymers that have multiple sites interacting with the nanotube shell can shift the equilibrium that leads to a static dispersion and more stable solutions.^[79] Such polymer–tube complexes remain after filtration and washing, prohibiting re-bundling of the tubes. This type of adsorption can influence the intrinsic properties of the tube even if no covalent bonds between the polymer and the tube are formed. Polymer wrapping for solubilization is known,^[81,82] in particular single-stranded DNA was found to be capable of sorting SWCNTs.^[83–85] Relatively recently, conjugated polymers have been found to disperse semiconducting SWCNTs efficiently and selectively. Nicholas and co-workers^[86] were first to report that poly(9,9-dioctylfluorenyl-2,7-diyl) (PFO) (entry 1 and 3, table 1) shows a specific selectivity towards semiconducting SWCNTs. It was found that the PFO-SWCNT dispersion in toluene contained only a small fraction of SWCNTs compared to the unselective dispersion of the same sample of SWCNTs with SDBS in water. As one can see clearly in figure 13 a and b dispersion with the polymer did not decrease the emission intensity of (8,6)-tubes compared to the solution with SDBS, but it decreased or even eliminated the presence of other tubes.

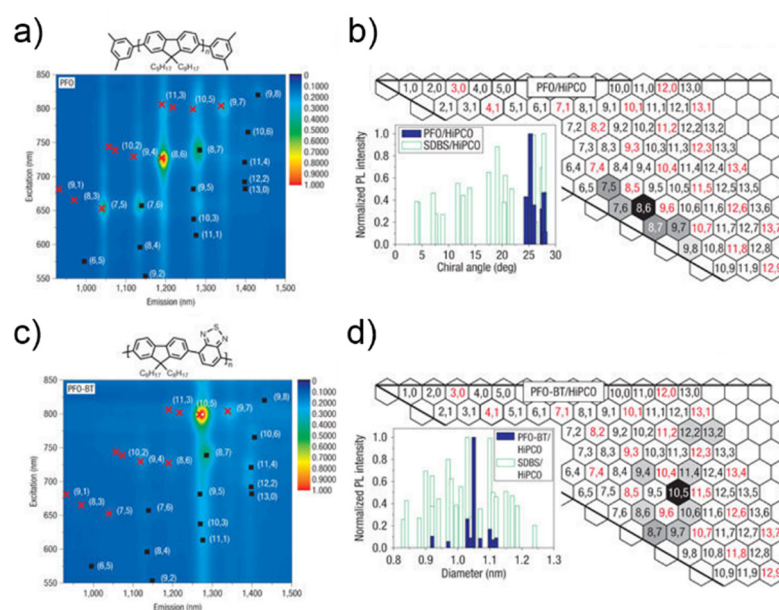


Figure 13. Dispersion ability of PFO and PFO-BT towards HiPco SWCNTs in comparison to SDBS. Measured photoluminescence excitation maps of the polymer-SWCNTs solutions a, c and corresponding graphene sheet maps b, d. First reported by Nicholas and co-workers. Reprinted with permission from A. Nish *et al.*^[86]

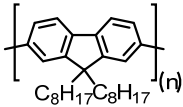
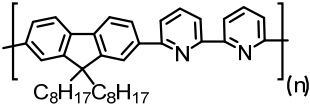
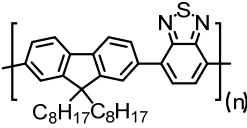
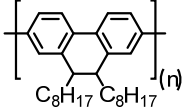
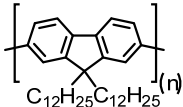
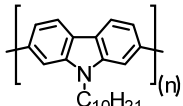
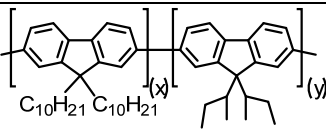
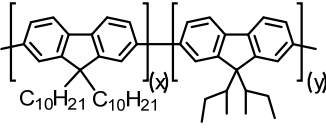
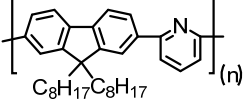
Interestingly, insertion of a benzothiadiazole into the polymer backbone (poly[9,9-dioctylfluorenyl-2,7-diyl]-co-1,4-benzo-{2,1'-3}-thiadiazole]) (PFO–BT or F8BT)) changed the selectivity towards (10,5) – SWCNTs addressing a larger diameter, but only a small subset of tubes was dispersed. The dispersion protocol involved sonication of a solution of the polymer and the tube, first for 60 minutes in a usual sonic bath and then for 15 min in a ultrasonic disintegrator, before centrifuging the sample for 3 minutes at 9,000 g to observe the desired dispersion. The authors postulated that the selectivity of the polymer towards the specific SWCNTs is enhanced with rigidity of the polymer backbone. Due to the limited conformational freedom in the polymer

backbone, the π - π stacking is limited to SWCNTs with suitably curved. Absorption, emission and Raman spectroscopies proved that the samples were enriched with SWCNTs of specific chirality and that the metallic tubes were absent. The selectivity changed if different solvents or SWCNT samples were used.^[87] For example, PFO and PFO-BT displayed the highest selectivity in toluene or xylene, while it decreased in THF and, in particular, in chloroform because the density of chloroform precluded the sedimentation of nanotube bundles during centrifugation. In the same paper, the influence of the rigidity of the polymers backbone was investigated. The authors concluded that more rigid polymers are more likely to be selective for specific SWCNTs.

Chen *et al.*^[88] (entry 3, table 1) used the same polymers (PFO and PFO-BT) and investigated their dispersing quality towards narrow-diameter distributed CNTs concluding that PFO disperses smaller diameter semiconducting SWCNTs than PFO-BT (0.83 – 1.03 nm, 1.03 – 1.07 nm respectively). In addition they were able to reproduce the results of Nicholas^[86] by using HiPco CNT material, which is remarkable because the diameter range of a given sample of SWCNTs is strongly dependent on the manufacturing process and varies even from batch to batch for any given synthesis. It is thus not surprising that the results obtained for a polymer depend on the sample of SWCNTs, which therefore requires a clear description of the SWCNTs sample.

Since the discovery of the dispersing power of PFO, various polymers were designed to selectively enrich samples with SWCNTs of specific chirality. This depends on the nature of the polymer, the production technique of the SWCNTs, the solvent used for the dispersion, the polymer : SWCNT ratio and on the dispersion conditions. A fluorene subunit represents the most popular building block in conjugated polymers which serve as semiconducting SWCNT dispersant. Thiophene- and carbazole- based polymers were investigated, too.^[89–91] Despite considerable efforts, there are no polymers to date that are known to disperse metallic SWCNTs exclusively. Table 1 highlights the performance of some of the polymers and the SWCNTs characteristics which they enrich in samples of SWCNTs.^[43]

Table 1. Highlighted selective conjugated polymers and their dispersion properties

entry	polymer structure	SWCNT production	enriched primary chirality (n,m)	diameter (nm)	chiral angle (°)	Solvent
1	 PFO	CoMoCAT	(7,5)	0.82	24.5	toluene
		HiPco	(8,6)	0.95	25.3	toluene
		Laser aplatation	(9,7)	1.09	25.9	toluene
2	 PFO-BPy	CoMoCAT	(6,5)	0.76	27.0	toluene
3	 F8BT or PFO-BT	HiPco	(10,5)	1.05	19.1	toluene
		HiPco	(9,4)	0.90	17.5	<i>o</i> -xylene
		Arc discharge	(15,4)	1.36	11.5	toluene
4	 PPhO	HiPco	(8,7)	1.03	27.8	toluene
5	 PFDD	HiPco	(7,6)	0.88	27.5	toluene
6	 P6	HiPco			$\varnothing < 20$	toluene
7	 P7 x:y=100:0	HiPco			$\varnothing > 24$	toluene
8	 P7 x:y=15:85	HiPco	(10,3)	0.94	12.7	toluene
9	 PFOPy	Laser aplatation	(13,5)	1.26	15.6	toluene

Ozawa *et al.* presented PFO-BPy as suitable polymer for enrichment of (6,5) SWCNTs out of a CoMoCAT nanotube sample (entry 2, table 1).^[92] The purity of the enriched sample was determined to be up to 97%. The sorting of HiPco SWCNTs by conjugated polymers was investigated extensively and with promising results regarding chirality. Entries 7 and 8 in table 1 show the results of Ozawa *et al.*, who systematically varied the ratio of the fluorine subunit with a linear and a branched, more bulky side chain in the polymer. With the different copolymers they revealed that the increase in steric bulk of the side chain leads to a dispersion of SWCNTs with smaller chiral angles.^[93] They also investigated the variation of the backbone and compared the selectivity of PFO and PPhO polymers.^[94] Their results indicate that PPhO preferably recognizes SWNTs with larger-diameter and higher chiral angles compared to those recognized by PFO. The influence of non-aromatic ring numbers of the backbone of PPhO results in different SWNT chirality recognition/extraction behaviors (entry 4, table 1).

The effect of the length of the solubilizing alkyl chains of PFO on the selectivity of the HiPco and arc plasma jet prepared SWCNT dispersion in toluene was examined by Loi and co-workers.^[95] Systematic elongation of the alkyl chain from 6 to 12 carbons in PFOs were tested. For dispersions with longer alkyl chain polymers, a higher SWCNT concentration was observed, together with a selectivity towards larger diameter semiconducting SWCNTs. However, the overall selectivity decreased and more metallic impurities were found in the samples. That sidechains affect the dispersing selectivity and quantity was as well shown by the work of Kappes and co-workers (entry 5, table 1).^[96] In addition, they were able to enrich predominantly specific SWCNT species, by optimization of polymer mass concentration in relation to the one of precursor SWCNT material. Obtaining specific enrichment of (7,5), (7,6), (10,5), or (9,7) SWCNTs, through the ratio optimization of various combinations of PFO or poly(9,9-di-*n*-dodecylfluorene) (PFDD) polymers and different produced SWCNT material. They postulate that limiting the polymer amount was critical for single-chirality selectivity. The impact that preparation conditions have on the dispersion selectivity is again underlined with these results.

Modifications in the polymer backbone was investigated to understand the selectivity towards other specific diameters of SWCNTs.^[97] A trend that overall high conformational rigidity in the polymer backbone correlates with the dispersion of tubes with larger diameter has been observed, while polymers which exhibit more flexible backbone were more selective to small diameter tubes.^[98]

The group of Mayor used a polycarbazole instead of PFO (entry 6, table 1) to disperse HiPco SWCNTs.^[91] Polycarbazoles possess an increased π - conjugation in the polymer backbone and lower steric hindrance due to the presence of a single alkyl sidechain, in contrast to two side chains in fluorene. In this study, the molecular weight of the polymers/oligomers was relatively low, due to the poor solubility of the carbazole unit, which made it difficult to compare directly with the results obtained for the fluorene-based polymers. Nevertheless, dispersion of semiconducting SWCNTs was observed. While PFO derivatives disperse selectively HiPco SWCNTs with a chiral angle $\theta \geq 20^\circ$, the polycarbazole derivative (P6) disperses tubes with a chiral angle of $\theta \leq 20^\circ$. Rice *et al.* presented a high molar mass polycarbazole including a different

solubilizing group which is selective towards small diameter semiconducting SWCNTs in toluene and THF.^[99-101]

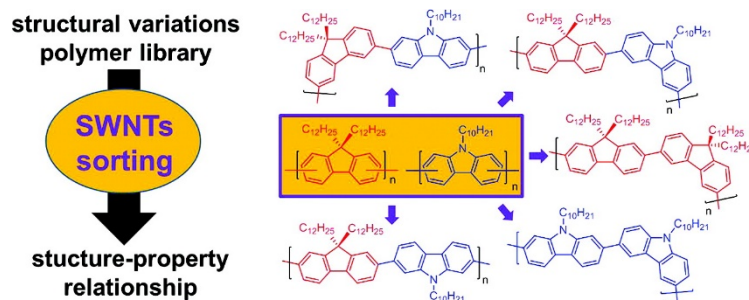


Figure 14. Structural variation in the polymers backbone of PFO and carbazole based polymers. Reprinted with permission from F. Lemasson *et al.*^[102]

In the context of structural variation of the polymer backbone, the Mayor group synthesized a library of fluorene and carbazole based homo- and copolymers, including naphthalene, anthracene, or anthraquinone linkers with different connection points in the individual subunits.^[102] The results generally show that the most stable suspension was formed with 2,7-connected fluorenyl and carbazole polymers, with an exception of (poly(*N*-decyl-3,6-carbazole) which unselectively dispersed a wide range of SWNT species (figure 14).

With PFOPy and laser ablation CNTs (entry 9, table 1), Tange *et al.* were able to capture SWCNTs with diameter size of 1.26 nm that emit light in the near infrared region, suitable for applications in telecommunication.^[103] Further they used PFO-BT polymers (entry 3, table 1) with Arc-discharge tubes to selectively address (15,4)-SWCNTs, which confirmed previous results that PFO-BT is selective towards tubes with larger diameters (~1.38 nm).^[104] This selectivity is attributed to the matching energy levels of the polymer and the tube. Considering that the band gaps of SWCNTs are related to their diameter, it is evident that recognition of SWCNT with various diameters has attracted considerable interest.

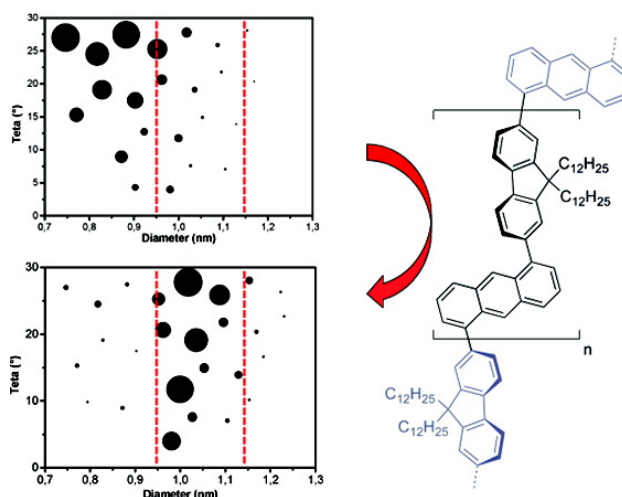


Figure 15. HiPco SWCNTs dispersed in aqueous solution using sodium cholate (upper graphic) and in toluene using organic copolymers (lower graphic). The graph shows the chiral angle of the tube versus its diameter and the size of the data points refers to the concentration of the specific SWCNTs. Reprinted with permission from N. Berton *et al.*^[105]

The anthracene group in poly(9,9-didodecylfluorene-2,7-diyl-*alt*-anthracene-1,5-diyl) is attributed to be the reason of the preference of the polymer to wrap around SWCNTs having a diameter of ≥ 0.95 nm.^[105] In figure 15 one can see the dispersion of HiPco SWCNTs in aqueous solution with only sodium cholate as reference (figure 15, top left) compared to the dispersion of the same SWCNT batch with the polymer in toluene (figure 15, bottom left). Blackburn and co-workers^[106] observed the same selectivity towards larger diameter semiconducting SWCNTs when the surface area of the aromatic rings in the repeating units in the copolymer backbone increased. A different connection of anthracene unit in a copolymer than discussed above increased the conjugated π -system and the selectivity of the copolymer towards large diameter (10,8)-SWCNTs (1.24 nm). Such correlation was also found in more recent studies.^[107–109]

In addition, SWCNTs with larger diameters (≥ 1.1 nm) were dispersed by copolymers comprising either fluorene/pyridine or carbazole/pyridine unites by Mayor and co-workers.^[110] The purification step of the sample after dispersion was shortened to a one-pot extraction where no further ultracentrifugation was needed. Even though the selectivity was reduced, the sorting yield could be enhanced. Similar results were obtained for the fluorene-based polymers presented by Mistry *et al.*^[106]

The influence of polymers chain length on the polymer dispersion ability was as well investigated by the groups of Mayor and Adronov.^[111,112] The sorting yield and the purity of SWCNTs after dispersion depend on the molar mass of the polymer. In the case of PFDD at least six fluorene subunits are needed to observe any dispersion activity. Although fast precipitation of the oligomers–SWCNTs complexes was observed, stability and dispersion was found to increase with higher molar mass of the polymer.^[111] Adronov and co-workers synthesized poly[2,7-(9,9-dioctylfluorene)-*alt*-2,5-(3-dodecyl-thiophene)] (PFTs) with a molar mass ranging from 5.7 up to 83 kg/mol.^[112] The maximum concentration of SWCNTs was reached with polymers with M_w between 10 and 35 kg mol⁻¹. Higher and lower M_w resulted in substantially reduced nanotube concentration, which is attributed to a weak π - π interaction between oligomers and the SWCNT surfaces, and the lower solubility of larger polymers and therefore their tendency to aggregate (figure 16), respectively.

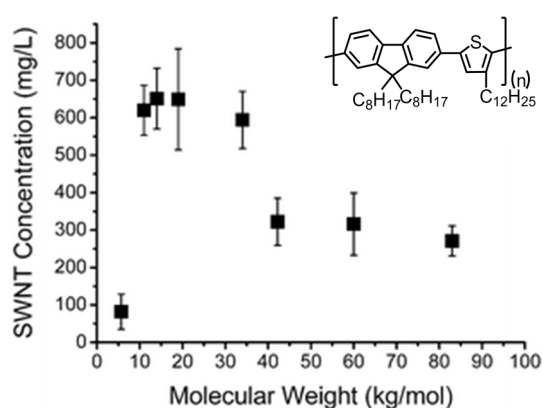


Figure 16. Dispersion concentration of PFT-SWCNT complex versus molecular length of the used polymer. Reprinted with permission from P. Imin *et al.*^[112]

A similar behavior was observed for PFDD by Ding *et al.*^[113] On the other hand, increasing the molar mass of the asymmetric polymer poly(9-dodecyl-9-methyl-fluorene) (PF-1-12) resulted in a reduced selectivity, most likely due to increased viscosity of the high-molar-mass polymer solution.^[114]

To increase the variety of polymers the group of Mayor explored the synthesis of copolymers by using click chemistry. These copolymers comprise a 1,2,3-triazole combined with a fluorene unit.^[115] These polymers were selective towards HiPco synthesized SWCNTs with $\varnothing > 20^\circ$. Overall the selectivity and the dispersion ability was found similar to POF. However, the preparation of the copolymer with click chemistry approach offers a number of advantages compared to polymerization by Suzuki coupling (figure 17).

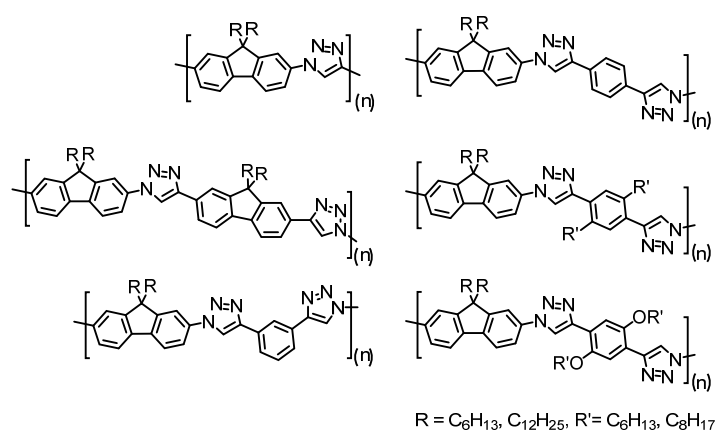


Figure 17. Structural diversification in conjugated copolymers backbone for SWCNT presented by Mayor *et al.*^[115]

The group of Bao investigated polythiophene derivatives and their sorting ability for CoMoCAT and HiPco SWNTs.^[89] Examination of the influence of side-chains was performed by randomly varying compositions of branched and linear alkyl chains in diketopyrrolopyrrole-*co*-terthiophene (PDPP-3T) (0 – 20% linear alkyl chains). Decreasing steric hindrance using linear alkyl chains increased the strength of the interaction of the polymer with the SWCNT. An ideal balance of sorting yield and selectivity was found for the polymer containing 10% of linear alkyl chains.^[116] Furthermore, excessive decrease of the amount of side chains results in complete loss of polymer dispersion ability. The sorting yield of semiconducting CoMoCAT tubes related directly to the length of side-chains used in the polymer (longer chains = higher sorting yield).^[97] The selectivity leaned towards smaller-diameter semiconducting tubes with larger bandgaps, which are ideal for the use in active layers of solar cells. With HiPco SWCNTs a high purity and selectivity with polythiophene as dispersing polymer was obtained (semiconducting SWCNTs purity > 99%).^[117] Overall both the length and the density of the side chain in the polymer influence the polymer dispersion ability. In addition, the same group addressed larger diameter semiconducting tubes by using copolymers with rigid backbones and increased surface area of aromatic units with improved selectivity towards larger diameter SWCNTs in accord with the studies using polyfluorenes.^[90,116,118]

Electronic properties of the polymer backbone influence the selectivity towards metallic or semiconducting SWCNTs.^[98] Currently, the use of electron rich π – conjugated building blocks like fluorene, thiophene and carbazole provide polymers that selectively disperse semiconducting SWCNTs. The group of Adronov

investigated the dispersion of electronically distinct polymers.^[119,120] They compared the dispersion ability of two fluorene based copolymers, one with an electron rich *p*-dimethoxyphenyl and one with an electron poor *p*-dinitrophenyl linker. While the electron rich copolymer dispersed semiconducting SWCNTs selectively, the electron poor copolymer was unselective and dispersed both semiconducting and metallic SWCNTs.^[119] In a subsequent work they investigated the dispersion of poly(fluorene-co-pyridine) copolymers and their positively charged methylated derivative. The decrease in electron density was found to strongly increase the amount of metallic SWCNTs that were dispersed.^[120] The results show that electron density in the polymer backbone has a strong impact on the amount of dispersed metallic SWCNTs.

From the perspective of device fabrication, not only the dispersion ability matters but as well the influence of the conjugated polymer on the properties of the tube. Even though fluorene containing polymers show good selectivity to semiconducting polymers, they exhibit unsuitable large bandgaps. In this context thiophene based polymers are better, though less selective. Nicholas and co-workers found that thiophene based polymers have higher affinity towards SWCNTs than fluorene based polymers even though they are less selective.^[121,122] Initially they dispersed semiconducting SWCNTs with PFO, to then perform a polymer exchange with the less selective but stronger binding poly(3-hexylthiophene) (P3HT) and by this enabled a better performance in electronic devices.

Earlier it was mentioned how dispersion by polymers was realized by Nicholas co-workers. It can be generally concluded, that a few parameters of the dispersion protocol influence the dispersion ability of a polymer as summarized in figure 18. The influence of the polymer structure, the type of nanotube material used for the dispersion and the influence of ratio of the two was already discussed before. That variation of solvent has an impact on dispersion was mentioned and it was highlighted that dispersion selectivity towards semiconducting SWCNTs tend to be much better in non-polar solvent, such as toluene.^[123] The fact that these solvents are unable to stabilize dipole moments is thought to be the reason that the more polarizable metallic SWCNT/polymer complexes can aggregate into bundles, due to dipole-dipole interactions and sediment during centrifugation as a result of the higher density bundles compared to the individual

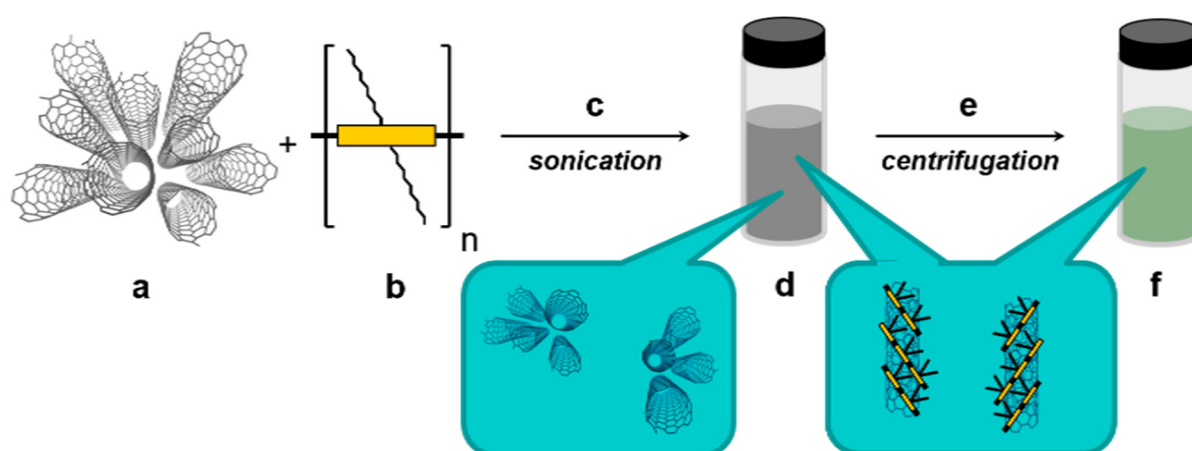


Figure 18. General overview of SWCNT dispersion and the parameters which can be influence during the dispersion protocol; a) type of SWCNT fabrication; b) solubilizing polymer: *backbone structure, molar mass, side chains; ratio* of a and b; c) *sonication time, solvent and temperature*; resulting in d) SWCNT bundles and soluble polymer coated SWCNTs; e) centrifugation to remove the SWCNT bundles: *speed* e) dispersed polymer coated SWCNTs.

semiconducting SWCNTs/polymer complexes.^[43,124] These trends are not absolute. Dispersions in polar THF tend to have poor selectivity, but individual examples exist in literature where selectivity towards semiconducting SWCNTs are reported in THF.^[91,100,120] Furthermore, several solvent properties like viscosity and density have shown to influence the dispersion selectivity and ability and are currently investigated.^[123,125,126] As well the sonication power, length and temperature and the centrifugation power can have an impact and should be considered. Different trends of these parameters are concluded in the review of Adronov.^[98]

Nakashima and co-workers were first to bring the complexation of SWCNTs and polymers a step further in terms of chirality.^[127] They were able to enrich either left or right handed semiconducting SWCNTs by using a bulky chiral fluorene-binaphthol copolymer. The binaphthol building block was responsible for the incorporation of the chiral moiety and the fluorene was chosen as it is already known to disperse semiconducting SWCNTs (figure 19). Through simple one-pot sonication of the copolymers and CoMoCAT SWCNTs, extraction of right-, respectively left-handed semiconducting SWCNT enantiomers with (6,5)- and (7,5)- enriched chirality was achieved as confirmed by Circular Dichroism (CD) spectroscopy.

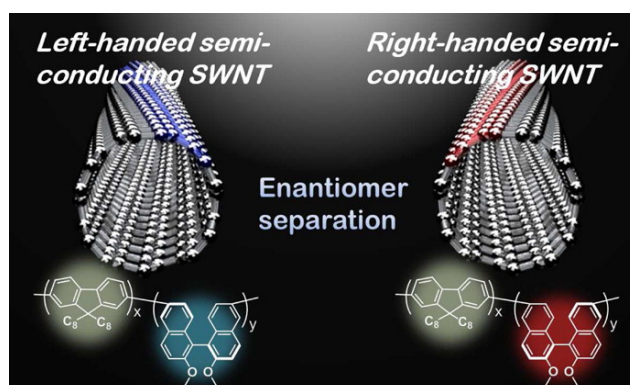


Figure 19. Copolymer presented by Nakashima and co-workers for enantiomeric separation of SWCNTs. Reprinted with permission from K. Akazai *et al.*^[127]

Selectivity for handedness was also achieved by Deria *et al.*^[128] They used highly charged semiconducting polymers including R respectively S conformers of 1,1'-bi-2-naphthol derivatives in the conjugated polymer backbone and achieved significant preference wrapping of SWCNT's single helical handedness.

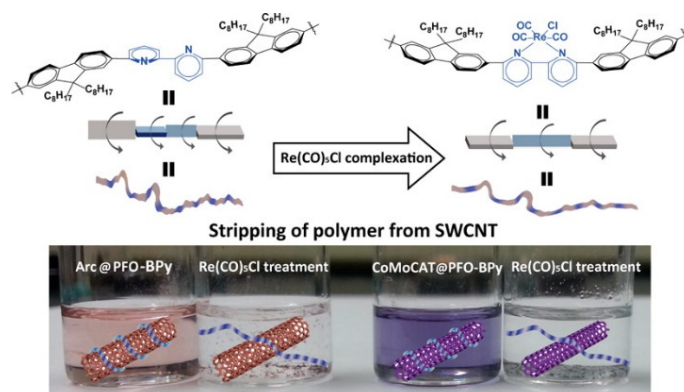


Figure 20. Ability to release the wrapping of the dispersed SWCNT on demand, through change of the polymers conformation. Reprinted with permission from Y. Joo *et al.*^[129]

In order to use the dispersed SWCNT's properties without interfering effects of the polymer, various attempts of polymers were realized which enable release of the wrapping after dispersion. In this context Joo *et al.*^[129] used the ability of the bipyridyl units in PFO-BPy to chelate rhenium. Through complexation to rhenium the conformation of the polymers backbone changes and therefore loses the adsorption interaction to the SWCNT during wrapping and allowed the release of the tube. Thus, as seen in figure 20, a combination of first use the selective wrapping and dispersion ability of PFO-BPy towards semiconducting SWCNT's followed by the disorientation and unwrapping of the polymer through metal complexation, it was possible to isolate a pristine semiconducting SWCNT sample.

Dynamic metal coordination chemistry was also used by Nakashima and co-workers.^[130] In their work they used supramolecular coordination chemistry to form metal linked polymers. The formed polymer consists of a fluorene unit with two phenanthroline moieties used for metal-complexation linkage to the next unit. Non-selective dispersion of metal and semiconducting SWCNT in benzonitrile was feasible with this polymers. Addition of toluene initiated sedimentation of the metallic tubes while keeping semiconducting SWCNT's dispersed. Subsequent release of the polymer was achieved by degradation of the polymer by addition of trifluoroacetic acid.

Another approach to address the release of a SWCNT from the polymer is to degrade the polymer which enwraps the semiconducting SWCNT after it's dispersion to enable a release as the multiple adsorption points of one molecule are lost. Using hydrogen bonding and imine hydrolysis Bao and co-workers were able to sort the desired tubes, release them from the polymers by degradation and not only isolate the purified SWCNT's but as well recycle and reuse the polymer (figure 21).^[124,131,132]

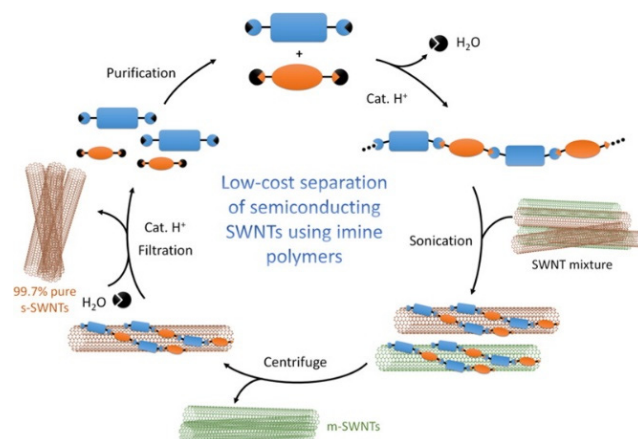


Figure 21. SWCNT wrapping release through hydrolysis of the imine bonded polymer and recycling via reformation of the re-polymerization of the monomeric units. Reprinted with permission from T. Lei *et al.*^[124]

Our group address this challenge with a photo cleavable polymer, containing a *o*-nitrobenzylether (Y) in the fluorene (X) backbone (figure 22).^[133] To ensure selectivity the X:Y ratio has to be at least three to one, meaning three consecutive fluorene subunits need to be present. Upon photo-Irradiation, the polymer which wrapped the SWCNT could be cut into small sections, which allowed removal of the tubes surface.

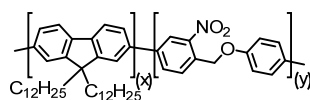


Figure 22. Structure of photo cleavable copolymer published by Mayor *et al.*¹³³

Postulated Sorting Mechanism of Conjugated Polymers towards SWCNTs

The SWCNT sorting ability of certain polymers by selective dispersion is multifaceted and not yet comprehensively understood. Considering the general procedure of dispersing SWCNTs with conjugated polymers, the selectivity could occur at two stages, either during centrifugation through formation of selective bundles or through selective exfoliation and wrapping of the polymer around the SWCNT during the sonication process (figure 18).^[98,134] These two concepts of selectivity (post-wrapping/exfoliation) do not necessarily exclude each other, selectivity is likely to feature a contribution from both.

Aspects in favor of selective aggregation were proposed by Bao *et al.*^[123] They postulated that polarizability of SWCNTs was one of the central parameters for selectivity. Calculations showed that semiconducting and metallic SWCNTs have markedly different polarizabilities, the metallic SWCNTs being $\sim 10^3$ times more polarizable than the semiconducting ones. Based on this knowledge, it follows that metallic SWCNT–polymer complexes aggregate into bundles during centrifugation in non-polar solvents while semiconducting complexes are dispersed due to pronounced dipole–dipole interactions between metallic complexes.^[123] This reasoning is underlined by the observed solvent dependency, where non-polar solvents – which are incapable of stabilizing dipole moments – usually display higher selectivities. There are, however, exceptions to this rule and some reports show selective aggregation/dispersion in polarizable solvents such as THF, which is able to stabilize dipole moments. Moreover, only a resolution of metallic and semiconducting SWCNTs would be feasible but selectivity towards a specific diameter of a SWCNT or even chirality would be challenging to explain. Adronov *et al.* suggested that selectivity arises in the exfoliation step.^[98] They postulated a thermodynamically driven process, with enough energy available from the sonication to overcome the activation energy of the polymer SWCNT complex formation. Additionally, it would allow to overcome the energy barrier to aggregate specific SWCNT bundles and therefore allowing reversibility of the exfoliation and bundling. Selectivity would thus arise from the stability of the polymer SWCNT complex and the stability of the bundles within the sample. In accord with this postulate is the fact that polymer exchange of P3HT and PFO-SWCNT complexes are feasible with sonication.^[121] Moreover, the displacement of fluorene oligomers with PFDD-BT polymers underline as well the likelihood of a selective exfoliation controlled process.^[111] That dispersion selectivity is enhanced by limiting the amount of available amounts of polymer during the dispersion also point towards a selective exfoliation process.

In this summary, various examples of the selective dispersion of SWCNTs through polymers were highlighted, demonstrating that variation of the polymer structure has an impact on the selectivity – even though the reason for selectivity is far from being completely understood.

Justification for our Work

This comprehensive overview about noncovalent wrapping and sorting of SWCNTs by conjugated polymers demonstrates the complexity of this quickly growing research field. Clearly, numerous variables influence the selectivity and quantity of SWCNTs dispersion. The polymer structure, its molar mass, the type of the used CNTs, the sonication temperature, the ratio of polymers and CNT material, the solvent used for the dispersion and other experimental conditions influence the selectivity.^[34,77,98] A full understanding of the observed selectivity principles and the underlying mechanism has not yet been achieved. The comparison of the results from different studies is also challenging because the results depend significantly on the experimental conditions and the samples of CNTs. The analysis of relationships between the experimental parameters is crucial to maintain the consistency during a study. But, systematic variation of the conjugated polymer structure to dedicate the CNT selectivity is non-trivial as structural changes of the monomer unit derive in different reactivity during the polymerization and therefore often resulting in different polymers length. It is nonetheless important to conduct these studies relentlessly, with the vision of achieving large amounts of monodisperse, and affordable SWCNTs one day.

Molecular Design

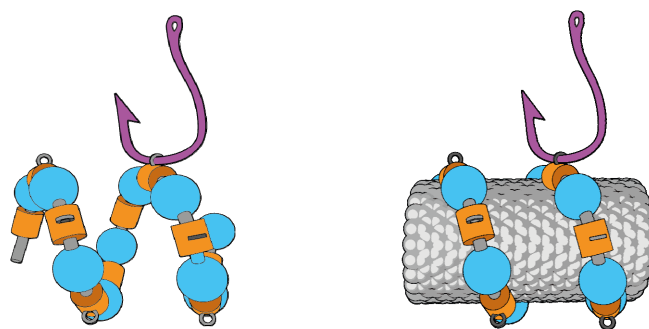


Figure 23. Schematic view of AB copolymer (left) and AB copolymer wrapping around a SWCNT.

We have a long standing interest to use polymers for dispersion of large, insoluble polyaromatic systems such as carbon nanotubes. Conceptually, the use of aromatic organic polymers to selectively solubilize certain types of single walled carbon nanotubes was first published by *Nish et al.*^[86] They found that poly(9,9-dioctylfluorenyl-2,7-diyl) (PFO) has a particularly strong selectivity for (8,6) SWCNT, if a HiPco mixture is solubilized in toluene. The selectivity for both chiral angle and tube diameter was found to be modulate strongly with small changes of the polymer structure. Since the publication of *Nish et al.* various polymers were found to be able to solubilize carbon nanotubes and the interest in this research field has grown.^[43,98,135] Our group focused as well on dispersing qualities of polymers. Instead of fluorene units, copolymers of carbazole were used. Poly(N-decyl-2,7-carbazole) as well as different copolymers of fluorene and carbazole units showed good dispersing qualities.^[91,102,105,110,111,115,133]

As outlined in the introduction, polymers can be tuned towards selective interactions with other macromolecular structures. Of particular interest are single-walled carbon nanotubes (SWCNTs), whose monodisperse isolation remains challenging. We envisioned that we can encode a strong interaction of a building block towards a curved π -surface and amplify this interaction across an entire copolymer (figure 23). Depending on the type of linkage, the formed copolymer should adopt a different tertiary structure and thus be selective towards a specific tube-diameter and n,m indices. The resulting tightly bound copolymer-tube assembly should dissolve in common organic solvents, depending on the solubilizing groups introduced into each monomeric building block and therefore be separable from the uncoated SWCNTs. The usage of chiral monomer units might allow selection for tube chirality – a feature that controls many of the properties of SWCNTs but is extremely challenging to obtain as monodisperse sample.

As previously outlined, the key requirements for the main building block are a) an efficient and modular assembly, with the potential of achieving multi-gram scales; b) high structural integrity, c) high solubility in common organic solvents; d) a platform to introduce chirality selectively and c) incorporation of a reactive moiety for efficient polymerization. Additionally, the assembly should be highly modular as it is challenging to predict the exact spatial requirement of each building block to show optimal selectivity.

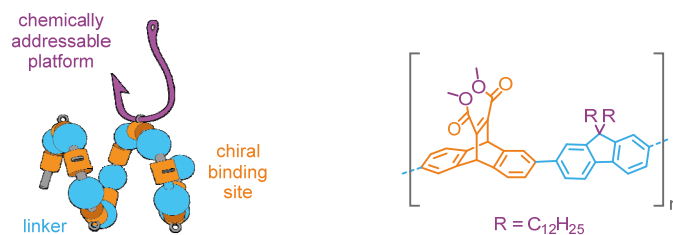
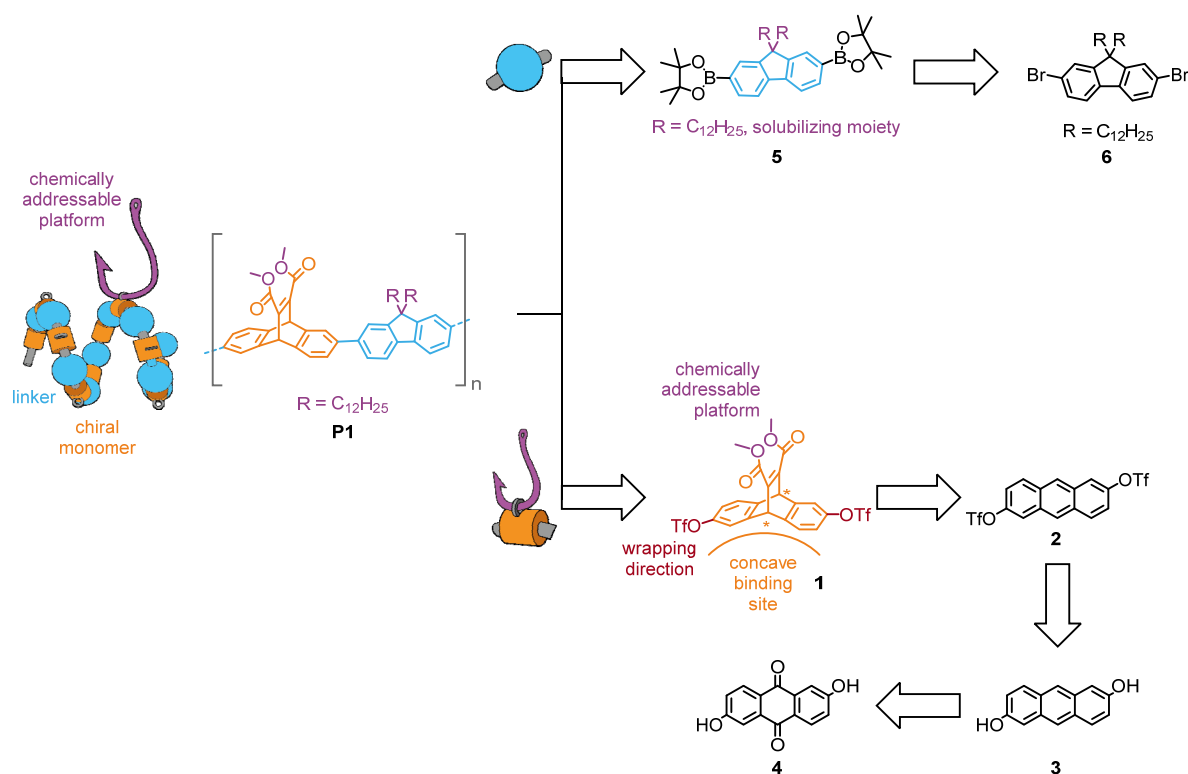


Figure 24. Conceptual drawing of the polymer (left) molecular representation of the envisaged polymer (right).

Eventually, we devised alternating A-B copolymers that consists of a chiral interface A and a linker B for connection and spatial resolution. The most prominent structural feature of our polymer is a triptycene analogue (ethenoanthracenes) as triptycenes are literature known as surfactants for CNT^[136] and possess a concave π -system for an efficient and selective surface π - π interaction with the desired carbon nanotube (figure 24). Deplanarization of a parent anthracene via regioselective Diels-Alder reaction introduces the concave binding interface and allows the overall physical and chemical properties of the polymer to be fine-tuned. To increase solubility of the polymer – before and after dispersion- long alkyl chains can be introduced, which also can be altered to introduce other features like solubility in other solvents or to immobilize the complex on a surface. Attachment of the linkers on opposite ends of the ethenoanthracene building block defines a preferred wrapping direction and introduces chirality upon deplanarization. Two enantiomeric centers are formed leading, due to the selectivity of the Diels-Alder step, exclusively to two enantiomers which can be separated by chiral chromatography. As the chiral centers of the monomer unit cannot racemise without decomposition of the molecule and the polymerization reaction has no influence on the chiral unit, the product should be an enantiomerically pure copolymer. Both enantiomers would be accessible from their respective enantiomeric monomers. As poly(9,9-dioctylfluorenyl-2,7-diyl) and their derivatives already showed adsorption affinity to SWCNTs, we intended to start with fluorene unit as linker. Varying the linkers allows to tune the selectivity for diameter, rigidity and to degrade the polymer after dispersion.

Building blocks

As outlined in the prior section our envisaged polymer features two main building blocks – the chiral interface (1) and the linker (5), which are assembled independently (scheme 2).



Scheme 2. Retrosynthesis of a representative target polymer **P1** and molecular representation of the individual building blocks

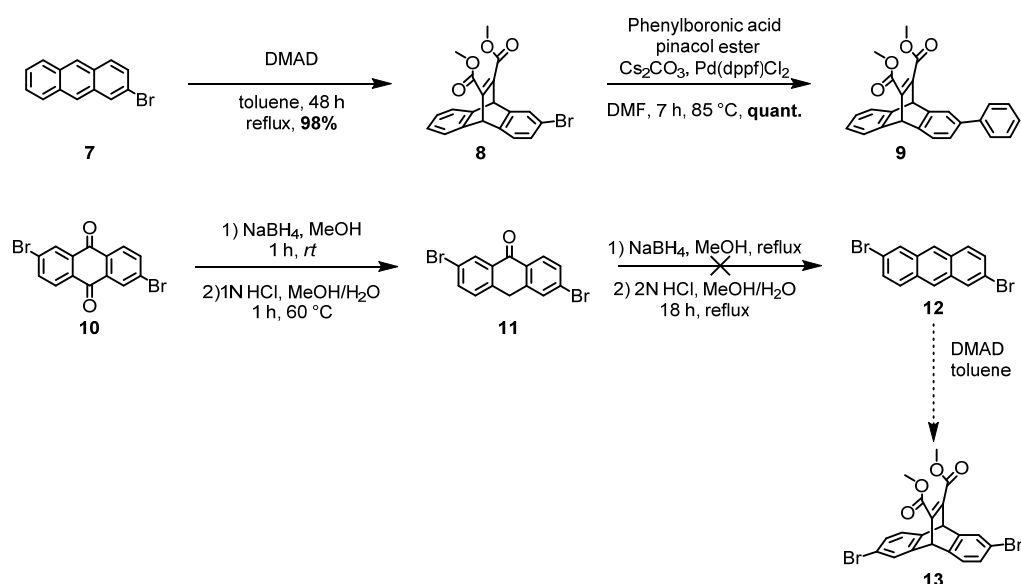
Chiral Interface. Anthracenes are abundant and well explored, making them ideal starting materials. To provide an addressable handle for interlinkage by cross-coupling and to make the molecule chiral once deplanarized, we settled on a 2,6-disubstituted anthracene derivative. Reduction of anthraflavic acid (4)^[137] and subsequent triflation of the formed 2,6 dihydroxyanthracene (3) installs handles for initiating polymerization, while reaction with dimethyl acethylene-dicarboxylate would give the desired ethenoanthracene **2** framework.

Linker. As polyfluorene is known to show dispersing quality, we decided to incorporate fluorene as a linker in our initial attempts. It provides two alkane chains, for increased solubility in organic solvents, an essential feature for good dispersing properties. Based on previous successes in our group we envisaged to copolymerize the linker **5** and ethenoanthracene **1** using a Suzuki-based polymerization. Suzuki cross-couplings are known to be highly regio –selective and tolerating a wide range of functional groups. Thus the linker needed boron moieties on each end. The synthesis of this initial linker is literature known and realized via a twofold borylation of 2, 7-dibromofluorene (6).^[133]

Results and Discussion

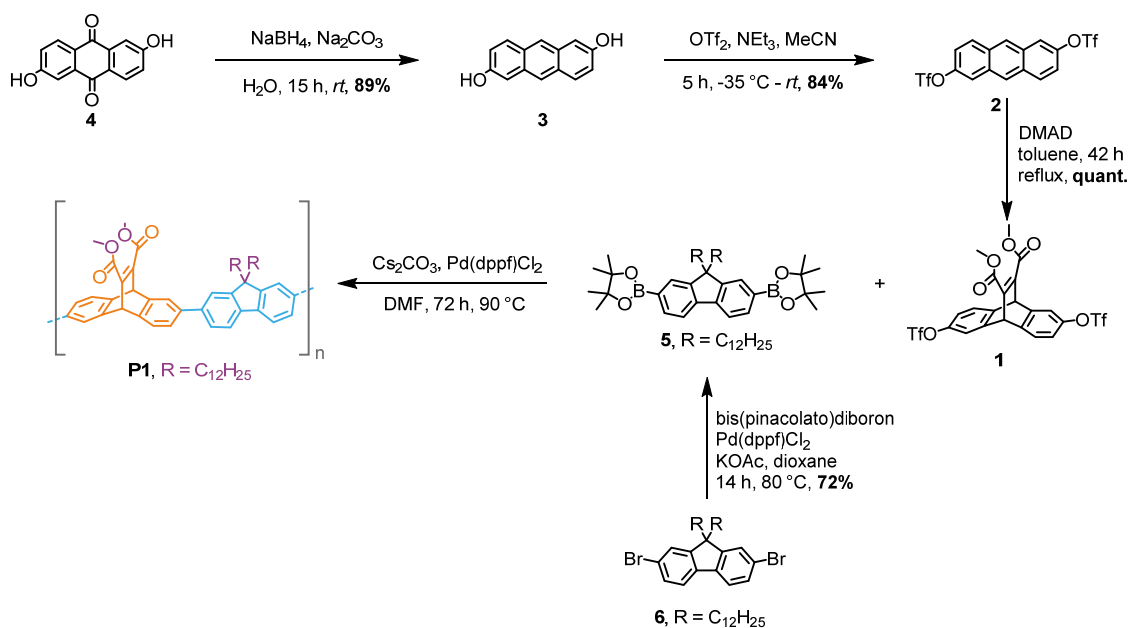
Synthesis of dimethyl polymer P1

We began our investigation on commercially available 2-bromoanthracene (**7**) with the intention on converting the structure to the corresponding ethenoanthracene and attach a model-linker via Suzuki-Miyaura cross-coupling. Indeed, we observed clean conversion of 2-bromoanthracene (**7**) into the corresponding ethenoanthracene **8** (98%) with dimethyl acetylene-dicarboxylate (DMAD) at elevated temperatures. Diels-Alder reactions are concerted pericyclic reactions and due to the substitution pattern of the starting material, two enantiomers (**8**, RS and SR) were observed. We found the structure **8** to be well soluble in organic solvents, on account of curvature and the incorporated ester moieties. These will allow for post-assembly modification of solubility etc. Pleasingly, the halogen was still present after the conversion and could be subjected to Suzuki cross-coupling with phenyl boronic acid. To avoid cleavage of the ester, mild conditions featuring Pd(dppf)Cl₂ were selected. Again, the conversion was excellent, validating the suitability of the chosen conditions for the model system (scheme 3). Due to the excellent yield, we decided to employ the same strategy for interlinking the individual building blocks into the corresponding polymer.



Scheme 3. Synthesis of mono functionalized model compound **9**, and initial trials towards dibromo-ethenoanthracene **13**.

To obtain a building block suitable for polymerization, we intended to use 2,6-dibromo-anthracene (**12**) in analogy to our initial model systems. As it is not commercially available, we began with the 2,6-dibromo-9,10-anthracenedione (**10**) precursor with the intention of reduction to the anthracene derivative **12**. Reductive conditions similar to literature^[138,139] gave the mono-reduced intermediate 2,6-dibromoanthracene-9(10H)-one (**11**) but no further reaction was observed, only partial retention of starting material was obtained (scheme 3).



Scheme 4. Synthetic route for copolymer **P1**

As the reduction of anthraflavic acid (**4**) is described in literature,^[138,140] we envisaged to convert the hydroxyl groups into triflates, which are known to undergo Suzuki couplings with a variety of boronic acids and esters. The overall approach would thus remain similar. Anthraflavic acid (**4**) was reduced with NaBH₄ in moderate yields to give 2,6-dihydroxy anthracene (**3**). We intended to carry out the Diels-Alder reaction as early as possible in the synthesis, which would allow us to separate the enantiomers on plentiful materials. However, heating diol **3** in dimethyl acethylene-dicarboxylate did not yield the desired Diels-Alder product in reasonable yields, likely because of precipitation. We reasoned that triflates could help to promote the DA step and converted the hydroxyl groups into triflates prior to the cycloaddition. Dry and degassed base was crucial for the success of the triflation, as well as low temperature to prevent hydrolysis of the triflates. Satisfyingly, compound **2** quantitatively reacted with dimethyl acethylene-dicarboxylate in refluxing toluene to the desired racemic Diels-Alder product **1** (scheme 4). Prior to polymerization, chiral resolution of the monomeric building blocks was crucial. A racemic building block would lead to a statistical mixture of a vast amount of stereoisomers. Consequently, ethenoanthracene derivative **1** was resolved into its enantiomers by HPLC on a chiral stationary phase. Screening was initiated using an analytical Daicel Chemical Industries, Ltd. CHIRALPAK IA column, (4,6 X 250 mm, particle size: 5 micron). Ultimately, ideal conditions were found (figure 25): 30:70 isopropanol/hexane, at 25 °C and a flowrate of 1 mL/min with UV detection at 254 nm. The resolution parameter of the two enantiomers was found to be $R_s = 8.07$ ($\alpha = 2.67$). The excellent baseline separation on the analytical column allowed upscaling to a preparative column with retention of the separation. A CHIRALPAK IA 250 x 30 mm 5 mic column was used for preparative separation and the flowrate was increased to 42.5 mL/min, with otherwise identical parameters. Per run, it was possible to separate 100 mg of racemate. Both fractions were subjected to CD spectroscopy giving identical spectra with opposite signs, as expected for enantiomers (**1-F1** and **1-F2**, figure 25). The NMR spectra of both enantiomers exhibit identical shifts and coupling constants for the resonances. Additionally, LC-MS of both compounds

revealed identical masses and retention times. Thus isolated, the enantiomerically pure building block **1** was ready to be subjected to copolymerization.

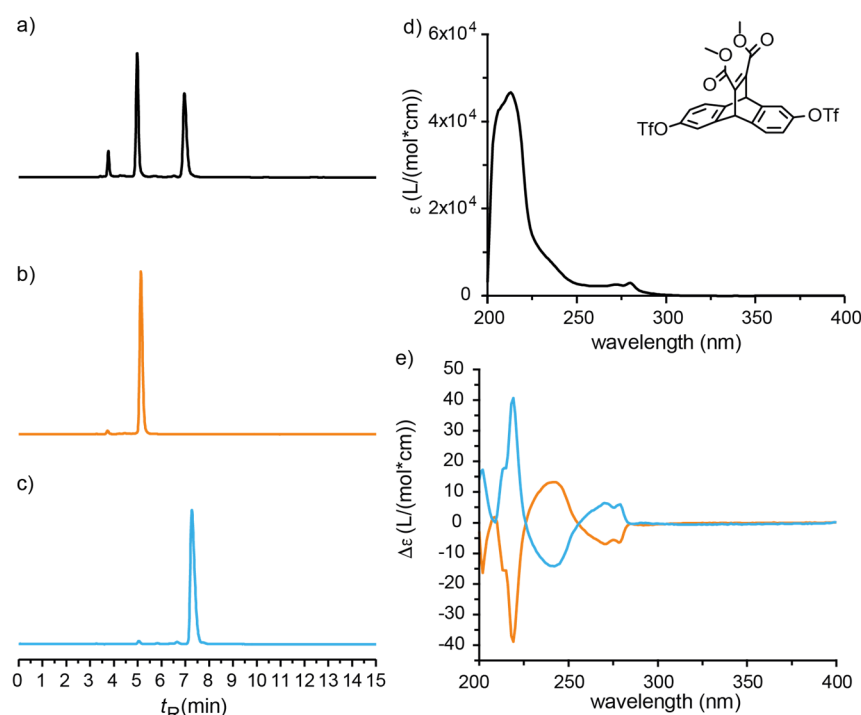
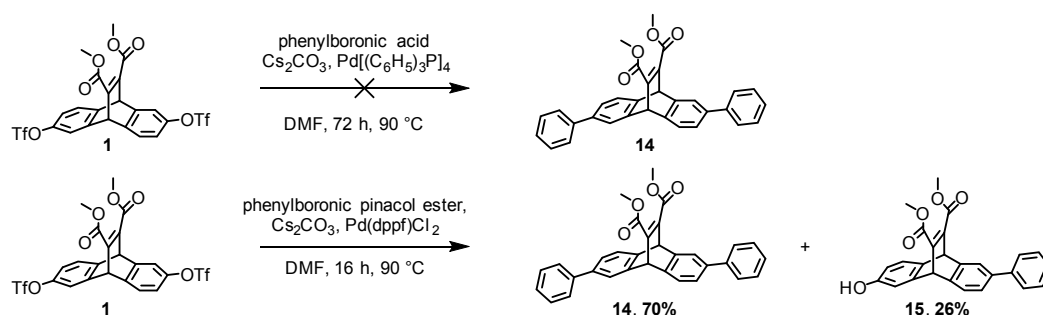


Figure 25. Chiral HPLC traces of **1**, (254 nm, 1 mL/min, 30:70 isopropanol:hexane, *n*); preparative separated enantiomers reinjected to the analytical HPLC under the same conditions a) crude (black) b) fraction 1 (orange) c) fraction 2 (blue); d) UV/vis spectrum of racemate **1** (black, 30:70 isopropanol:hexane, 1 cm cuvette, *n*); e) CD spectra of the enantiomers **1-F1** and **1-F2** (30:70 isopropanol:hexane, 1 cm cuvette, *n*) fraction 1 (orange) fraction 2 (blue).

As outlined, we intended to interlink the building blocks with a linker to introduce modularity at a late stage of the assembly. We chose diboronic ester **5** bearing two pinacol esters as initial linker, which was obtained by efficient Miyaura borylation of the dibromofluorene derivative **6**.^[105]

We now turned our attention to initiate a first Suzuki-based polymerization using the ditriflate monomer **1** and the obtained diboronic ester **5**.



Scheme 5. Screening reaction conditions for the Suzuki based polymerization.

For convenience, a mono-functionalized linker (phenyl boronic acid) was used to establish Suzuki conditions (scheme 5). Ideally, these conditions could then be used to enable co-polymerization of **P1**. Initially, reaction of the monomer unit **1** with phenyl boronic acid, a source of Pd⁰ (tetrakis(triphenylphosphine)palladium) as catalyst, and Cs₂CO₃ as base in DMF led to decomposition of the starting material. Exchanging the acid for the corresponding pinacol ester instigated slow release of the boronic acid by hydrolysis under the employed

conditions. Together with a catalyst ($\text{Pd}(\text{dppf})\text{Cl}_2$) known for functional group tolerance, the target ethenoanthracene moiety **14** was obtained in 70% after heating for 12 hours, together with the mono reacted side product **15** (26%). These conditions were transferred to the target polymerization. Before initiating polymerization, an exact 1:1 ratio of monomer and linker was established by $^1\text{H-NMR}$ spectroscopy, as polycondensation reactions are crucially dependent on stoichiometric ratios.

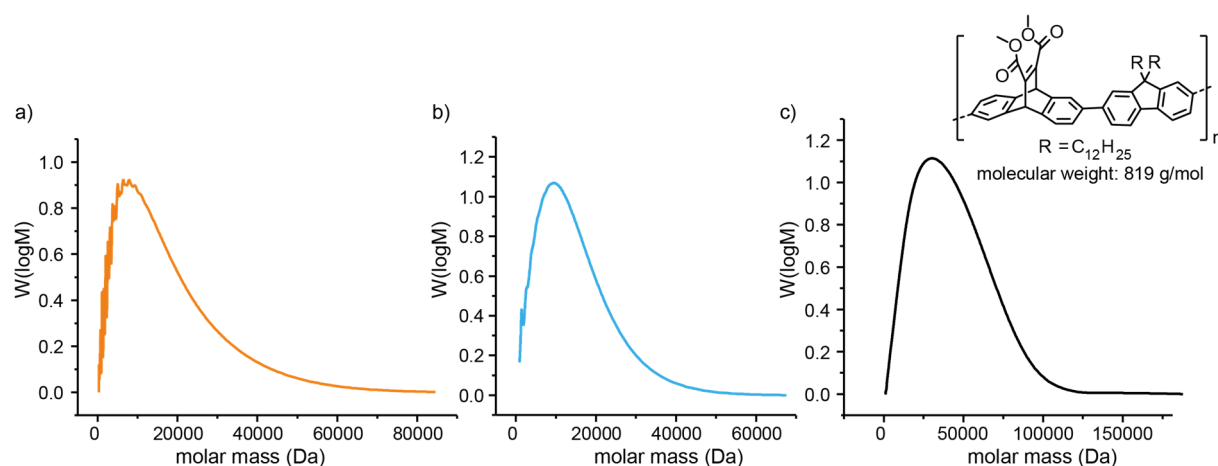


Figure 26. GPC analysis of the two enantiomeric copolymers **P1-F1** and **P1-F2**; a) deriving from monomer **1** fraction 1 (orange) b) synthesized from monomer **1** fraction 2 (blue) c) the racemic equivalent **1** (black) obtained by Suzuki cross coupling reaction

Gel permeation chromatography (GPC) was used for relative molar mass determination of the obtained polymeric compounds **P1-F1**, **P1-F2** and **P1** (figure 26). GPC traces were recorded and analyzed in WinGPC UniCrom (V 8.30 - build 8217, Polymer Standard Service (PSS), Germany). The measurements were performed on an Agilent-based system with linear-S SDV columns (pre-column (5 cm), three analytical columns (30 cm) all 5 μm particles and 0.8 cm in diameter, PSS, Germany) or a pair of SDV columns (pre-column (5 cm), a 10^3 Å and a 10^5 Å both 30 cm, all 5 μm particles and 0.8 cm in diameter, PSS, Germany). Detector and columns were kept at 35 °C using chloroform (stabilized with EtOH), with a flowrate of 1 mL/min and sample loading of 100 μL per run. The system was calibrated against narrowly dispersed polystyrene standards.

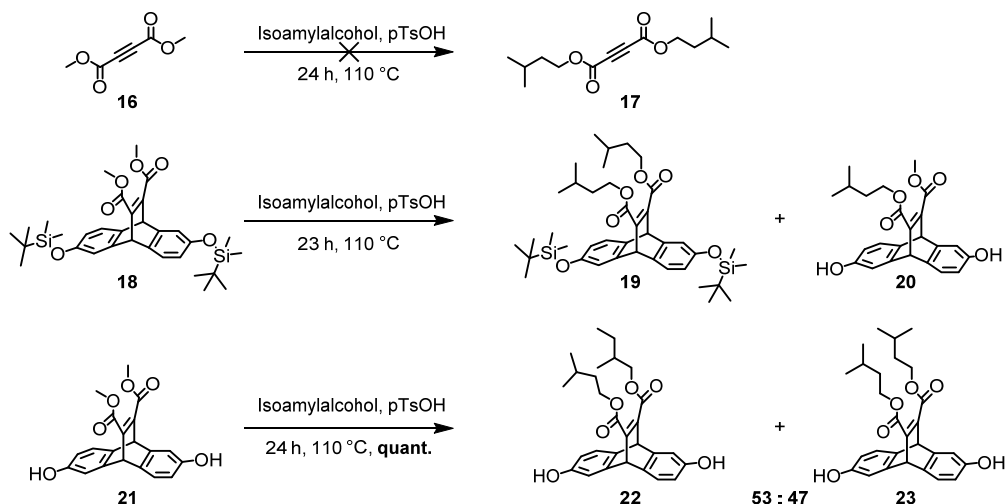
According to GPC analysis, the mass average molar mass (M_w) of the two enantiomeric polymers/oligomer **P1-F1** and **P1-F2** are both shorter than the racemic polymer **P1**. Polymerization with enantiomer **1-F1** eluting first on the chiral column showed almost no polymeric material (theoretical $M_w = 1.11 \cdot 10^3$ Da, 1.35 monomer units). The peak maximum is located at 7551 Da, which corresponds to an oligomer with 9 repeating units. Enantiomer **1-F2** gave a higher density of longer chains. The measured M_w equals $9.15 \cdot 10^3$ Da (11 repeating units). A high polydispersity of $D = 2.01$ was found with masses up to 40000 Da (48 units). The difference between **P1-F1** and **P1-F2** is likely not related to the chirality of the starting material. We speculate that the purity of the starting materials and the stoichiometry of the components is detrimental for the success of the polymerization. With the small amounts of starting material available for copolymerization these parameters were challenging to keep consistent. The M_w of the racemic polymer **P1** was determined to be $2.86 \cdot 10^4$ Da, which equals 34 repeating units. We observed diminished solubility for the formed

oligomers/copolymers. It appears that the short alkyl chains on the esters are only marginally suited to enable solubility which likely inhibits the polymer from growing to higher molecular weight. Furthermore, it makes purification and characterization of the obtained systems challenging.

The SWCNT dispersion ability of the longer copolymer **P1-F2** was investigated by the group of Professor M. Kappes at the Karlsruhe Institute of Technology (KIT). The copolymer did not show dispersion of SWCNT, likely on account of the short length of the polymer. Dispersion is mediated by cooperativity, which enables strong binding after reaching a threshold of units. Short copolymers provide less docking units and are therefore more likely to go back into solution rather than staying bound to the SWCNT. Additionally, the solubility of the final copolymer in common organic solvent is a concern. If the solubility of the polymer-SWCNT is too poor, the complex precipitates during centrifugation together with the SWCNTs. We therefore had to redesign the structure of the copolymer.

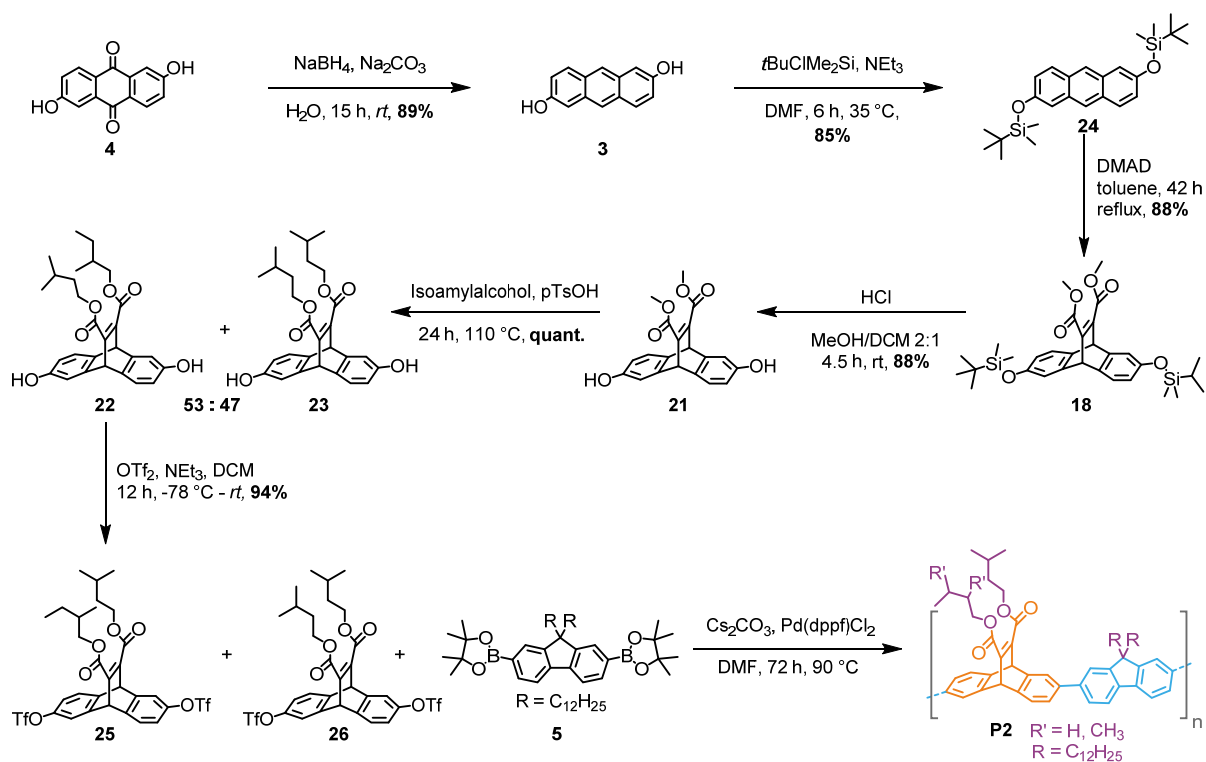
Synthesis of diisoamyl polymer P2

To improve the solubility of the polymer and with that hopefully increase the molecular weight of the individual polymers, the polymer was redesigned: we adapted the synthesis to have better variability of the ester moiety, which in turn allows to screen for a variety of solubilizing side chains.



Scheme 6. Transesterifications of the carboxyl groups at different stages of the synthetic route towards copolymer **P2**.

To enhance solubility by the incorporation of long alkyl chains, the ester moieties are particularly suited. Transesterification could, in principle, be performed at any stage of the assembly. Ideally however, it is tested as early as possible in the synthesis on less precious starting materials. Two particular points were desirable, either modification of the dienophile **16** or transesterification after the Diels-Alder step. It was found that transesterification of dimethyl acetylene-dicarboxylate (**16**) using isoamylalcohol as solvent led to decomposition (scheme 6). We therefore shifted to transesterification at the ethenoanthracene state. To encourage the anthracene derivative to undergo the DA-step, the free hydroxyl groups were protected with tert-butyldimethylsilyl, which are cleavable with strong bases or acids, the protected anthracene underwent good conversion to the desired ethenoanthracene derivative **18** in 88% yield (scheme 7). However, the subsequent transesterification lead to preferential cleavage of the protection group, with some observable traces of mono- transesterificated compound **20**. This result clearly hinted at performing the deprotection prior to transesterification.



Scheme 7. Synthesis of copolymer **P2**.

Acidic deprotection of the silyl protected hydroxyl groups was performed with HCl in a mixture of methanol and dichloromethane, as the starting material showed poor solubility in pure methanol. At room temperature, the two methylesters were stable towards the employed reaction conditions. Transesterification was realized by refluxing ethenoanthracene derivative **21** in freshly distilled isoamylalcohol. The conversion was quantitative yielding 47% to the desired di isopropyl ester derivative **23** in a mixture with an undesired unknown compound with the same molecular mass. Determination of the unknown compound (**22**, 53% yield) was possible by 2D NMR analysis directly on the mixture. Ultimately, the side-product was determined to be a rearranged isomer of the isoamyl sidechain of the target compound **23**. This (stereochemically) unselective rearrangement introduces a new chiral center in one alkyl chain leading to diastereomers which can be identified by NMR (figure 27). The ^1H NMR spectrum obtained from the mixture of enantiomer **23** and diastereomers **22** show resonances for the aryl protons (figure 27, marked orange) with nearly identical shifts, even though they are obtained from different compounds. Two additional, split resonances (purple) were observed, belonging to the protons directly next to the new chiral center. The additional stereocenter is however remote from the chiral backbone of the system and is unlikely to affect the chiral selectivity of the SWCNT dispersion. The chemical similarities of the species **23-RR** and **22-RRR/RRS** (**23-SS** and **22-SSS/SSR**, respectively) prevented separation of the constitutional isomers by column chromatography, crystallization or GPC and were consequently carried forward as mixtures (scheme 8).

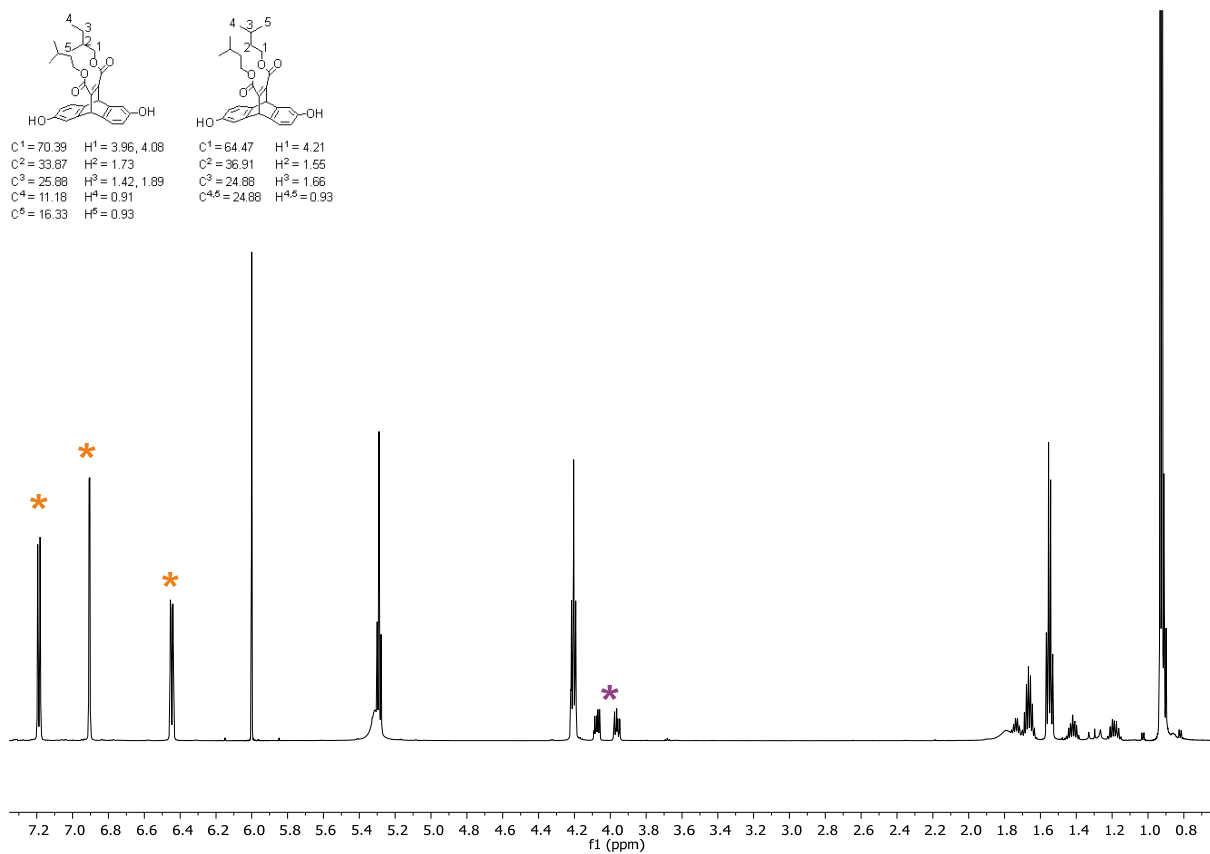
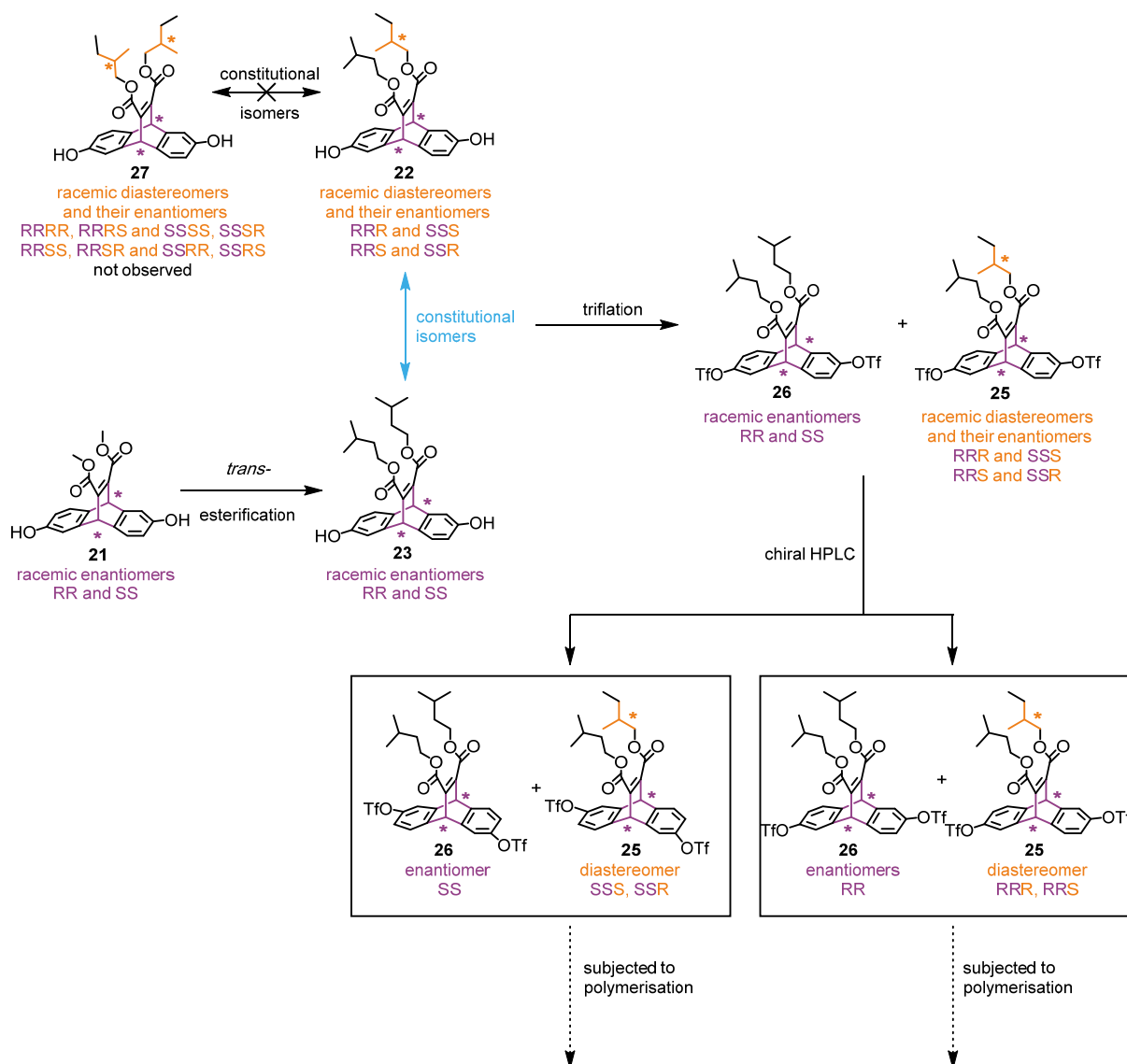


Figure 27. ¹H-NMR of the isolated mixture of isoamyl derivative **23** and its constitutional isomer **22**. The proton spectra was recorded in C₂D₂Cl₄, at 298 K, 600 MHz.

The longer sidechain did result in improved solubility in organic solvents as intended, allowing to substitute acetonitrile for CH₂Cl₂ as solvent in the triflation step. This allowed to use lower temperatures below the freezing point of acetonitrile (-78°C instead of -35°C) leading to an improved 94% yield.



Scheme 8. Overview of the formation of different isomers during transesterification and their possible separation after triflation

For the purpose of the following discussion, we define the enantiomeric isomers eluting first of the column E1 and the second E2. As E1/E2 can either contain the desired (**26**) or the rearranged chain (**25**), we label the undesired chain with (*). The first peak to elute from the column contains a mixture of E1 and E1* due to the short retention time. The second enantiomer elutes substantially later and can thus be partially resolved into E1 (fraction 2, figure **28** F2) and E2* (fraction 3, figure **28** F3). The separation did not lead to pure samples, but substantial enrichment of E2 was observed for fraction 2. Nevertheless, it was not possible even upon repeated injections and intense investigation in different solvent systems, to obtain pure fractions of E2. The resolution parameter of fraction 1 and 2 is $R_s = 8.57$ with a selectivity parameter of $\alpha = 3.67$.

CD spectroscopy of fractions 1 (containing E1/E1*) and 2 (containing E2>E2*) gave mirrored CD spectra, demonstrating the negligible influence of the additional chiral center on the overall chirality.

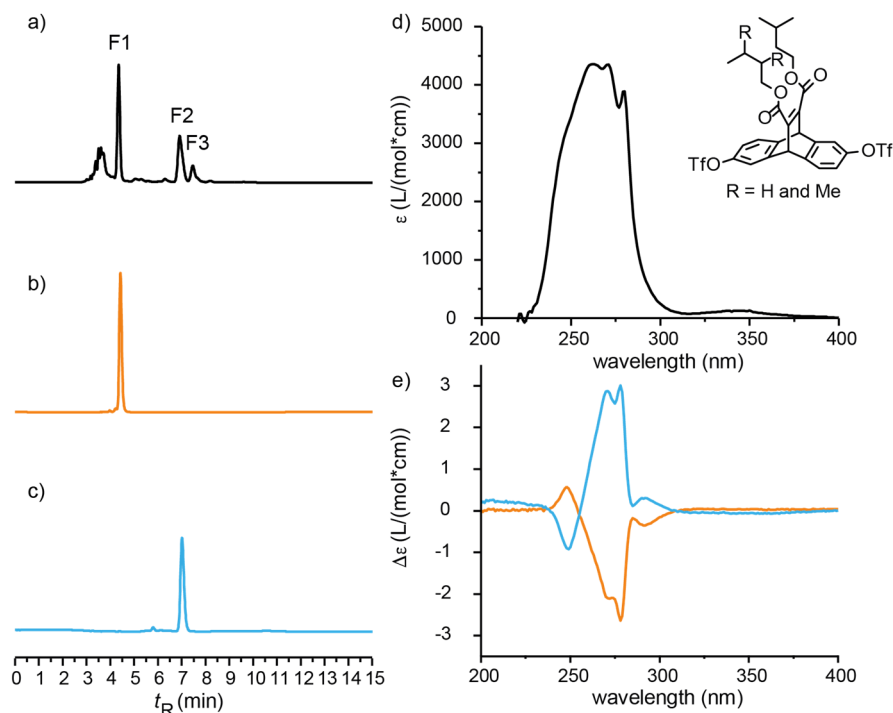


Figure 28. Chiral HPLC of ditriflate-ethenoanthracene **26/25**, (254 nm, 1 mL/min, 20:80 isopropanol:hexane, n_t) preparative separated enantiomers reinjected to the analytical HPLC under the same conditions a) crude (black, fraction 1 (F1, 52%), fraction 2 (F2, 38%), fraction 3 (F3, 10%) relative uv intensity), b) fraction 1 (orange) c) fraction 2 (blue) d) UV/vis spectrum of racemate **26/25** (black, THF, 1 cm cuvette, n_t), e) Cd spectra of the enantiomers **E1/E2** (THF, 1 cm cuvette, n_t) fraction 1 (orange) fraction 2 (blue).

Polymerization of enantiomeric derivative **26/25** (E2>E2*, fraction 2, figure **28**, (b)) was initiated under the same conditions as the methyl derivative **1** (Cs₂CO₃, Pd(dppf)Cl₂, DMF, 72 h, 90 °C). After completion, threefold precipitation from chloroform/hexane yielded three batches. Batch I after one precipitation cycle contained insoluble waste material. The third precipitation batch III (figure **29**, purple) included low molecular weight copolymers and oligomers according to GPC analysis. However, batch II (figure **29**, black) gave broad proton resonances in the expected area of chemical shifts as well as a Gaussian polymer distribution as indicated by ¹H NMR and GPC, respectively. The change to a longer solubilizing chain appears to positively influence the obtained polymer lengths - the mass average molar mass (M_w) of the second batch II was found to be 1.929 * 10⁴ Da, which is around 20 repeating units. The polydispersity is high (1.67) as expected for endcapped polymerizations, with a mass range of ~2300 (2.5 units) up to ~57000 (61 units). The dispersion quality of this copolymer towards SWCNTs is currently under investigation by the group of M. Kappes.

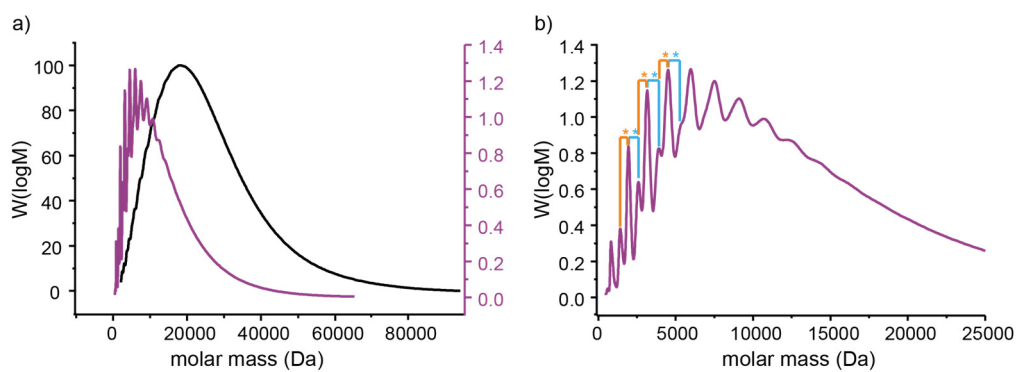
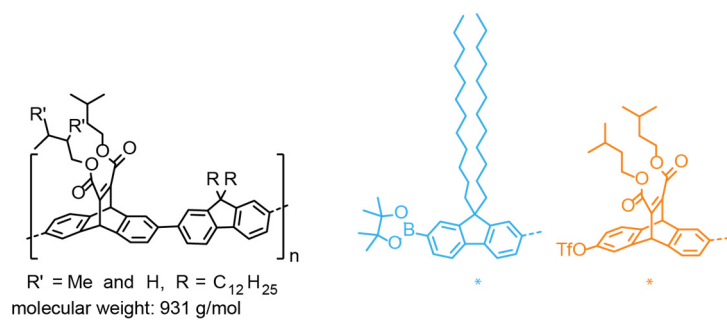


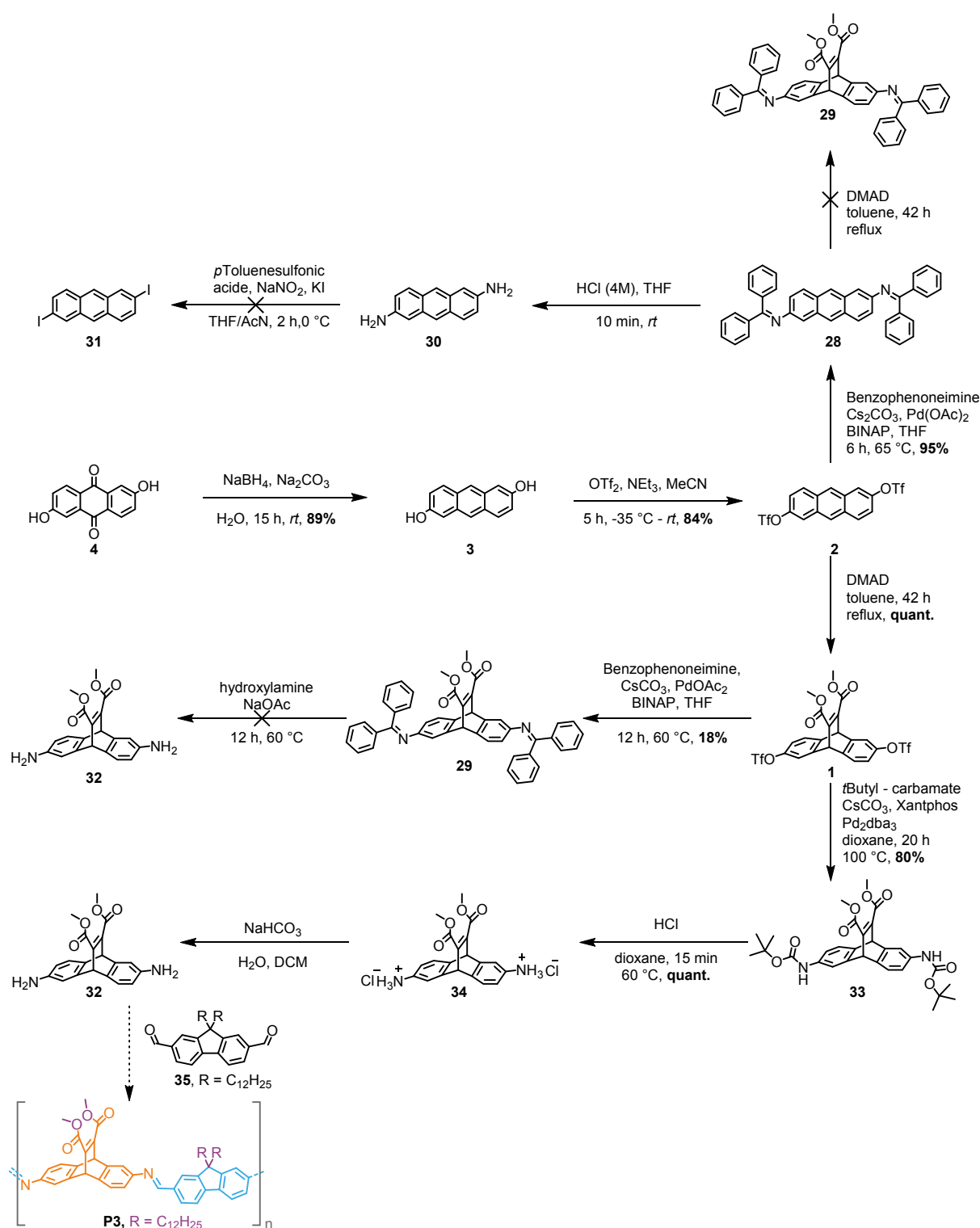
Figure 29. GPC traces of enantiomeric copolymer **P2 F2** synthesised from monomer unit **26/25** fraction 2 (E2>E2*) a) Two different length of the same enantiomeric polymer: batch II precipitate (black) batch III precipitate (purple), c) magnified of the low molecular batch III.

Synthesis towards imine linked polymer **P3**

So far, covalently linked polymers were investigated. While the rigidity of the linkages allows to subject the obtained polymers to an array of purification and characterization techniques, the initial estimate parameters such as chain-length or linker size is detrimental to the dispersion properties and selectivity of the polymer. In contrast stands a polymer that would self-assemble around a suitable tube. Not only would the polymer be formed into a thermodynamic minimum (good fit), the reversibility of the linkage would allow the polymer to overcome structural defects (self-healing). Another interesting feature would be release of the wrapping after the dispersion of the tubes by chemical cleavage of the linker, giving access to the properties of the “clean”, sorted SWCNT.

We envisaged a Schiff-base topology to interlink a diamine-ethenoanthracene monomer with a previously described bis-aldehyde fluorene linker. Schiff-bases are known to form by mild condensation of an amine with an aldehyde and cleavage under acidic conditions. Taking our modular building block **1** and formally substituting both triflates for amines and the diboronic esters of the fluorine linker for aldehydes gives the proposed target building blocks **32** and **35** (scheme 9).

Initially we envisaged to introduce a masked amine at the anthracene level, by a double Buchwald-Hartwig amination. The previously synthesized 2,6-bis(trifluoromethanesulfonate)-anthracene (**2**) was cross coupled twice with benzophenone imine with excellent 95% yield. However, no subsequent Diels-Alder product **29** with dimethyl acetylenedicarboxylate (**16**) was observed, probably on account of either the steric congestion of the diimine or the electronic change inflicted on the diene. Instead obtaining the desired Diels-Alder adduct, starting material was re-isolated accompanied by substantial amounts of decomposition. Consequently, it was decided to deprotect the amine prior to the Diels-Alder reaction. Treatment of **28** with acid in THF resulted in immediate precipitation of the highly unstable diamine **30**, which decomposed before the completion of full characterization. In principle, it would be possible to convert the diamine compound **30** into the diiodo derivative **31** *in situ* by a Sandmeyer-type reaction. The compound would be an interesting starting material for any cross coupling polymerization reactions. Unfortunately, procedures as described^[141] by Knochel *et al.* resulted exclusively in insoluble decomposition material. To circumvent the troublesome Diels-Alder reaction between **16** and diimine **28** we decided to perform the cycloaddition prior to the Buchwald-Hartwig reaction (quant.). The subsequent transformation of the triflate moiety to the corresponding imine **29** did proceed in poor 18% yield without observable liberation of the amine upon treatment with acid or base. Using a sterically less demanding Boc-protected amine, the transformation worked in considerable better yield (80%): Isolation of the corresponding chlorine salt **34** by precipitation was quantitative. The free amine derivative **32** was subsequently obtained by basic extraction.



Scheme 9. Synthesis of a diamine functionalized monomer **32** for a self-assembling polymer **P3**.

Screening of the enantiomeric resolution was performed after the C-N coupling with compound **33** and not with the free amine **32** (Chiralpak IA column, 250 x 4,6 mm 5 mic, 1 ml/min, 70/30 hexane:isopropanol, 25°C) giving resolution of the two enantiomers of $R_S = 2.996$ and a selectivity parameter of $\alpha = 1.383$. A better resolution of $R_S = 5.054$ was achieved with less percentage of isopropanol (80/20, hexane:isopropanol, $\alpha = 1.334$, figure **30**). Due to better separation of the corresponding enantiomers at the triflate state **1**

compared to the boc amide **32**, enantiomeric separation in preparative amounts were performed on compound **1** and the Buchwald-Hartwig type reaction was performed with the enantiomerically pure compounds. Copolymerization of the free amine **32** and the dialdehyde fluorene **35** and subsequent SWCNT dispersion is currently under investigation by M. Valasek at the KIT.

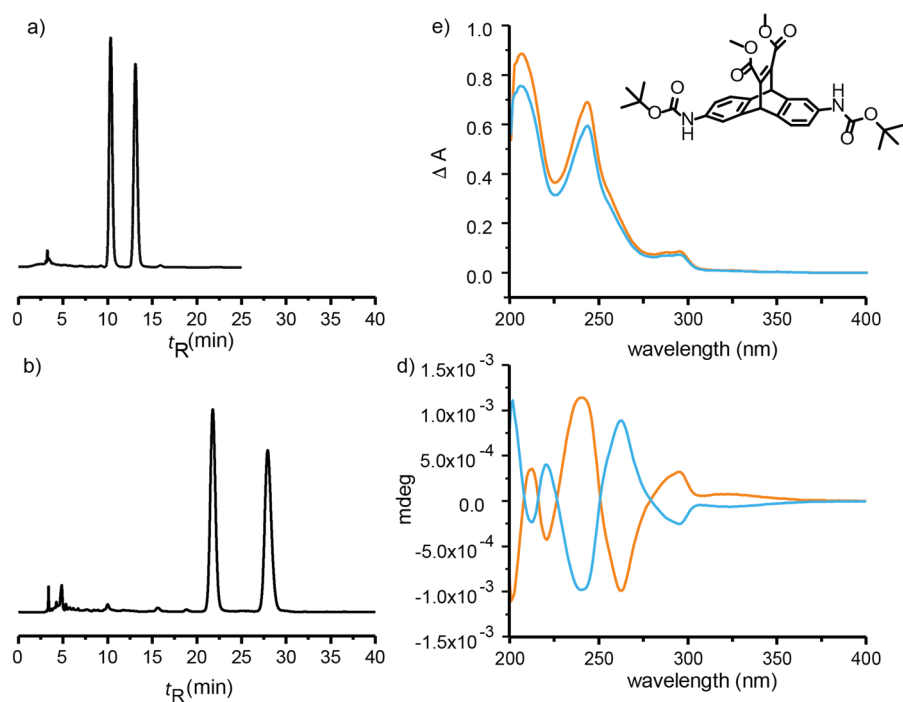
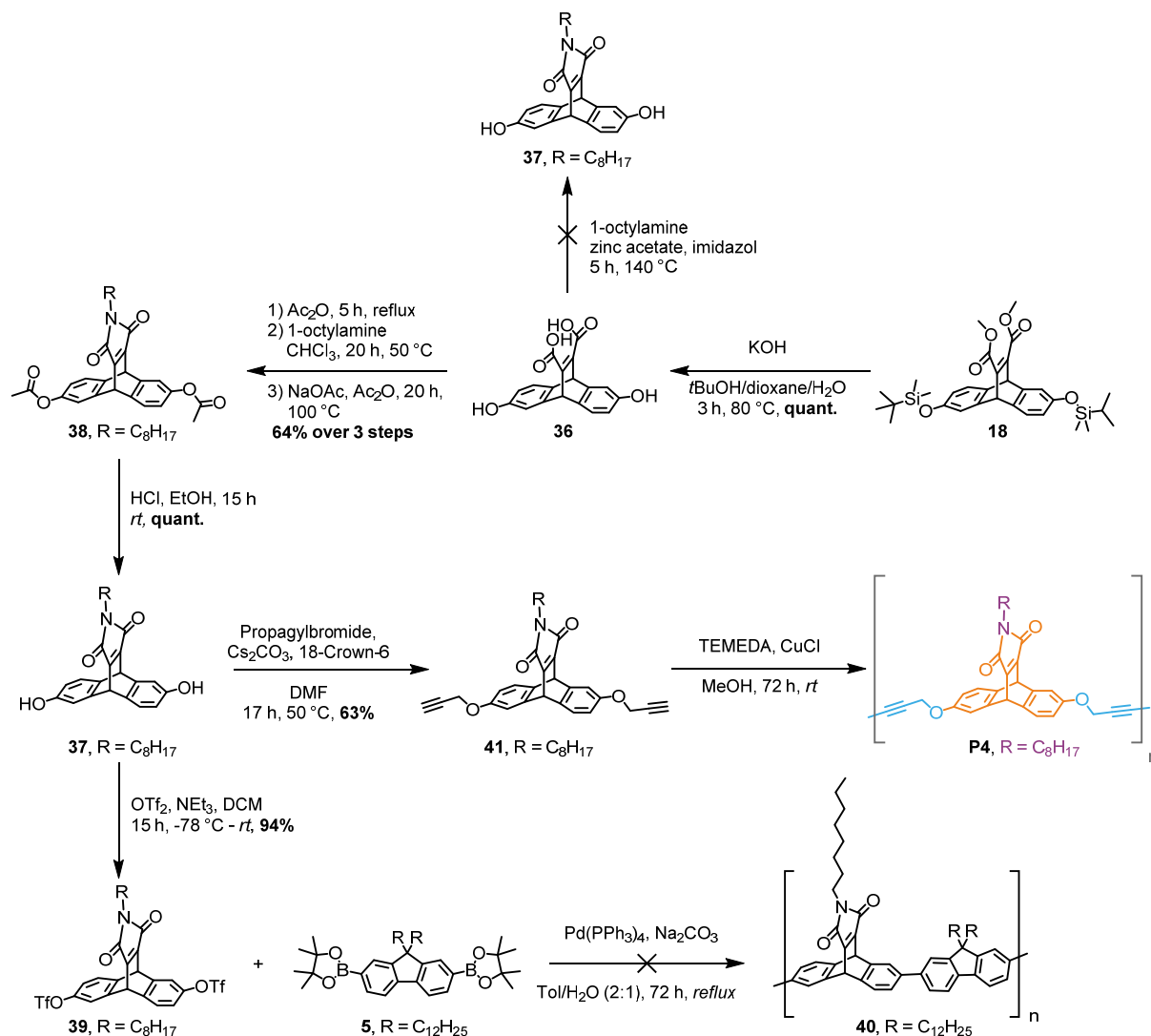


Figure 30. a) Chiral HPLC of diamide derivative **33**, (254 nm, 1 mL/min, 30:70 isopropanol:hexane, *rt*), b) Chiral HPLC of diamide derivative **33**, (254 nm, 1 mL/min, 20:80 isopropanol:hexane, *rt*). c) UV/vis spectrum of enantiomers **33-F1** and **33-F2** (20:80 isopropanol:hexane, 1 cm cuvette, *rt*). d) CD spectra of the enantiomers **33-F1** and **33-F2** (20:80 isopropanol:hexane, 1 cm cuvette, *rt*) fraction 1 (orange) fraction 2 (blue).

Synthesis of imide polymer P4

While it was found that longer alkyl chains have a dramatic effect on the resulting polymer length, sterical interference of the solubilizing chain eventually becomes a concern. We reasoned that a spatial control of the chain would allow us to employ longer chains and thus further increase the length of polymers. Structure **37** features an imide-based bridge. While the amount of present solubilizing chains is halved, the resulting chain originates perpendicularly to the polymer, which allows to use substantially longer alkyl groups. Imides are usually obtained by condensation of a diester with a variety of primary amines, which retains modularity of the building block.



Scheme 10. Synthesis of imide-based polymer P4.

The synthesis remained largely identical to isopropyl compound **26** up to the silyl protected ethenoanthracene **18**. Instead of treating this building block with acid to deprotect the phenols, treatment with aqueous base to hydrolyze the esters simultaneously with the deprotection of the phenols quantitatively gave diacid ethenoanthracene **36**. Unfortunately, heating diacid **36** in imidazole with octylamine and a zinc acetate as catalyst did not yield the desired imide derivative **37**. However, a stepwise introduction involving two subsequent hydrolysis steps (scheme 10) resulted in imide **38** in 64% (over three steps). Under the reaction

conditions the phenol groups were acylated as well, which could be liberated using hydrochloric acid in ethanol yielding the desired diphenol imide triptycene derivative **37** quantitatively. It is noteworthy, that reduction with DIBAL-H did not give **37**. The conversion of the alcohol to the triflate in the presence of the imide functionality was challenging. Various reaction conditions were screened (table 2). The use of the suitable base (NEt_3), temperature ($0 - 25\text{ }^\circ\text{C}$) under exclusion of water (dry solvent/bases) were crucial for the success of the reaction (table 2, entry 5).

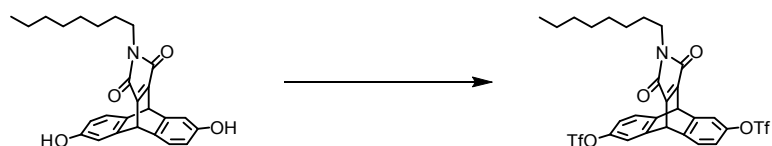


Table 2. Screening of triflation conditions

entry ^a	base / equiv.	solvent ^b	Δ [$^\circ\text{C}$]	reaction time	yield ^c
1	pyridine	pyridine	$0 - 25$	15 h	SM
2	pyridine / 10.0	THF	$0 - 25$	1 h	SM
3	Cs_2CO_3 / 2.4	DMF	$0 - 50$	5 h	decomposition
4	K_3PO_4 / 4.0	toluene/ H_2O	$0 - 25$	15 h	mostly SM
5	NEt_3 / 4.8	DCM	$-78 - 25$	15 h	94%

^aTrifluoromethanesulfonic anhydride (2.5 equiv.); ^b6 mL; ^c SM = starting material recovered

Analytical chiral separation of the enantiomers of the ditriflate derivative **39** was possible on a Chiralpak IA column ($250 \times 4,6\text{ mm}$, 5 mic). The column conditions used for the HPLC traces shown in figure 31, were: 30/70 isopropanol:hexane, 25°C , flowrate = 1 mL/min detection at 254 nm. The resolution parameter of the two enantiomers was obtained as $R_s = 3.01$ and a selectivity parameter of $\alpha = 1.67$. The parameters were unsuited to upscale the separation on a preparative system, (no baseline separation of the two enantiomers).

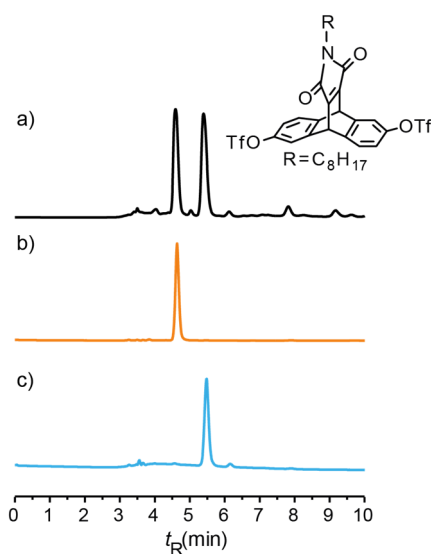


Figure 31. Chiral HPLC traces of ditriflate imide derivative **39**, (254 nm, 1 mL/min, 30:70 isopropanol:hexane, *rt*). a) Crude mixture (black) b) reinjected fraction 1 (orange), c) reinjected fraction 2.

We decided to attempt the chiral resolution at the stage of the dihydroxy imide compound **37**, due to observation that the hydroxyl group seemed to enhance the chiral resolution. Racemization of enantiomer **37** would proceed through an unlikely *retro* Diels – Alder and subsequent Diels – Alder reaction, and we reasoned that it would be possible to triflate after chiral resolution.

The two enantiomers of diphenol derivative **37** were resolved by chiral HPLC (figure 32). To test separation conditions an analytical Chiralpak IA, column (250 x 4,6 mm, 5 mic) was used and later successfully upscaled to a preparative Chiralpak IA column (250 x 30 mm, 5 mic). The resolution of the two enantiomer was substantially improved in comparison to triflate **39**, ($R_s = 7.74$ vs $R_s = 3.01$). The selectivity parameter was found to be $\alpha = 2.64$. The preparative column could be loaded with 200 mg of racemate **37**, still giving baseline separation of the two enantiomers. The limiting factor was the solubility of the monomer unit **37** in the mobile phase (~100 mg/ml). On a side note, the ditriflate enantiomer **39** derived from dihydroxyl enantiomer **37-F1** elutes second from the chiral column, while its parent structure elutes first.

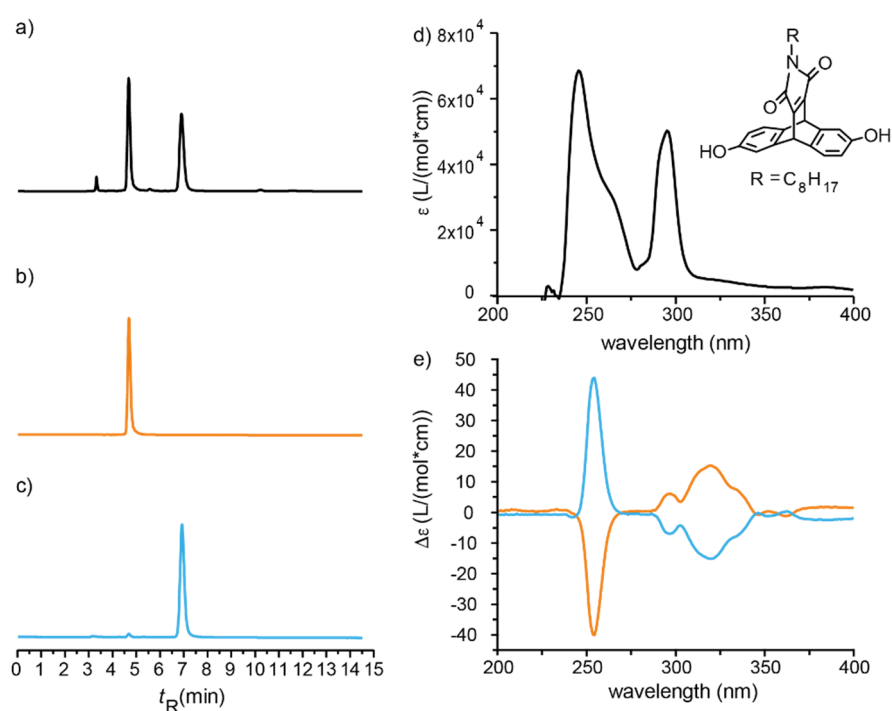


Figure 32. Chiral HPLC traces of di hydroxy imide ethenoanthracene derivative **37**, (254 nm, 1 mL/min, 30:70 isopropanol:hexane, *n*); a) crude (black), preparative separated enantiomers reinjected to the analytical HPLC under the same conditions b) fraction 1 (orange) c) fraction 2 (blue) d) UV/vis spectrum of racemate **37** (black, THF, 1 cm cuvette, *n*); e) CD spectra of the enantiomers **37-F1** and **37-F2** (THF, 1 cm cuvette, *n*). fraction 1 (orange) fraction 2 (blue).

To instigate polymerization, chiral imide ethenoanthracenes **39** were subjected to Suzuki conditions ($\text{Pd}(\text{PPH}_3)_4$ as catalyst, Na_2CO_3 as base, reflux 2:1, water/toluene). After three days of reflux, 65% of bispinacolatoboron **5** was recovered along with some poorly soluble material without any resonances similar to a bridged ethenoanthracene proton. Therefore we decided to test the stability of the ditriflate derivative **39** in aqueous solution. A sample was dissolved in deuterated chloroform with deuterated water, an excess of sodium carbonate was added and heated to 50 °C for 3 days while incrementally monitoring by ^1H NMR spectroscopy. The compound was found to be stable for about 1h under the used conditions, but decomposed

afterwards (figure 33). If decomposition is occurring as low as 50 °C, it stands to reason that continuous refluxing will similarly result in decomposition, which explains the poor conversion in the reaction.

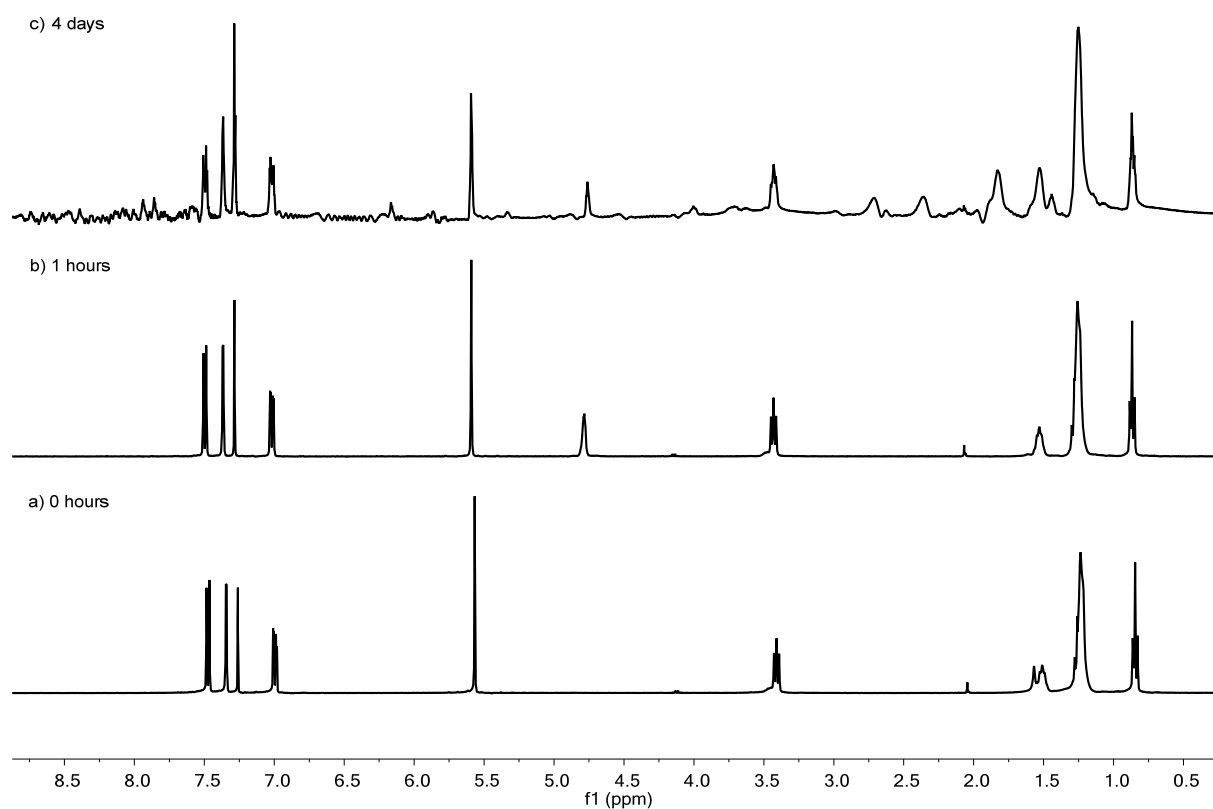
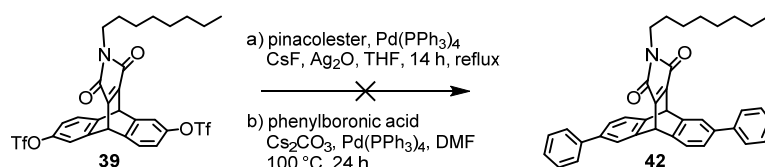


Figure 33. Stability test of ditriflate **39** by ^1H – NMR. a) Measured in CDCl_3 ; b) after heating for 1 h at 50 °C and addition of Na_2CO_3 D_2O ; c) after heating for 4 days under the same conditions.

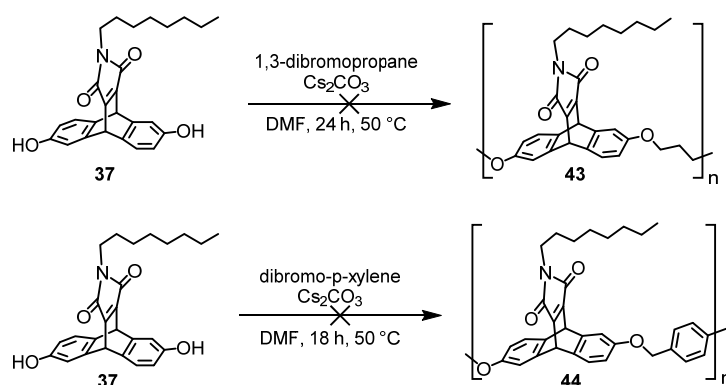
The conditions which were suited for Suzuki-polymerization of the dimethyl ester derivative **1** did equally fail, even when substituting water for dry DMF, $\text{Pd}(\text{PPh}_3)_4$ for $\text{Pd}(\text{dppf})\text{Cl}_2$, and using dried cesium carbonate as base. Even using either monofunctionalized pinacolester or –acid, respectively, (figure 11) resulted in either detriflation of the starting material or decomposition.



Scheme 11. Coupling attempts of imide **39** with either phenyl boronic ester or -acid.

Considering the instability of the triflate **39** under polymerization conditions, we reasoned that we could employ $\text{S}_{\text{N}}2$ reactions to instigate polymerization starting from dihydroxy derivative **37**. The rationale was that we would not only circumvent the troublesome stability of the triflates but also investigate a flexible linker motif. Adsorption to the tube would be driven exclusively from the interaction of the ethenoanthracene with the tube. As a starting point, we envisaged to use dibromopropane as linker, that would react with dihydroxy derivative **37** to form an alkyl-linked polymer **43**. Over the course of the reaction traces of pentamer(s) were

be observed by MALDI-ToF even though the trimeric adduct was prominent (figure 34). After workup however, only decomposition material was obtained. A similar observation was made when using dibromo-*p*-xylene as linker.



Scheme 12. Attempts at S_N2 -initiated polymerization.

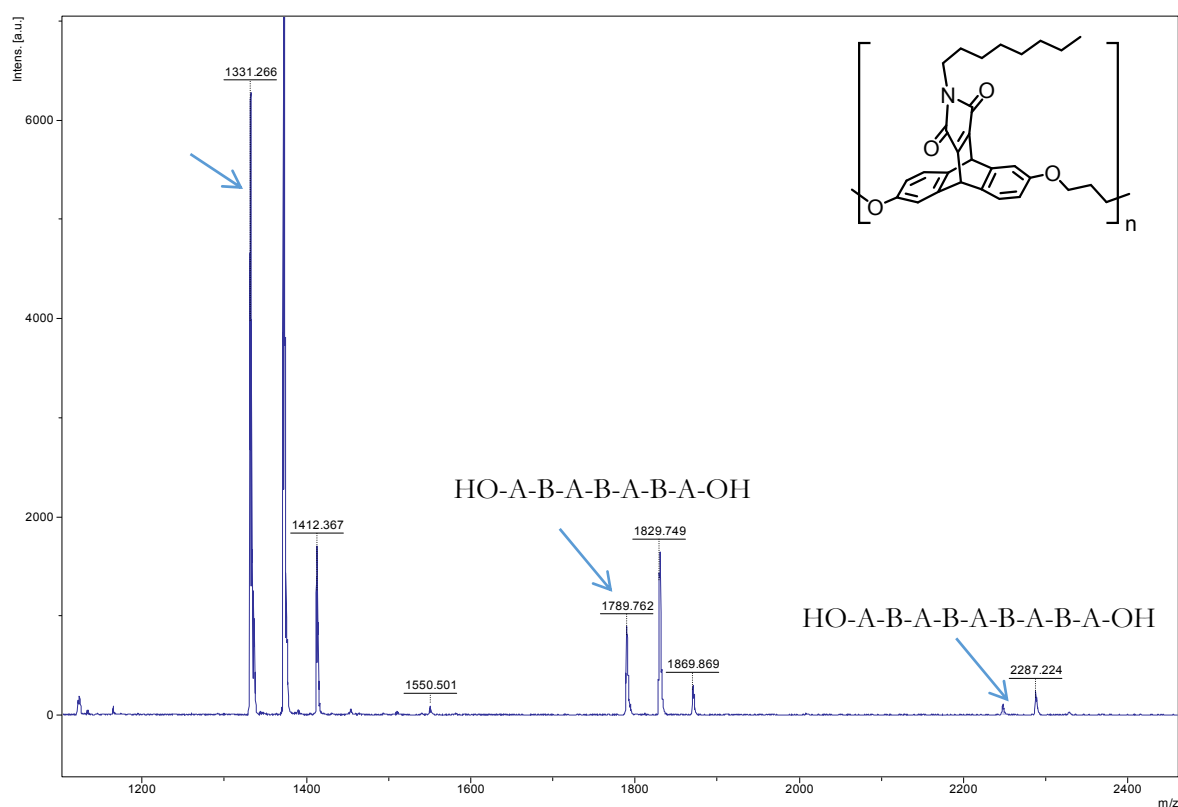


Figure 34 Reaction control by MALDI-ToF of S_N2 copolymerisation **43** (dihydroxy derivative **37** and 1,3 dibromo propane)

Having attempted a variety of conditions to initiate polymerizations (Suzuki, S_N2) we began investigating milder protocols. In particular Glaser-Hay conditions were appealing, as they require neither high temperatures nor the presence of water. Glaser-Hay couplings require the presence of free acetylenes, which we introduced directly at the hydroxyl terminus by a mild S_N2 reaction with propargylbromide (Cs_2CO_3 as base, 18-Crown-6, in DMF, 17 h, 50 °C, 63%). The obtained bis-acetylene **41** was then subjected to Glaser-Hay polymerization conditions (TEMEDA, CuCl, MeOH, 72 h, *rt*).

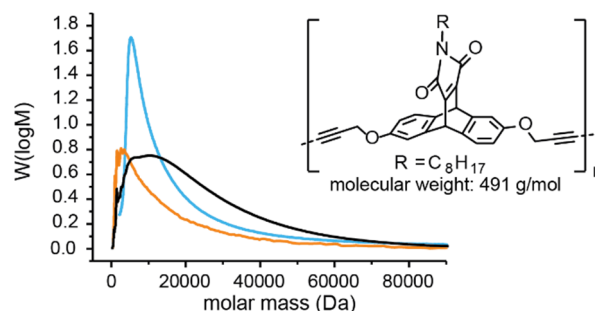
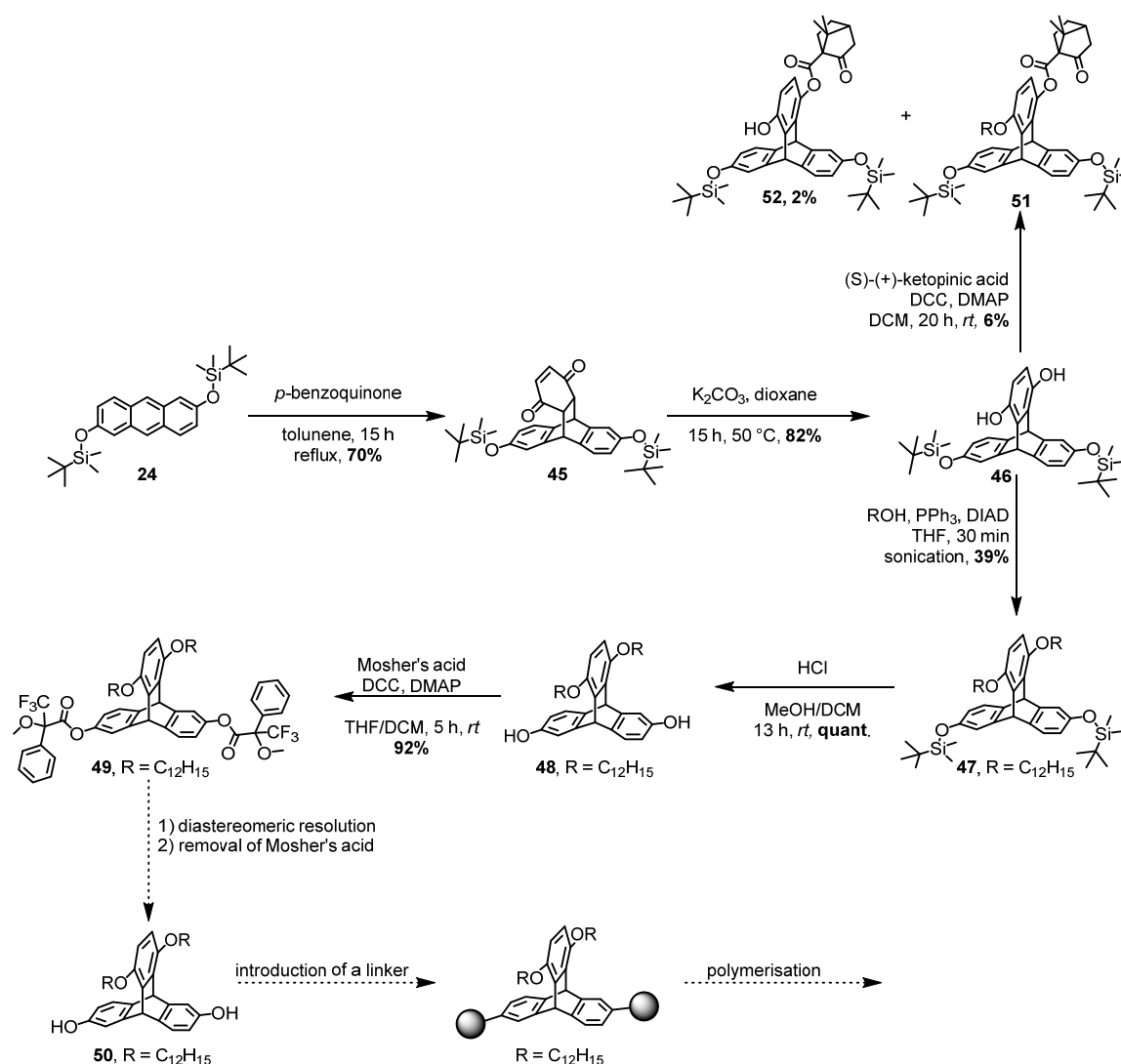


Figure 35. GPC analysis of the two enantiomeric polymers **P4-F1** and **P4-F2** deriving from monomer **41** fraction 1 (orange); synthesized from monomer **41** fraction 2 (blue) and the racemic equivalent **P4** (black) obtained by Glaser-Hay coupling reaction

The polymer derived from the racemic starting material **41** showed pronounced polydispersity ($D = 4.25$, $M_w = 1.11 \times 10^4$ Da, 23 repeating units, figure 35, black). GPC analysis of the polymerization of the enantiomer **P4-F1** gave an oligomer with M_w of 6.40×10^3 Da which corresponds to approximately 13 repeating units (figure 35, orange). The observed polydispersity was high with a value of 3.37 mostly as oligomers. As preparative GPC purification was carried out prior to characterization for the 2nd enantiomer **P4-F2**, a narrower polydispersity (1.67) was observed but with higher M_w (1.10×10^4 Da, 22 repeating units). Selective dispersion ability of the polymer **P4-F2** and oligomer **P4-F1** towards SWCNTs was tested at KIT by the group of Professor M. Kappes. Neither dispersed SWCNT to an observable extend under initial conditions. Coupled with the short overall length of the polymer/oligomer, it is especially the poor overall yield (40 – 60 mg) that makes the screening of suitable dispersion protocols challenging.

Synthesis towards triptycene derivative polymer

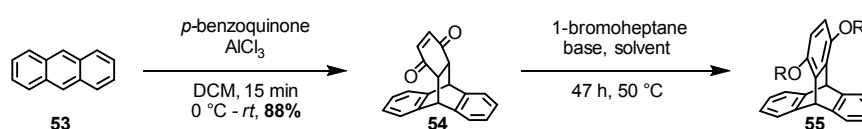
The bottleneck of the synthesis of any polymers presented herein is the requirement for chiral resolution by HPLC. To maintain efficient separation, the injection volume is typically limited to below 100 mg per run. We were therefore interested in transforming the enantiomeric separation into a diastereomeric resolution. Especially crystallization techniques after chiral functionalization with an enantiomerically pure moiety were appealing. At the same time, we desired a compound stable towards higher temperatures needed for efficient crystallization in our context translating to inhibition of the *retro* Diels – Alder reaction. For these purposes, we designed a triptycene moiety with two hydroxyl moieties in *para* positions of an aromatic upper ring. Said aromatic system should prevent the *retro* Diels – Alder reaction and, in comparison to the ester groups, the solubilizing ether groups should point further away from the binding cavity.



Scheme 13. Synthesis of diastereomeric monomer units for resolution trials.

To assemble the triptycene unit we intended to perform a Diels – Alder reaction with commercially available *para*-benzoquinone and an anthracene derivative and then aromatize the upper ring. The cyclisation reaction did not proceed with the free 2,6-dihydroxy anthracene (**3**) and *para*-benzoquinone. Even after addition of aluminum chloride as Lewis acid catalyst, only insoluble decomposition material was observed. Hence, our

already synthesized silyl protected anthracene derivative **24** together with the *para*-benzoquinone was successfully subjected to Diels – Alder reaction (reflux in toluene, 70%, scheme **13**). To improve the yield of 70%, two attempts were done; either to elevate the reaction temperature by changing toluene to *para*-xylene or to introduce aluminum chloride as known catalyst for Diels – Alder reactions. The catalyst prevented the reaction completely and the higher reaction temperature did neither accelerate the reaction duration nor raised the yield. Therefore it was proceeded with toluene and a reaction yield of 70%. The formed compound **45** was isolated as a diastereomeric product as the Diels – Alder reaction induced four new stereogenic centers, by which two are lost again after the aromatization of the upper ring. The introduction of the solubilizing alkyl chains and the aromatization of the upper ring, was planned to be the next step. As the introduction of the alkyl chains were challenging, a less functionalized test system **54** (scheme **14**) was used to figure out suitable reaction conditions. The aromatization and alkylation was realized in one step at the test system **54**. Different solvents and bases were investigated: acetonitrile with potassium carbonate and dimethyl formamide with either potassium carbonate, sodium *tert*-butoxide, or sodium hydride was tried out. The combination of the strong polar aprotic solvent DMF and potassium carbonate as a base yielded the highest results with 96%.



Scheme 14. Test system for the introduction of the alky chains and aromatizing the upper ring.

For the target compound **47** it did not work in one step, using potassium carbonate as base and the corresponding bromo alkyne did not give the desired enolate formation and S_N2 reaction but to the aromatization of the upper ring. Therefore we followed a two steps reaction mechanism where we first aromatized the system, with a yield of 82% and coupled the alkyne chain with a Mitsunobu reaction (39%). The deprotection of the silyl groups gave quantitatively the desired triptycene moiety **48**. To ensure and confirm the chirality of the compound chiral chromatography was performed and cd spectra measured (figure **36**).

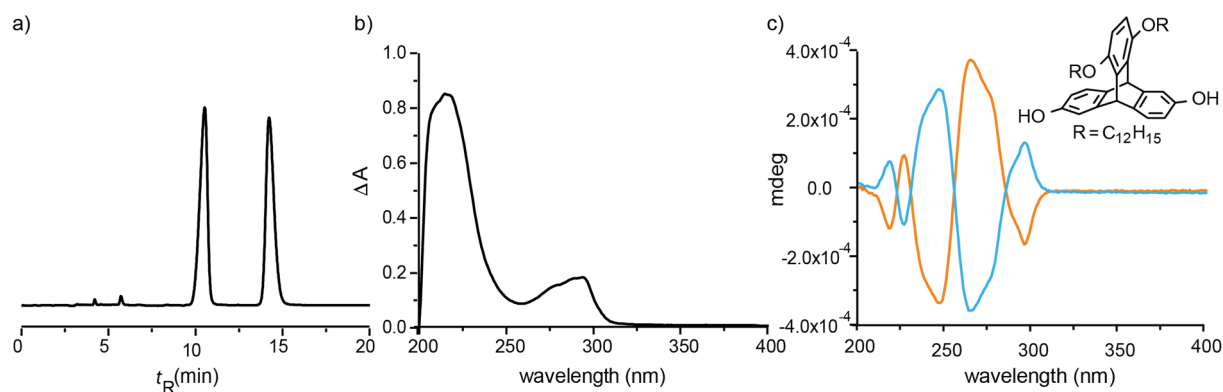
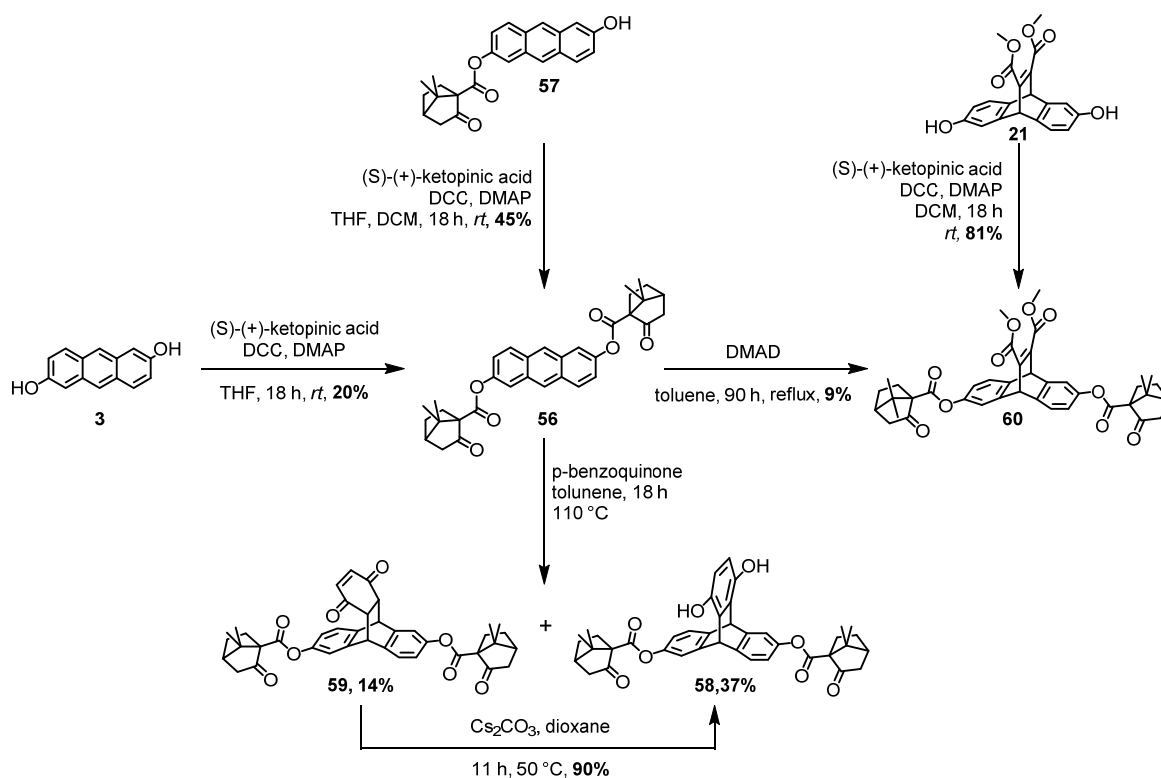


Figure 36. a) HPLC trace of compound **48**, (254 nm, 1 mL/mi, 12:88 isopropanol:hexane, *rt*) with $R_S=4.28$ and $a=1.633$. b) UV spectrum of racemate **48** (12:88 isopropanol:hexane, 1 cm cuvette, *rt*). c) CD spectra of enantiomers **48-F1** and **48-F2** (12:88 isopropanol:hexane, 1 cm cuvette, *rt*) fraction 1 (orange) fraction 2 (blue)

To instigate diastereomeric resolution, Mosher's acid was introduced at the two phenol moieties via Steglich – esterification conditions. The diastereomers showed the same retention times on silica and were obtained as colorless, oily compounds, which could not be solidified by precipitation/slow diffusion, preventing diastereomeric resolution. A possible reason is the long alkyl chains introduced in the upper ring.

To help the diastereomeric resolution and support crystallization, the idea was to introduce the additional enantiomerically pure chiral center (and therefore the formation of diastereomers) before the alkylation of the compound. The goal was to assemble this new chiral center closer to the two chiral centers of the triptycene moiety to have a more pronounced impact. As keptopic acid is known for diastereomeric resolution and substantially cheaper than Mosher's acid we decided to introduce the keptopic acid on the upper diphenol moiety of compound **46**. However, with Steglich – esterification only 6% of the desired compound **51** was formed, as a side product we could isolate 2% of the mono ester product **52** and a mixture of starting material and decomposition. Subsequent upscaling failed forcing us to abandon this approach.

Instead of silyl protection on the 2,6 – dihydroxy anthracene the keptopic acid was assembled already at the protection step of 2,6 – dihydroxy anthracene (**3**) to give di-ester **56** as an enantiomerically pure white crystalline compound (scheme 15). The product was only formed in 20% but the mono functionalized **57** could also be isolated in 38% and converted into the desired di – ester product **56** in 45%. Purification of this di-ester was troublesome in the beginning. On usual column chromatography hydrolysis of an ester moiety occurred as it can be seen on the 2D TLC (figure 37).



Scheme 15. Synthesis towards diastereomeric unit for resolution trials.

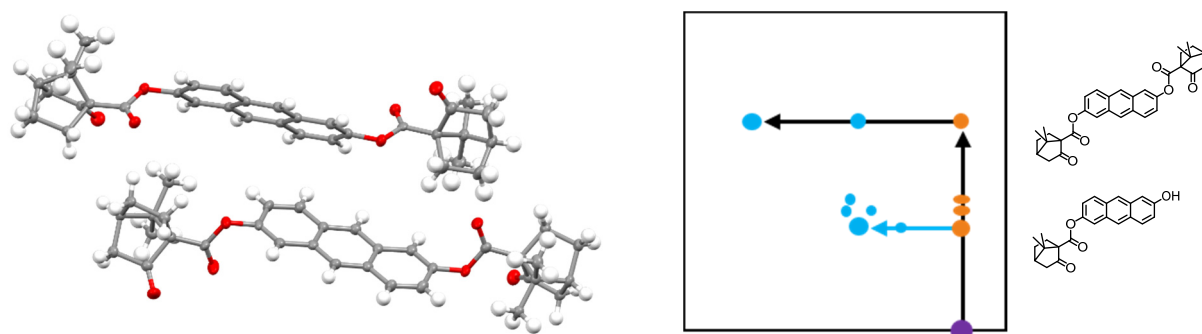


Figure 37. Crystal structure of enantiomerically pure compound **56** on the left and 2D TLC stability analysis of compound **56** in 1:10 ethylacetate:toluene on the right

Recrystallization in hexane, toluene or ethyl acetate did not lead to a clean fraction. Furthermore, solubility of the compound was marginal in dichloromethane, excluding GPC as means for purification. Purification was ultimately possible by iterative column chromatography on a Biotage Isolera ACI system and subsequent recrystallization in ethyl acetate. Additionally, the mono functionalized compound **57** could be isolated and converted to the desired compound. The Diels – Alder reaction with *para*-benzoquinone and the sterically demanding anthracene derivative **56** yielded 37% of the directly aromatized triptycene derivative **58**. Only 14% of the diastereomeric Diels – Alder product **59** was formed which could be converted into the desired target **58** by heating in solution of potassium carbonate in dioxane at 50 °C. The obtained diastereomers of compound **58** did not show different retention times on silica nor crystallized differently in any of the array of solvent mixtures tried.

Due to the lack of diastereomeric resolution of the diastereomers **58** we decided to change the monomer structure back to the di – ester ethenoanthracene moiety, instead of the triptycene. The first intention to form the diastereomers **60** was the Diels – Alder reaction with keptopic protected anthracene derivative **56** and dimethyl acetylenedicarboxylate (**16**). The product was formed in poor 9% yield, most likely due to low solubility and steric hindrance. Therefore we decided to perform the Diels – Alder reaction prior to the introduction of the new chiral center. The already synthesized di-phenol di-ester derivative **21** was used as starting material for a Steglich– esterification and the keptopic acid was successfully introduced improving the yield to 81 %. The product **60** was isolated as a white crystalline product. On reversed phase and normal phase column chromatography the diastereomers did not show any separation. Recrystallization in dichloromethane and methanol and hexane did lead to diastereomeric crystals as shown by the crystal structure of compound **60** (figure **38**).

The diastereomeric packing seems to be favorable compared to the enantiomeric pure one. It seems that the diastereomeric resolution by introducing an additional “chiral center” like keptopic or Mosher’s acid to our bridged racemic structures is not enough for effective diastereomeric separation.

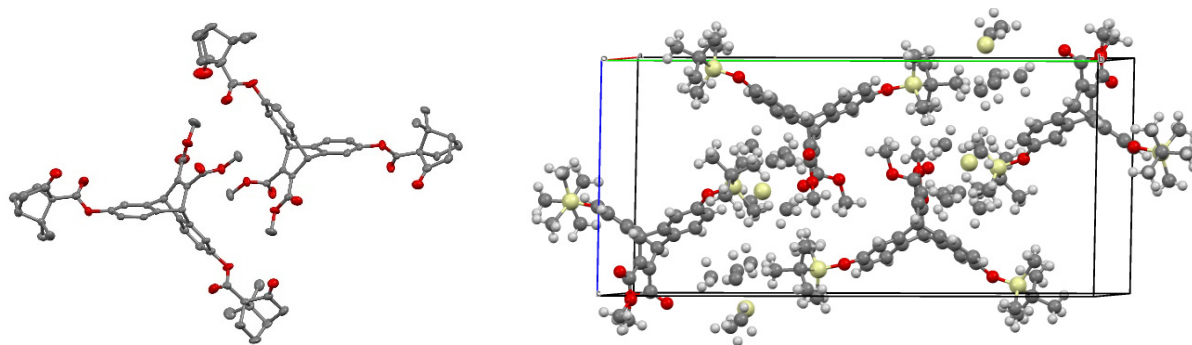


Figure 38. Crystal structure of diastereomeric triptycene derivative **60**

Conclusion

Carbon exists in a multitude of allotropes. Amongst those, single walled carbon nanotubes (SWCNT) are attractive targets on account of their tensile strength, their topology, and the broad range of electronic properties. Besides considerable efforts, the synthesis of SWCNTs still largely results in polydisperse mixtures with a broad range of diameters, chiralities and lengths. Consequently, research is invested in the development of efficient purification techniques such as density gradient ultracentrifugation, two phase extractions, Gel and size exclusion chromatography. Amongst those, dispersion techniques hold great appeal. Not only could they selectively target a specific type of tube (diameter, chirality) but they enable the subsequent study and transformation of the originally insoluble tube in solution. Encouraging progress has been made over the last decade but to date, the dispersion of nanotubes still results in poor overall yield.

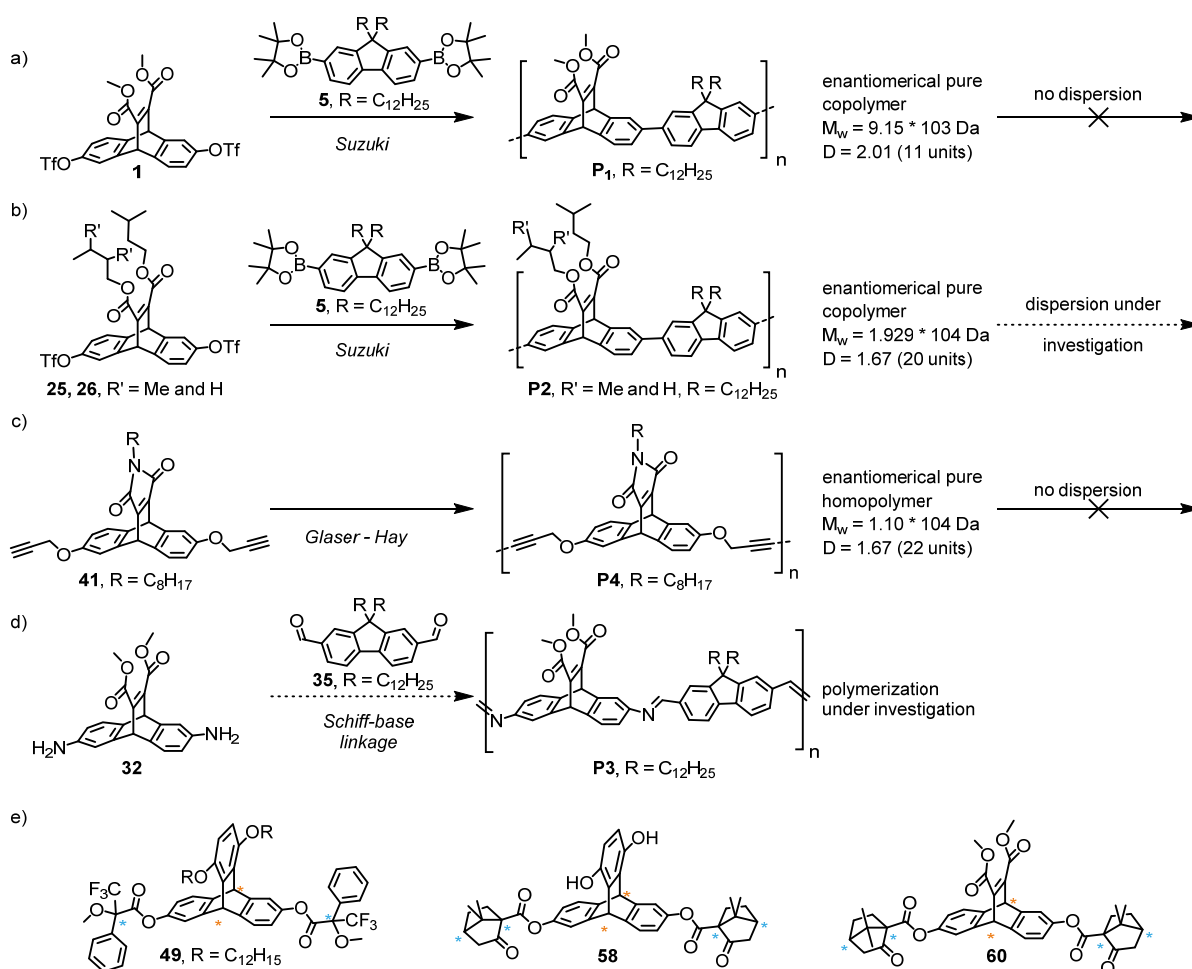
The scope of this thesis was to develop an ethenoanthracene-based chiral copolymer to disperse chiral nanotubes. The thesis describes the successful synthesis of a variety of soluble ethenoanthracene derivatives, their chiral resolution and polymerization. Dispersion of SWCNT by the formed polymers was then studied by the group of Prof. Dr. M. Kappes at the Karlsruhe Institute of Technology (KIT, Germany).

From suitably functionalized anthracene derivatives, three ethenoanthracene-types were realized (scheme **16**, a, b and c), either bearing dimethylester **1**, dialkylester **25/26** or imide **41** functionalized bridge. All three allow to modulate solubility by the choice of solubilizing (alkyl)-chain, for the ester and imide based systems even post-assembly. They differ in their strategic use. The ester moiety was selected for its synthetic availability and robustness under the required subsequent chemical transformations. The parent dimethyl acetylenedicarboxylate (**16**) is known to undergo efficient Diels-Alder cycloadditions and thus an ideal synthetic target to explore the chemistry towards the desired copolymers. The imide system **41** moves the solubilizing chain out of proximity to the binding site into a perpendicular position resulting in a sterically less congested system that should increase the required π - π interaction with the SWCNT thus show increased dispersion qualities. For both ester systems, retro-DA under elevated temperatures could potentially release a dispersed tube. However, it constrains the synthesis of the building blocks to lower temperatures. We thus complemented the series by a triptycene based system (scheme **16**, e). Retro-DA would require to break aromaticity, which is thermodynamically unfavored.

Besides the ethenoanthracene derivatives, considerable effort was dedicated to the development of suitable linker topologies. Three types were described: aryl-aryl and Schiff-base-linked fluorenes, as well as butadiynes. Fluorenes are known to undergo efficient polymerization and have been used as main unit in SWCNT dispersing polymers. The sp^3 -center allows to install additional side-chains, while the backbone provides rigidity. Suitable functionalization allows the formation of a labile linkage between ethenoanthracene **32** and fluorine **35** (Schiff-base) giving potential self-assembly and -healing properties as well as SWCNT release after dispersion. A concern for the fluorine-based linking approach was the interference of the linker when dispersing. Glaser-Hay homo-coupling of propargyl ethers gave a butadiyne based topology with reduced strain to maximize the π - π interactions. Because the required acetylene were directly installed on the monomer

41, the polymer could be realized through homo-polymerization, with the profound advantage that the degree of polymerization is not depending on an exact 1:1 ratio of the monomer units.

Of the library of synthesized compounds, the following were selected for polymerization both from their respective enantiomers and racemate:



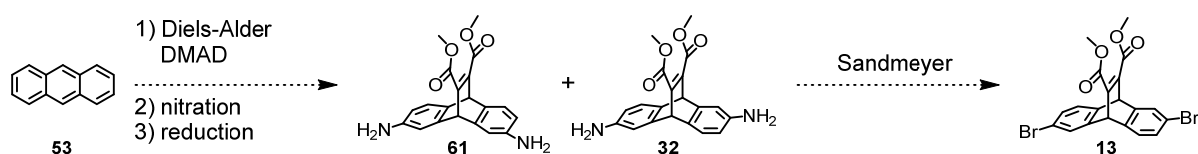
Scheme 16. Summary of synthesized monomers, copolymers and observed dispersions.

Two key factors have limited the amount of obtained polymers. Availability of the enantiomerically pure starting materials and efficiency of polymerization. Enantiomeric resolution relied largely on chiral HPLC, which limited the throughput substantially. Crystallization was considered as a potential bypass to HPLC. Diastereomeric resolution by derivatization of a racemic mixture of suitably functionalized monomers by Mosher's acid or keptopic acid either lead to the formation of racemic crystals or amorphous material, eventually forcing to return to resolution by chiral HPLC. Besides the availability of the building blocks, it is polymerization itself that was found to be challenging. Either the employed conditions were found to mediate each coupling inefficiently – for polymerization, even a yield of 90% per coupling will result in early chain termination. This is in particular true for the Suzuki-based methodologies. Switching to highly efficient Glaser-Hay coupling was atom-efficient and found to yield longer polymers with well-behaved purification ability of the resulting polymer.

Despite the small amounts of each polymer, initial dispersion of SWCNT was performed with copolymers **P1** and **P4** (**P2** and **P3** are still under investigation). To date, only marginal dispersion was observed. Because of the limited amounts available, the trials were restricted to a very small number, preventing extensive screening of conditions. Additionally, the dispersed SWCNT are challenging to detect and investigate. On the employed scale, it is therefore difficult to draw firm conclusions and adopt the molecular design accordingly.

Outlook

The key issues to address are the amount of available chiral material and the lengths and the solubility of the polymer. Considering literature, the length of the used conjugated polymer can have dramatic effects on dispersion ability and selectivity. Under the employed Suzuki-conditions, the chain length is mainly determined by defunctionalization of the monomer unit, deactivation of the catalyst, uncertainties in the molar ratios of the reaction partners and decreasing solubility of the growing polymers. The modularity of the molecular design allows to address these issues on multiple levels. Solubility can be enhanced by even longer, branched sidechains the isoamyl/octyl chains used so far. Additionally, this might even allow to completely change the solubility to polar or aqueous media, which in turn might be used to drive dispersion. Optimization of the Suzuki conditions is another handle to improve chain length. Exchanging the used triflates to a less reactive bromine, might give a better rate match to the slow transmetalation step and slow down the chain-terminating dehalogenation. A suitable dibrominated triptycene derivative **13** can be accessed from the corresponding diamine by Sandmeyer reaction which in turns is accessed by nitration and reduction (scheme 17). Formation of two regioisomers **61** and **32** are expected for the nitration which can be separated by diastereo selective gelation (recently published by Schneebeli and co-workers^[142] 99 % *ee* in gram scale).^[143,144] This approach would give access to the diamine derivative **32** in larger quantities and allows to explore the Schiff-base linked polymer. The conclusions of linker and side-chain design are valid here as well.



Scheme 17. Projected synthesis towards dibromo ethenoanthracene **13**.

Additionally, diastereomeric resolution by crystallization is still an attractive methodology to obtain large amounts of enantiomerically pure material. It is likely that the differences in the diastereomers are more pronounced if the chiral centers of the bridge and the additive (Moshers acid, keptoic acid) are brought closer together. In this context, modification of the diester moiety instead of the anthracene could be beneficial.

The Glaser-Hay coupling of the monomer holds great appeal, as it is a very atom efficient approach and known to yield polymers efficiently. A concern is the potential interference of the ether moiety while dispersing, which can be addressed by introduction of a directly aryl-linked acetylene. Likely, Sonogashira cross-coupling on the dibrominated anthracene or triptycene would yield the desired bis-acetylene precursor.

It is possible to explore other polymerization techniques. A promising polymerization protocol would include copper catalyzed click chemistry, as they end up in both *regio* and *stereo* specific triazoles linkage under mild reaction conditions. As outlined in the introduction, triazole linked polymers showed promising dispersion capabilities. Such a polymerization would be realizable with either ethenoanthracene or triptycene bearing a directly aryl-linked acetylene or azide, both of which are accessible by conventional chemistry.

A final approach to be considered is the immobilization of an initial building block on a solid support. Not only would this allow to gain better control of the growth of the polymer, the issues with solubility could be completely circumvented. Intriguingly, the polymer would not have to be released to disperse SWCNTs and would allow to monitor the dispersion directly on the solid support.

Experimental section

General Procedure

Reagent and Solvents: All chemical were used as received without any further purification unless explicitly stated otherwise. Dry Solvents were purchased from Fluka or Accros. NMR solvent were obtained from Cambridge Isotope Laboratories, Inc. (Andover, MA,USA).

¹H and ¹³C Nuclear Magnetic Resonance (NMR): were recorded on a Bruker DPX-NMR (400 MHz, 101 MHz respectively) instrument. All chemical shifts are reported relative to trimethylsilane (TMS) or to the used solvent. The measurements were performed at room temperature if stated otherwise. The multiplicities are written as: s = singlet, d = doublet, t = triplet, dd = doublet of doublets and m = multiplet.

GC/MS: For GC/MS analysis a Shimadzu GCMS-QP2010 SE gas chromatograph system was used, with a Zebron 5 MS Inferno column (30 m x 0.25 mm x 0.25 mm), at 1 mL/min He-flow rate (split = 20:1) with a Shimadzu mass detector (EI 70 eV).

Mass spectroscopy (MS): MALDI-TOF analyses were performed on a Bruker microflex system.

High-resolution mass spectra (HRMS): HR-ESI-ToF-MS were measured with a Maxis 4G instrument from Bruker with the addition of NaOAc.

Direct Analysis in Real Time (DART-MS): DART-MS was measured on an IonSense DART-SVP100 (He, 450 °C) connected to a Shimadzu LC-2020.

Column Chromatography: For column chromatography SiliaFlash® P60 from SILICYCLE was used with a particle size of 40-63 μm (230-400 mesh), and TLC was performed on silica gel 60 F254 glass plates with a thickness of 0.25 mm purchased from Merck.

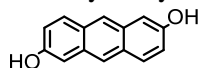
High performance liquid chromatography (HPLC): was performed on a Shimadzu LC-20AT HPLC equipped with diodearray UV/Vis detector (SPD-M10 VP from Shimadzu, λ = 200 - 600 nm) equipped with the corresponding column (regular chiral: chiralpak IA 0.46 x 25 cm; Daicel Chemical Industries Ltd.; GPC: 2 x Repro-Gel GPC 500, 5 μm 20 x 600 mm).

UV-Vis Spectroscopy: The UV-Vis spectra were recorded on a Shimadzu UV spectrometer UV-1800 at room temperature.

CD measurements were performed on a Chirascan CD Spectrometer with the indicated solvent at room temperature in 1 cm quartz glass cuvettes directly after the chiral HPLC. All solutions were prepared and measured under air saturated conditions.

Experimental Section of Poly[9,10-dihydro-11,12-dicarbomethoxyethenoanthracene-2,6-diyl-*alt*-(9,9-didodecylfluorene-2,7-diyl)] (P1)

2,6-Dihydroxyanthracene (3)

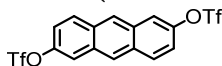


Anthraflavic acid (**4**, 1.00 g, 4.16 mmol, 1.00 equiv.) was added in portions to a suspension of Na₂CO₃ (5.29 g, 50.0 mmol, 12.0 equiv.) and NaBH₄ (2.46 g, 62.4 mmol, 15.0 equiv.) in H₂O (50 mL). The mixture was stirred at *rt* overnight, poured on ice-cold 6 N HCl (5 mL), which was covered with a layer of EtOAc (5 mL). The precipitate was filtered and taken up in acetone and filtered over a short pad of celite. The solvent was evaporated yielding in the first batch of product. The aqueous layer was extracted three times with EtOAc (probably more than 3 times are required) and the combined organic layers were washed with saturated NaHCO₃ solution, dried over Na₂SO₄ and concentrated to yield crude product (**3**, 775 mg, 3.69 mmol, **89%**), which was used without further purification.^[140]

¹H NMR (400 MHz, DMSO-*d*₆) δ = 9.64 (s, 2H), 8.14 (s, 2H), 7.83 (d, ³J_{H,H} = 9.0 Hz, 2H), 7.14 (d, ⁴J_{H,H} = 2.3 Hz, 2H), 7.08 (dd, ³J_{H,H} = 9.0, ⁴J_{H,H} = 2.4 Hz, 2H).

¹³C NMR (101 MHz, DMSO-*d*₆) δ = 153.6, 130.8, 129.0, 127.7, 123.0, 120.4, 106.7.

2,6-Bis(trifluoromethanesulfonate)-anthracene (2)



To an oven dried and argon-flushed Schlenk tube was added 2,6-Dihydroxyanthracene (**3**, 2.06 g, 9.80 mmol, 1.00 equiv.) and NEt₃ (6.60 mL, 47.0 mmol, 4.80 equiv., freshly dried over CaH₂) along with ACN (50 mL). The reaction mixture was cooled down to -41 °C and stirred for 10 minutes. Trifluoromethanesulfonic anhydride (3.9 mL, 23.5 mmol, 2.40 equiv.) was added dropwise and the reaction mixture was stirred for another 5 hours at -41 °C. The solvent was removed under reduced pressure and the residue was purified by column chromatography (SiO₂; cyclohexane/toluene, 2:1 to pure toluene) to give 2,6-bis(trifluoromethanesulfonate)-anthracene (**2**, 3.89 g, 9.80 mmol, **85%**) as an off white solid.

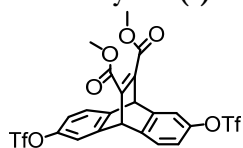
¹H NMR (400 MHz, CDCl₃) δ = 8.54 (s, 2H), 8.12 (d, ³J_{H,H} = 9.1 Hz, 2H), 7.95 (d, ⁴J_{H,H} = 2.5 Hz, 2H), 7.43 (dd, ³J_{H,H} = 9.3, ⁴J_{H,H} = 2.4 Hz, 2H).

¹³C NMR (101 MHz, CDCl₃) δ = 147.4, 131.5, 131.4, 130.9, 127.7, 120.9, 119.4, 119.0 (q, ¹J_{C,F} = 320.8 Hz).

¹³⁵DEPT (101 MHz, CDCl₃) δ = 131.4, 127.7, 120.9, 119.4.

HRMS (ESI) calcd for C₁₆H₇F₆O₆S₂ [M-H]⁻ 472.9594, found 472.9593.

Dimethyl 2,6-bis(trifluoromethanesulfonate)-9,10-dihydro-9,10-ethenoanthracene-11,12-dicarboxylate (1)



To an oven dried round bottom flask 2,6-bis(trifluoromethanesulfonate)-anthracene (**2**, 1.00 g, 2.11 mmol, 1.00 equiv.) and DMAD (1.50 mL, 10.6 mmol, 1.00 equiv.) were added under argon atmosphere and dissolved in toluene (10 mL). The reaction mixture was heated to reflux and stirred for 42 hours. The solvent was removed under reduced pressure and the crude product was purified by column chromatography (SiO₂; cyclohexane/toluene, 2:3 to pure toluene and then to pure EtOAc). The target compound was isolated as an off white solid (**1**, 1.29 g, 2.11 mmol, **quant.**).

¹H NMR (400 MHz, CDCl₃): δ = 7.46 (d, ³J_{H,H} = 8.2 Hz, 2H), 7.33 (d, ⁴J_{H,H} = 2.4 Hz, 2H), 6.99 (dd, ³J_{H,H} = 8.1, ⁴J_{H,H} = 2.4 Hz, 2H), 5.55 (s, 2H), 3.82 (s, 6H).

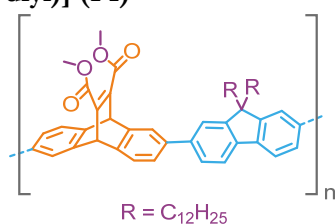
¹³C NMR (101 MHz, CDCl₃): δ = 165.1, 147.2, 146.5, 145.9, 143.2, 125.5, 118.8 (q, ¹J_{C,F} = 320.9 Hz), 118.8, 117.8, 52.9, 51.7.

¹³⁵DEPT (101 MHz, CDCl₃): δ = 125.5, 118.8, 117.8, 52.9, 51.7.

¹⁹F NMR (376 MHz, CDCl₃): δ = -72.84 (s).

HRMS (ESI) calcd for C₂₂H₁₅F₆O₁₀S₂ [M+H]⁺ 617.0005: found 617.0002.

Poly[9,10-dihydro-11,12-dicarbomethoxyethenoanthracene-2,6-diyl-*alt*-(9,9-didodecylfluorene-2,7-diyl)] (P1)



An oven dried and argon-flushed 20 ml Schlenk tube was charged with 2,6-Bis(trifluoromethane-sulfonate)-9,10-dihydro-11,12-dicarbomethoxyethenoanthracene (**1**, 100 mg, 0.162 mmol, 1.00 equiv.), 9,9-Didodecyl-2,7-bis(4,4,5,5-tetramethyl-1,3,2-dioxaborolane)fluorene (**5**, 126 mg, 0.126 mmol, 1.00 equiv.) and Cs_2CO_3 (267 mg, 0.810 mmol, 5.00 equiv). The vial was sealed and evacuated/backfilled with nitrogen (3 \times). Dimethylformamide (3 mL) was added, and the reaction was flushed again with nitrogen (3 \times) under sonication. $Pd(dppf)Cl_2 \cdot CH_2Cl_2$ (26.5 mg, 0.0324 mmol, 0.20 equiv.) was added and the reaction mixture was evacuated and backfilled with nitrogen under sonication once more before heated to 90 °C. The reaction mixture was stirred for 3 days at 90 °C. The reaction was cooled to room temperature, diluted with dichloromethane (40 mL) and washed with Water. The aqueous layer was back extracted with dichloromethane (3 x 20 mL), the combined organic layers were dried over $MgSO_4$ and the solvent was removed under reduced pressure. The residue was solved in a minimal amount of chloroform and the product was precipitated with hexane. The precipitate was filtered and the polymer was obtained as a brown solid (**P1**, 89.0 mg).

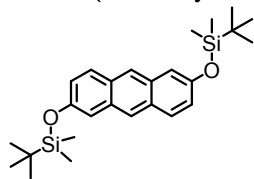
SEC (DA) $M_w = 9.15 \times 10^3$ Da, $D = 2.01$

1H NMR (400 MHz, $CDCl_3$): $\delta = 7.83 - 7.63$ (m, 4H), 7.58 - 7.43 (m, 6H), 7.39 - 7.29 (m, 2H), 5.64 (s, 2H), 3.84 (s, 6H), 2.02 (br, 4H), 1.35 - 0.98 (m, 32H), 0.93 - 0.78 (m, 8H), 0.66 (br, 6H).

^{135}C DEPT (101 MHz, $CDCl_3$): $\delta = 126.1, 124.4, 124.4, 124.1, 124.1, 123.0, 123.0, 121.6, 121.6, 120.0, 119.9, 52.5, 52.3, 40.6, 31.9, 30.1, 29.6, 29.6, 29.3, 23.9, 22.7, 14.1$.

Experimental section of Poly[Diisopentyl-9,10-dihydro-9,10-ethenoanthracene-11,12-dicarboxylate-2,6-diyl-*alt*-(9,9-didodecylfluorene-2,7-diyl)] (P2)

2,6-Bis(tert-butyldimethylsiloxy)anthracene (24)



2,6-Dihydroxyanthracene (**3**, 3.22 g, 15.3 mmol, 1.00 equiv.) and tert-butyldimethylsilyl chloride (7.06 g, 45.9 mmol, 3.00 equiv.) were dissolved under stirring in DMF (100 mL) under argon. Triethylamine (6.52 mL, 45.9 mmol, 3.00 equiv.) was added, and the reaction turned dark red immediately. The reaction was stirred at 35 °C for 6 h and then cooled to room temperature. The DMF was removed under vacuum yielding an orange-black semisolid that was suspended in 100 mL of petroleum ether/ether (9/1), placed on a flash silica pad, and eluted with more solvent. The yellow band was collected and the solvent was evaporated yielding an orange red solid (**24**, 5.74 g, 15.3 mmol, **86%**).^[137]

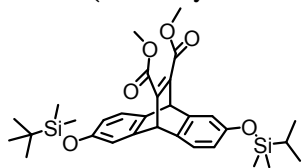
¹H NMR (400 MHz, CDCl₃): δ = 8.19 (s, 2H), 7.84 (d, ³J_{H,H} = 9.1 Hz, 2H), 7.28 (d, ⁴J_{H,H} = 2.3 Hz, 2H), 7.09 (dd, ³J_{H,H} = 9.1, ⁴J_{H,H} = 2.3 Hz, 2H), 1.05 (s, 18H), 0.28 (s, 12H).

¹³C NMR (101 MHz, CDCl₃): δ = 152.4, 131.6, 129.4, 128.9, 124.3, 123.6, 113.5, 25.9, 18.5, -4.1.

¹³⁵DEPT (101 MHz, CDCl₃): δ = 129.4, 124.3, 123.6, 113.5, 25.9.

HRMS (ESI) no ms laut paper sollte ESI gehen

2,6-Bis(*tert*-butyldimethylsiloxy)-9,10-dihydro-11,12-dicarbomethoxyethenoanthracene (18)



To an oven dried and argon-flushed Schlenk tube (50 mL) 2,6-bis(*tert*-butyldimethylsiloxy)anthracene (**24**, 1.08 g, 2.46 mmol, 1.00 equiv.) and dimethylacetylenedicarboxylate (1.59 mL, 12.3 mmol, 5.00 equiv.) were added and dissolved in toluene (10 mL). The mixture was flashed with argon and heated to reflux for 72 hours. The solvent was removed under reduced pressure and the remaining starting material was removed by bulb to bulb distillation (100 °C, 5×10^{-1} mbar). The crude product was purified by column chromatography (SiO_2 ; cyclohexane/ethyl acetate, 1:4) to yield the target compound as off white solid (**18**, 1.30 g, 2.46 mmol, **91%**).

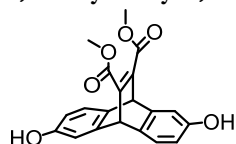
^1H NMR (400 MHz, CDCl_3): δ = 7.17 (d, $^3J_{\text{H,H}} = 7.9$ Hz, 2H), 6.87 (d, $^4J_{\text{H,H}} = 2.3$ Hz, 2H), 6.43 (dd, $^3J_{\text{H,H}} = 7.9$, $^4J_{\text{H,H}} = 2.3$ Hz, 2H), 5.29 (s, 2H), 3.79 (s, 6H), 0.96 (s, 18H), 0.16 (d, 12H).

^{13}C NMR (101 MHz, CDCl_3): δ = 166.2, 153.3, 147.4, 145.9, 136.4, 124.2, 116.4, 115.6, 52.5, 51.9, 25.8, 18.2, -4.3.

$^{135}\text{DEPT}$ (101 MHz, CDCl_3): δ = 124.1, 116.3, 115.4, 52.4, 51.8, 25.6.

HRMS (ESI) calcd for $\text{C}_{32}\text{H}_{45}\text{O}_6\text{Si}_2$ $[\text{M}+\text{H}]^+$: 581.2749 found 581.2750.

2,6-dihydroxy-9,10-dihydro-11,12-dicarbomethoxyethenoanthracene (**21**)



In a 50 mL round bottom flask 2,6-bis(tert-butyltrimethylsilyloxy)-9,10-dihydro-11,12-dicarbomethoxyethenoanthracene (**18**, 807 mg, 1.39 mmol, 1.00 equiv.) was suspended in methanol (10 mL). Dichloromethane was added until a solution was formed (4 mL), then aq. HCl (37%, 1.01 mL, 12.2 mmol, 8.75 equiv.) was added and the reaction mixture was stirred at room temperature for 4.5 hours. The reaction mixture was concentrated and the crude mixture was purified by column chromatography (SiO₂; cyclohexane/dichloromethane, 3:2) to yield the target compound as off white solid (**21**, 520 mg, 1.39 mmol, **quant.**).

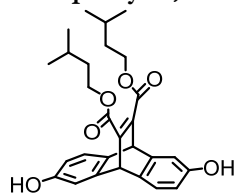
¹H NMR (400 MHz, acetone-*d*₃): δ = 8.21 (s, 2H), 7.21 (d, ³J_{H,H} = 7.9 Hz, 2H), 6.95 (d, ⁴J_{H,H} = 2.4 Hz, 2H), 6.44 (dd, ³J_{H,H} = 7.9, ⁴J_{H,H} = 2.4 Hz, 2H), 5.38 (s, 2H), 3.73 (s, 6H).

¹³C NMR (101 MHz, acetone-*d*₃): δ = 166.6, 155.9, 148.2, 147.5, 135.9, 125.0, 112.7, 111.4, 52.5, 52.4.

¹³C DEPT (101 MHz, acetone-*d*₃): δ = 125.0, 112.7, 111.4, 52.5, 52.4.

HRMS (ESI) calcd for C₂₀H₁₆NaO₆ [M+Na]⁺: 375.0839 found 375.0841.

Diisopentyl-2,6-dihydroxy-9,10-dihydro-9,10-ethenoanthracene-11,12-dicarboxylate (**23**)



To an oven dried and argon flushed 10 mL round bottom flask 2,6-dihydroxy-9,10-dihydro-11,12-dicarbomethoxyethenoanthracene (**21**, 520 mg, 1.48 mmol, 1.00 equiv.) and freshly distilled isoamylalcohol (5.01 mL, 45.4 mmol, 30.7 equiv.) were added. The reaction mixture was heated up to 100 °C and then *para*-toluenesulfonic acid monohydrate (45.0 mg, 0.986 mmol, 0.158 equiv.) was added. The reaction mixture was stirred at 100 °C for 24 hours. Ethyl acetate was added to the reaction mixture and then it was washed with brine, saturated NaHCO₃ and water. The organic layer was dried over MgSO₄ and the solvent was removed under reduced pressure. The crude mixture was purified by column chromatography (SiO₂; cyclohexane/ethyl acetate, 1:1) and the remaining isoamylalcohol was removed by bulb to bulb distillation (40 °C, 5 x 10⁻¹ mbar) to yield the target compound as colorless solid (**22**, **23**, 687 mg, 1.48 mmol, **quant.**).

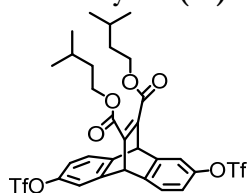
¹H NMR (400 MHz, CDCl₃): δ = 6.92 (d, ³J_{H,H} = 7.9 Hz, 2H), 6.71 (d, ⁴J_{H,H} = 2.3 Hz, 2H), 6.19 (dd, ³J_{H,H} = 7.9, ⁴J_{H,H} = 2.4 Hz, 1H), 6.07 – 5.57 (m, 1H), 5.11 (d, ³J_{H,H} = 3.1 Hz, 1H), 4.07 (t, ³J_{H,H} = 7.0 Hz, 3H), 3.98 – 3.78 (m, 1H), 1.64 – 1.45 (m, 2H), 1.39 (q, ³J_{H,H} = 7.0 Hz, 2H), 1.29 – 0.98 (m, 1H), 0.76 (d, ³J_{H,H} = 6.6 Hz, 6H).

¹³C NMR (101 MHz, CDCl₃): δ = 166.5, 153.7, 147.1, 146.2, 135.6, 124.4, 112.0, 111.1, 70.6, 64.7, 51.8, 37.2, 34.1, 27.0, 26.1, 25.1, 22.6, 16.5, 11.3.

¹³⁵DEPT (101 MHz, CDCl₃): δ = 124.4, 112.0, 111.1, 70.6, 64.7, 51.8, 37.2, 34.1, 26.1, 25.2, 22.6, 16.5, 11.3.

HRMS (ESI) calcd for C₂₈H₃₃O₆ [M+H]⁺: 465.226 found 465.2266.

Diisopentyl-2,6-bis(trifluoromethanesulfonate)-9,10-dihydro-9,10-ethenoanthracene-11,12-dicarboxylate (26**)**



To an oven dried and argon flushed Schlenk tube (25 mL) diisopentyl-2,6-dihydroxy-9,10-dihydro-9,10-ethenoanthracene-11,12-dicarboxylate (**23**, 340 mg, 0.732 mmol, 1.00 equiv.) and NEt₃ (494 μL, 3.51 mmol, 4.80 equiv., freshly dried over CaH₂) was added along with dichloromethane (6 mL). The reaction mixture was cooled down to -78 °C and stirred for 10 minutes. Trifluoromethanesulfonic anhydride (292 μL, 1.76 mmol, 2.40 equiv.) was added dropwise over 10 minutes and the reaction mixture was stirred for another 6 hours at -41 °C. The Reaction mixture was filtered over celite and the solvent was removed under reduced pressure. The residue was purified by column chromatography (SiO₂; cyclohexane/ethyl acetate, 10:1) to gain Diisopentyl-2,6-bis(trifluoromethylsulfonate)-9,10-dihydro-9,10-ethenoanthracene-11,12-dicarboxylate (**26**, 500 g, .732 mmol, **94%**) as a colorless foam.

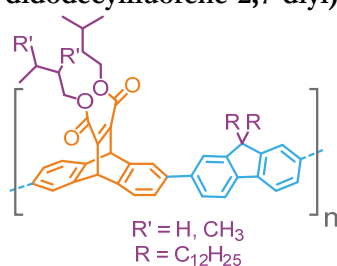
¹H NMR (400 MHz, CDCl₃): δ = 7.45 (dd, J = 8.2, 1.4 Hz, 2H), 7.34 (t, J = 1.8 Hz, 2H), 6.98 (dt, J = 8.0, 1.8 Hz, 2H), 5.57 (d, J = 3.5 Hz, 2H), 4.24 (t, J = 6.9 Hz, 3H), 4.15 – 3.96 (m, 1H), 1.70 (ddq, J = 26.6, 13.2, 6.6 Hz, 1H), 1.56 (q, J = 6.9 Hz, 3H), 1.49 – 1.15 (m, 2H), 0.96 – 0.90 (m, 12H).

¹³C NMR (101 MHz, CDCl₃): δ = 164.7, 147.2, 147.2, 146.1, 146.1, 146.0, 146.0, 143.3, 125.3, 118.8 (q, ¹J_{C,F} = 320.7 Hz), 118.6, 117.6, 117.6, 70.7, 64.8, 51.8, 51.7, 51.7, 42.8, 37.1, 34.1, 29.8, 26.0, 25.1, 22.4, 16.4, 13.9, 11.2.

¹³⁵DEPT (101 MHz, CDCl₃): δ = 125.3, 125.3, 118.6, 117.6, 117.6, 70.7, 64.8, 51.8, 51.7, 51.6, 42.7, 37.1, 34.1, 29.7, 26.0, 25.1, 25.1, 22.4, 22.4, 16.4, 13.9, 11.2.

HRMS (ESI) calcd for C₃₀H₃₁F₆O₁₀S₂ [M+H]⁺: 729.1257 found 729.1255.

Poly[Diisopentyl-9,10-dihydro-9,10-ethenoanthracene-11,12-dicarboxylate-2,6-diyl-*alt*-(9,9-didodecylfluorene-2,7-diyl)] (P2)



A an oven dried and argon-flushed 25 ml Schlenk tube was charged with diisopentyl-2,6-bis(trifluoromethylsulfonate)-9,10-dihydro-9,10-ethenoanthracene-11,12-dicarboxylate (**26**, 133 mg, 0.183 mmol, 1.00 equiv.), 9,9-Didodecyl-2,7-bis(4,4,5,5-tetramethyl-1,3,2-dioxaborolane)fluorene (**5**, 142 mg, 0.183 mmol, 1.00 equiv.) and Cs_2CO_3 (301 mg, 0.915 mmol, 5.00 equiv). The vial was sealed and evacuated/backfilled with nitrogen (3 \times). Dimethylformamide (3 mL) was added, and the reaction was flushed again with nitrogen (3 \times) under sonication. $\text{Pd}(\text{dppf})\text{Cl}_2 \cdot \text{CH}_2\text{Cl}_2$ (29.9 mg, 32.4 μmol , 0.20 equiv.) was added and the reaction mixture was evacuated and backfilled with nitrogen under sonication once more before heated to 90 $^\circ\text{C}$. The reaction mixture was stirred for 3 days at 90 $^\circ\text{C}$. The reaction was cooled to room temperature, diluted with dichloromethane (40 mL) and washed with Water. The aqueous layer was back extracted with dichloromethane (3 x 20 mL), the combined organic layers were dried over MgSO_4 and the solvent was removed under reduced pressure. The residue was solved in a minimal amount of chloroform and side products were precipitated with hexane. The solvent of the mother layer was removed under reduced pressure and the precipitation procedure was repeated once more. The precipitate of the second batch was filtered and to obtain the target polymer **P2** as a brown solid (56.0 mg).

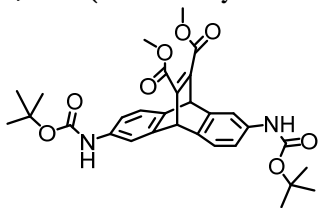
SEC (DA) $M_w = 1.929 \times 10^4$ Da, $D = 1.67$

$^1\text{H NMR}$ (400 MHz, CDCl_3): $\delta = 7.88 - 7.31$ (m, 12H), 5.62 (br, 2H), 4.26 (br, 4H), 2.15 - 0.46 (m, 68H).

$^{13}\text{C NMR}$ (101 MHz, CDCl_3): $\delta = 165.7, 151.6, 151.4, 150.9, 146.5, 144.6, 142.7, 140.0, 139.8, 139.5, 131.7, 131.4, 131.3, 128.8, 128.4, 128.2, 127.2, 126.1, 124.4, 124.1, 122.9, 121.6, 120.0, 75.0, 74.1, 74.0, 73.5, 70.3, 64.3, 55.3, 55.2, 52.5, 40.6, 37.2, 34.1, 31.9, 30.2, 30.1, 29.7, 29.7, 29.6, 29.6, 29.4, 29.3, 26.1, 25.1, 24.9, 23.9, 22.7, 22.5, 16.5, 14.1, 11.3$.

Experimental section towards Schiff base polymer

2,6-Bis(*tert*-butoxycarbonyl-amino)-9,10-dihydro-11,12-dicarbomethoxyethenoanthracene (**33**)



An oven dried and argon-flushed 100 ml Schlenk tube was charged with Dimethyl 2,6-bis(trifluoromethanesulfonate)-9,10-dihydro-9,10-ethenoanthracene-11,12-dicarboxylate (**1**, 565 mg, 917 μmol , 1.00 equiv.), *tert*-butyl carbamate (280 mg, 2.34 mmol, 2.55 equiv.), Pd₂dba₃ (84.0 mg, 91.7 μmol , 0.100 equiv.), Xantphos (162 mg, 0.275 mmol, 0.300 equiv.) and Cs₂CO₃ (845 mg, 2.57 mmol, 2.80 equiv.). The vial was sealed and evacuated/backfilled with nitrogen (3 \times). Dioxane (9 mL) was added, and the reaction was flushed again with nitrogen (3 \times). The reaction mixture was stirred at 100 °C for 20 h. It was then cooled to room temperature, filtered over Celite with DCM and the solvent was evaporated. The residue was purified by column chromatography (SiO₂; EtOAc/toluene, 2:8) to afford the target compound (**33**, 444 mg, 917 μmol , **88%**) as a yellowish solid.

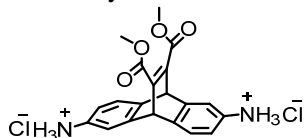
¹H NMR (400 MHz, CDCl₃): δ = 7.68 (s, 2H), 7.23 (d, ³J_{H,H} = 8.0 Hz, 2H), 6.77 (dd, ³J_{H,H} = 7.9, ⁴J_{H,H} = 2.1 Hz, 2H), 6.52 – 6.44 (m, 2H), 5.38 (s, 2H), 3.79 (s, 6H), 1.51 (s, 18H).

¹³C NMR (101 MHz, CDCl₃): δ = 166.0, 152.9, 147.2, 145.2, 138.3, 135.9, 124.0, 115.0, 114.9, 80.7, 52.5, 52.0, 28.4.

¹³⁵DEPT (101 MHz, CDCl₃): δ = 123.90, 115.0, 114.8, 52.4, 51.9, 28.3.

HRMS (ESI) calcd for C₃₀H₃₅N₂O₈ [M+H]⁺ 551.2388: found 551.2386.

9,10-Dihydro-11,12-dicarbomethoxyethenanthracene-2,6-diaminium chloride (**34**)



An oven dried and argon-flushed 50 ml two neck round bottom flask was charged with 2,6-Bis(*tert*-butoxycarbonyl-amino)-9,10-dihydro-11,12-dicarbomethoxyethenanthracene (**33**, 160 mg, 291 μmol , 1.00 equiv.) and dissolved in dioxane (10 mL). The solution was heated to 60 $^{\circ}\text{C}$ and dry HCl gas was bubbled through for 18 minutes. The reaction mixture was stirred for another hour at 60 $^{\circ}\text{C}$. The suspension was cooled down to room temperature, filtered and the product was washed with cold dioxane. The product was isolated as yellow solid (**34**, 123 mg, 0.291 mmol, **quant.**).

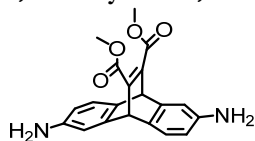
$^1\text{H NMR}$ (400 MHz, D_2O): δ = 7.64 (d, $^3J_{\text{H,H}} = 7.9$ Hz, 2H), 7.56 (s, 2H), 7.16 (d, $^3J_{\text{H,H}} = 7.9$ Hz, 2H), 5.88 (s, 2H), 3.85 (s, 6H).

$^{13}\text{C NMR}$ (101 MHz, D_2O): δ = 167.7, 147.9, 146.1, 144.5, 128.4, 126.0, 121.1, 119.6, 53.9, 51.4.

$^{135}\text{DEPT}$ (101 MHz, D_2O): δ = 126.0, 121.1, 119.6, 53.9, 51.4.

HRMS (ESI) calcd for $\text{C}_{18}\text{H}_{19}\text{N}_2\text{O}_2$ [$\text{M}-\text{HCl}$, $-\text{Cl}$] $^+$ 351.1339: found 351.1343.

9,10-Dihydro-11,12-dicarbomethoxyethenanthracene-2,6-diamine (**32**)



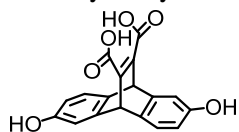
9,10-Dihydro-11,12-dicarbomethoxyethenanthracene-2,6-diaminium chloride (**34**, 90.0 mg, 214 μmol , 1.00 equiv.) was taken up in water (5 mL) diluted with saturated NaHCO_3 (5 mL) and extracted three times with DCM (3 x 10 mL). The organic layer was washed with brine and the solvent was evaporated under reduced pressure. The target compound was isolated as yellow solid (**32**, 74.0 mg, 212 μmol , **quant.**).

$^1\text{H NMR}$ (400 MHz, CDCl_3): δ = 6.99 (d, $^3J_{\text{H,H}} = 7.8$ Hz, 2H), 6.64 (d, $^4J_{\text{H,H}} = 2.2$ Hz, 2H), 6.16 (dd, $^3J_{\text{H,H}} = 7.8$, $^4J_{\text{H,H}} = 2.2$ Hz, 2H), 5.11 (s, 2H), 3.68 (s, 6H), 3.55 – 3.26 (br, 4H).

HRMS (ESI) calcd for $\text{C}_{18}\text{H}_{19}\text{N}_2\text{O}_2$ [$\text{M}+\text{H}$] $^+$ 351.1339: found 351.1343.

Experimental section Poly[*N*-octyl-(2,6- bis(propargyl-1-oxy))-9,10-dihydro-9,10-maleimidoanthracene] (P4)

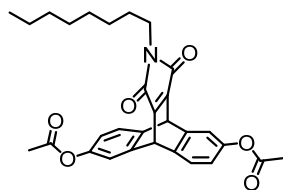
2,6-dihydroxy-9,10-dihydro-9,10-ethenoanthracene-11,12-dicarboxylic acid (36)



A solution of 2,6-bis(*tert*-butyldimethylsiloxy)-9,10-dihydro-11,12-dicarbomethoxyethenoanthracene (**18**, 4.10 g, 7.06 mmol, 1.00 equiv.) in a mixture of *tert*-butanol (200 mL) and dioxane (20 mL) was heated to 80 °C in a round bottom flask under atmosphere. Potassium hydroxide (1.98 g, 35.3 mmol, 5.00 eq.) was added after 10 min and the reaction mixture was stirred for 7 hours. The solvent was removed under reduced pressure and the residue was suspended in DCM and washed with brine. The aqueous layer was acidified with concentrated HCl and was extracted three times with EtOAc. The combined organic layers were dried over Na₂SO₄ and the solvent was removed under reduced pressure. The residue was purified by flash column chromatography (*reversed-phase* - C₁₈; water/acetonitrile, 1:1). The product was obtained as a yellow solid (**36**, 2.28 g, 7.06 mmol, **quant.**).

¹H NMR (400 MHz, MeOD-*d*₄) : δ = 7.16 (d, ³*J*_{H,H} = 7.9 Hz, 2H), 6.85 (d, ⁴*J*_{H,H} = 2.3 Hz, 2H), 6.40 (dd, ³*J*_{H,H} = 7.9, ⁴*J*_{H,H} = 2.4 Hz, 2H), 5.41 (s, 2H).

***N*-octyl-(2,6-diacetate)-9,10-dihydro-9,10-maleimidoanthracene (38)**



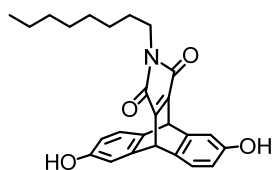
An oven dried and argon-flushed round bottom flask (250 mL) was charged with 2,6-dihydroxy-9,10-dihydro-9,10-ethenoanthracene-11,12-dicarboxylic acid (**36**, 1.00 g, 3.08 mmol, 1.00 equiv.) and acetic anhydride (20 mL). The solution was heated to 130 °C for 5 hours and then the solvent was removed under reduced pressure. The crude mixture was dissolved in freshly dried chloroform (20 mL) and 1-octanamine (freshly distilled before use, 1.03 mL, 6.16 mmol, 2.00 equiv.) was added. The solution was heated to 50 °C for 20 hours and then the solvent was removed under reduced pressure. The crude mixture was dissolved in acetic anhydride (20 mL), sodium acetate (1.03 g, 12.3 mmol, 4.00 equiv.) was added and the reaction mixture was heated to 100 °C for 20 hours. The solvent was removed under reduced pressure and the residue was taken up in ethyl acetate and washed with water. The aqueous layer was back extracted with ethyl acetate (3x) and the combined organic layers were washed once with brine and dried over MgSO₄. The solvent was removed under reduced pressure and the residue was purified by column chromatography (SiO₂; cyclohexane/ethyl acetate, 4:1) to yield the target compound as off white solid (**38**, 1.01 g, 2.01 mmol, **65%**).

¹H NMR (400 MHz, DMSO - *d*₆): δ = 7.52 (d, ³*J*_{H,H} = 8.0 Hz, 2H), 7.33 (d, ⁴*J*_{H,H} = 2.3 Hz, 2H), 6.78 (dd, ³*J*_{H,H} = 8.0, ⁴*J*_{H,H} = 2.3 Hz, 2H), 5.78 (s, 2H), 3.27 (t, ³*J*_{H,H} = 7.2 Hz, 2H), 2.23 (s, 6H), 1.41 (q, ³*J*_{H,H} = 7.1 Hz, 2H), 1.26 – 1.10 (m, 10H), 0.81 (t, ³*J*_{H,H} = 6.9 Hz, 3H).

¹³C NMR (101 MHz, DMSO - *d*₆): δ = 169.3, 165.9, 155.8, 147.7, 146.0, 141.4, 125.0, 118.8, 118.1, 45.2, 37.5, 31.1, 28.4, 28.4, 28.1, 26.2, 22.0, 20.7, 13.9.

HRMS (ESI) calcd for C₃₀H₃₁NO₆Na [M+Na]⁺: 524.2004 found 524.2050.

***N*-octyl-(2,6-dihydroxy)-9,10-dihydro-9,10-maleimidoanthracene (37)**



To a round bottom flask was added *N*-octyl-(2,6-diacetate)-9,10-dihydro-9,10-maleimidoanthracene (**38**, 400 mg, 0.797 mmol, 1.00 equiv.) and ethanol (40 mL). Concentrated aqueous hydrochloric acid (200 μ L, 2.41 mmol, 3.03 equiv.) was added dropwise and the reaction mixture was stirred for 15 hours. The solvent was removed under reduced pressure and the residue was purified by column chromatography (SiO₂; cyclohexane/ethyl acetate, 5:1) to yield the target compound as yellow solid (**37**, 332 mg, 0.797 mmol, **quant.**).

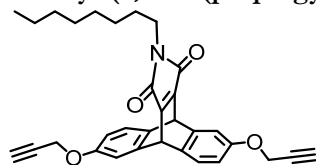
¹H NMR (400 MHz, CDCl₃): δ = 7.15 (d, ³*J*_{H,H} = 7.9 Hz, 2H), 6.90 (d, ⁴*J*_{H,H} = 2.4 Hz, 2H), 6.41 (dd, ³*J*_{H,H} = 7.9, ⁴*J*_{H,H} = 2.5 Hz, 2H), 5.32 (s, 2H), 3.37 (t, ³*J*_{H,H} = 7.4 Hz, 2H), 1.48 (q, ³*J*_{H,H} = 7.2 Hz, 2H), 1.31 – 1.14 (m, 10H), 0.85 (t, ³*J*_{H,H} = 7.0, 3H).

¹³C NMR (101 MHz, CDCl₃): δ = 167.0, 156.5, 153.5, 146.8, 136.1, 125.1, 112.9, 111.1, 46.5, 38.3, 31.9, 29.2, 29.0, 26.9, 25.4, 22.7, 14.2.

¹³⁵DEPT (101 MHz, CDCl₃): δ = 125.1, 112.9, 111.1, 46.5, 38.3, 31.9, 29.2, 29.0, 26.9, 22.7, 14.2.

HRMS (ESI) calcd for C₂₆H₂₆NO₄ [M+H]⁺: 416.1867 found 416.1872.

***N*-octyl-(2,6-bis(propargyl-1-oxy))-9,10-dihydro-9,10-maleimidoanthracene (41)**



To an oven dried and argon-flushed Schlenk tube (25 mL) *N*-octyl-(2,6-dihydroxy)-9,10-dihydro-9,10-maleimidoanthracene (**37**, 105 mg, 251 μmol , 1.00 equiv.), CsCO_3 (197 mg, 602 μmol , 2.40 equiv.), and 18-Crown-6 (1.38 mg, 5.17 μmol , 0.0206 equiv.) were added and dissolved in dimethylformamide (2 mL). The tube was subjected shortly to vacuum under sonication and backfilled with argon (3x). Propargyl bromide (80% solution in toluene, 89.6 mg, 602 μmol , 2.40 equiv.) was added and the mixture was heated to 50 $^\circ\text{C}$ for 17 hours. The reaction mixture was filtered and washed with dichloromethane. The solvent was removed under reduced pressure and the residue was purified by column chromatography (SiO_2 ; cyclohexane/ethyl acetate, 5:1) to yield the target compound as a yellow solid (**41**, 78.0 mg, 0.251 mmol, **63%**).

^1H NMR (400 MHz, CDCl_3): δ = 7.28 (d, $^3J_{\text{H,H}}$ = 8.1 Hz, 2H), 7.05 (d, $^4J_{\text{H,H}}$ = 2.4 Hz, 2H), 6.59 (dd, $^3J_{\text{H,H}}$ = 8.1, $^4J_{\text{H,H}}$ = 2.5 Hz, 2H), 5.38 (s, 2H), 4.62 (d, $^4J_{\text{H,H}}$ = 2.4 Hz, 4H), 3.43 – 3.31 (m, 2H), 2.50 (t, $^4J_{\text{H,H}}$ = 2.4 Hz, 2H), 1.54 – 1.44 (m, 2H), 1.26 – 1.16 (m, 10H), 0.85 (t, $^3J_{\text{H,H}}$ = 6.8 Hz, 3H).

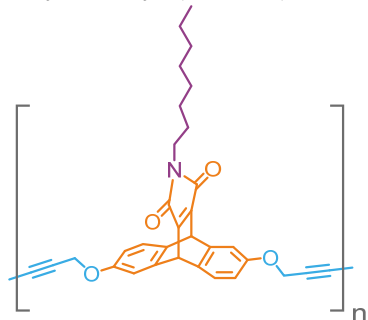
^{13}C NMR (101 MHz, CDCl_3): δ = 166.7, 156.3, 155.5, 146.5, 136.9, 124.9, 112.9, 110.1, 78.5, 75.9, 56.2, 46.6, 38.2, 31.9, 29.2, 29.2, 29.0, 26.9, 22.7, 14.2.

167.0, 156.5, 153.5, 146.8, 136.1, 125.1, 112.9, 111.1, 46.5, 38.3, 31.9, 29.2, 29.2, 29.0, 26.9, 25.4, 22.7, 14.2.

$^{135}\text{DEPT}$ (101 MHz, CDCl_3): δ = 124.9, 112.9, 110.1, 78.5, 75.9, 56.2, 46.6, 38.2, 31.9, 29.2, 29.2, 29.0, 26.9, 22.7, 14.2.

HRMS (ESI) calcd for $\text{C}_{32}\text{H}_{32}\text{NO}_4$ $[\text{M}+\text{H}]^+$: 494.2326 found 494.2329.

Poly[*N*-octyl-(2,6-bis(propargyl-1-oxy))-9,10-dihydro-9,10-maleimidoanthracene] (P4)



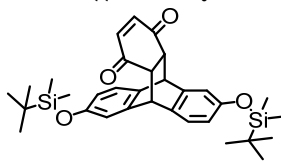
To a 100 mL round bottom flask was added *N*-octyl-(2,6-bis(propargyl-1-oxy))-9,10-dihydro-9,10-maleimidoanthracene (**41**, 100 mg, 203 μmol , 1.00 equiv.), TEMEDA (47.4 mg, 406 μmol , 2.00 equiv.), and copper(I)chloride (41.4 mg, 406 μmol , 2.00 equiv.). The mixture was dissolved in methanol (55 mL) and stirred at room temperature for 72 hours. The reaction mixture was diluted with chloroform and washed with saturated aqueous NH_4Cl and then with brine. The organic layer was dried over MgSO_4 and the solvent was concentrated. The residue was purified over an automated recyclable Gel-Permeations-Chromatographic (GPC, CHCl_3) yielding the target polymer (**P4**, 40 mg).

SEC (DA) $M_w = 1.10 \times 10^4 \text{ Da}$, $D = 1.67$.

$^1\text{H NMR}$ (400 MHz, CDCl_3): $\delta = 7.36 - 7.19$ (m, 2H), 7.08 - 6.90 (m, 2H), 6.61 - 6.46 (m, 2H), 5.73 (br, 1H), 5.52 (br, 1H), 4.77 - 4.57 (m, 4H), 3.27 (br, 2H), 1.56 - 1.44 (m, 2H), 1.36 - 1.18 (m, 10H), 0.94 - 0.78 (m, 3H).

Experimental section diastereomeric resolution

2,6-Bis((*tert*-butyldimethylsilyloxy)-11,12-dihydro-triptycene-13,16-dione (**45**)



To an oven dried round bottom glass 2,6-bis(*tert*-butyldimethylsilyloxy)anthracene (**24**, 4.09 g, 9.32 mmol, 1.00 equiv.) and *p*-benzopinone (2.02 g, 18.6 mmol, 2.00 equiv.) were added before subjecting the flask to vacuum. The mixture was flashed with argon and dissolved in toluene (50 mL). After heating the reaction mixture to reflux it was stirred overnight. The reaction mixture was filtered and the solvent was removed under reduced pressure. The crude product was purified by column chromatography (SiO₂; EtOAc:Cyc, 1:8) to yield the target compound as off white solid (**45**, 3.58 g, 6.55 mmol, **70%**).

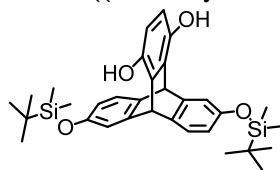
¹H NMR (400 MHz, CDCl₃): δ = 7.20 (d, $^3J_{\text{H,H}} = 8.0$ Hz, 1H), 7.00 (d, $^3J_{\text{H,H}} = 8.0$ Hz, 1H), 6.87 (d, $^4J_{\text{H,H}} = 2.4$ Hz, 1H), 6.67 (d, $^4J_{\text{H,H}} = 2.4$ Hz, 1H), 6.62 (dd, $^3J_{\text{H,H}} = 8.0$, $^4J_{\text{H,H}} = 2.4$ Hz, 1H), 6.53 (dd, $^3J_{\text{H,H}} = 8.0$, $^4J_{\text{H,H}} = 2.4$ Hz, 1H), 6.29 (s, 2H), 4.69 (dd, $^3J_{\text{H,H}} = 4.4$, $^4J_{\text{H,H}} = 2.0$ Hz, 2H), 3.07 (s, 2H), 0.97 (s, 9H), 0.93 (s, 9H), 0.18 (s, 6H), 0.11 (s, 6H).

¹³C NMR (101 MHz, CDCl₃): δ = 198.9, 198.7, 154.6, 154.5, 143.3, 141.5, 140.7, 140.6, 134.1, 132.3, 125.5, 124.7, 117.9, 117.5, 117.1, 115.9, 49.6, 49.5, 48.8, 48.7, 25.8, 25.8, 18.3, 18.3, -4.2, -4.3, -4.3, -4.3.

¹³⁵ DEPT (101 MHz, CDCl₃) : 140.5, 140.5, 125.4, 124.6, 117.8, 117.4, 116.9, 115.7, 49.4, 49.3, 48.6, 48.6, 25.7, 25.6.

MS (APCI) calcd for C₃₂H₄₂O₄Si₂ [M+H]⁺: 547.26 found 547.20.

2,6-Bis((*tert*-butyldimethylsilyl)oxy)-13,16-dihydroxy-triptycene (**46**)



A mixture of 2,6-bis((*tert*-butyldimethylsilyl)oxy)-11,12-dihydro-triptycene-13,16-dione (**45**, 300 mg, 549 μmol , 1.00 equiv.) and K_2CO_3 (460 mg, 3.29 mmol, 6.00 equiv.) was put under vacuum for 10 minutes. The mixture was floated with argon and dissolved in dioxane (14 mL). The reaction mixture was heated to 50 $^\circ\text{C}$ for 17 h under a nitrogen atmosphere. The solvent was removed under reduced pressure and the residue was dissolved in DCM. The mixture was washed with saturated NH_4Cl and the organic layer was separated. The aqueous layer was extracted twice with dichloromethane. The combined organic layers were washed with saturated NaHCO_3 , dried over Na_2SO_4 , filtered, and evaporated in *vacuum*. The residue was purified by column chromatography (SiO_2 ; EtOAc/cyclohexane, 1:4) to give the desired product as off white solid (**46**, 245 mg, 0.448 mmol, **82%**).

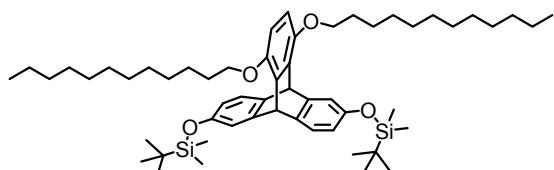
$^1\text{H NMR}$ (400 MHz, Acetone- d_6): δ = 7.76 (s, 2H), 7.24 (d, $^3J_{\text{H,H}} = 7.9$ Hz, 2H), 6.95 (d, $^4J_{\text{H,H}} = 2.4$ Hz, 2H), 6.45 (dd, $^3J_{\text{H,H}} = 7.9$, $^4J_{\text{H,H}} = 2.4$ Hz, 2H), 6.38 (s, 2H), 5.78 (s, 2H), 0.96 (s, 18H), 0.16 (s, 12H).

$^{13}\text{C NMR}$ (101 MHz, Acetone- d_6): δ = 153.5, 149.1, 145.9, 139.9, 133.9, 124.9, 116.8, 115.8, 113.9, 47.6, 26.0, 18.7, -4.3, -4.3.

$^{13}\text{C DEPT}$ (101 MHz, Acetone- d_6): δ = 124.9, 116.8, 115.8, 113.9, 47.6, 26.0, -4.3, -4.3.

HRMS (ESI) calcd for $\text{C}_{32}\text{H}_{43}\text{O}_4\text{Si}_2$ $[\text{M}+\text{H}]^+$: 547.2694 found 547.2698.

2,6-Bis((*tert*-butyldimethylsilyl)oxy)-13,16-bis(dodecyloxy)-tritycene (47)



To an argon-flushed Schlenk tube was added 2,6-bis((*tert*-butyldimethylsilyl)oxy)-13,16-dihydroxy-tritycene (**46**, 200 mg, 366 μmol , 1.00 equiv.), 1-dodecanol (170 μL , 767 μmol , 2.10 equiv.), triphenylphosphine (203 mg, 0.767 mmol, 2.10 equiv.), and THF (1 mL). The reaction mixture was degassed under sonication. The reaction vessel was then lowered into a 40-kHz sonication bath and sonicated for several minutes (to allow for mixing). While sonicating, diisopropylazodicarboxylate (160 μL , 767 μmol , 2.10 equiv.) diluted in 1 mL THF was added dropwise to the reaction mixture over the course of 7 min. Overall, the reaction mixture (amber color) was sonicated for 15 min. The reaction mixture was purified by flash chromatography (SiO_2 ; EtOAc/cyclohexane, 1:100 to 40:100) to give 2,6-bis((*tert*-butyldimethylsilyl)oxy)-13,16-bis(dodecyloxy)-tritycene (**47**, 127 mg, **39%**) as an oil.

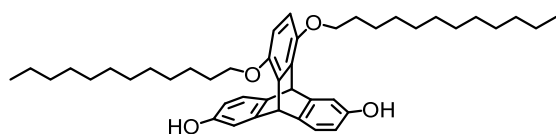
^1H NMR (400 MHz, CDCl_3): δ = 7.16 (d, $^3J_{\text{H,H}} = 7.9$ Hz, 2H), 6.86 (d, $^4J_{\text{H,H}} = 2.3$ Hz, 2H), 6.46 (s, 2H), 6.37 (dd, $^3J_{\text{H,H}} = 7.8$, $^4J_{\text{H,H}} = 2.3$ Hz, 2H), 5.66 (s, 2H), 3.91 (t, $^3J_{\text{H,H}} = 6.5$ Hz, 4H), 1.86 – 1.75 (m, 4H), 1.37 – 1.22 (m, 36H), 0.94 (s, 18H), 0.91 – 0.85 (m, 6H), 0.13 (s, 12H).

^{13}C NMR (101 MHz, CDCl_3): δ = 124.0, 116.1, 114.9, 110.7, 69.9, 46.9, 32.1, 29.8, 29.6, 29.5, 26.4, 25.8, 22.9, 18.2, 14.3, 0.2, -4.3.

$^{135}\text{DEPT}$ (101 MHz, CDCl_3): δ = 124.0, 116.1, 114.9, 110.7, 69.8, 46.8, 31.9, 29.8, 29.7, 29.7, 29.7, 29.5, 29.5, 29.4, 26.2, 25.6, 22.7, 14.1.

DART MS (550 $^\circ\text{C}$, +): m/z (%) 829.6 (16.6), 883.6 (M^+ , 88.2), 883.6 (47.5), 884.6 (52.1), 885.7 (21.8), 900.7 ($\text{M} + \text{NH}_4^+$, 100.0), 901.6 (48.5), 902.7 (20.3), 1767.5 (2M^+ , 14.5), 1767.8 (11.5), 1783.3 ($2\text{M} + \text{NH}_4^+$, 42.3), 1784.0 (72.7), 1784.9 (78.1), 1786.5 (33.8), 1786.6 (17.1).

2,6-Dihydroxy-13,16-bis(dodecyloxy)-triptycene (48)



To an argon-flushed Schlenk tube was added 2,6-bis((tert-butyldimethylsilyloxy)-13,16-bis(dodecyloxy)-triptycene (**47**, 135 mg, 153 μmol , 1.00 equiv.), MeOH (2 mL) and DCM (2 mL). Concentrated aqueous HCl (37%, 152 μL , 1.83 mmol, 12.00 equiv.) was added, the clear solution changed immediately to a milky solution. The reaction mixture was stirred for 13 hours at room temperature. The reaction mixture was diluted in DCM (100 mL) and washed with aqueous NaHCO_3 . The aqueous layer was extracted twice with DCM. The combined organic layers were washed with brine, dried over Na_2SO_4 and the solvent was removed under reduced pressure. The residue was purified over a silica plug (SiO_2 ; EtOAc). The product was obtained as an off white solid (**48**, 101 mg, 153 μmol , **quant.**).

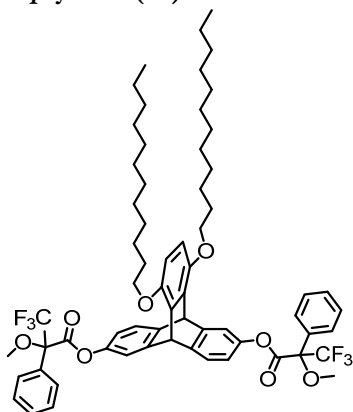
$^1\text{H NMR}$ (400 MHz, CDCl_3): δ = 7.19 (d, $^3J_{\text{H,H}} = 7.9$ Hz, 2H), 6.89 (d, $^4J_{\text{H,H}} = 2.4$ Hz, 2H), 6.48 (s, 2H), 6.38 (dd, $^3J_{\text{H,H}} = 7.9$, $^4J_{\text{H,H}} = 2.5$ Hz, 2H), 5.70 (s, 2H), 4.45 (br, 2H), 3.91 (t, $^3J_{\text{H,H}} = 6.5$ Hz, 4H), 1.86 – 1.76 (m, 4H), 1.56 – 1.45 (m, 4H), 1.44 – 1.21 (m, 32H), 0.93 – 0.85 (m, 6H).

$^{13}\text{C NMR}$ (101 MHz, CDCl_3): δ = 153.0, 148.3, 148.2, 138.2, 135.8, 124.4, 111.9, 110.9, 110.6, 100.1, 69.8, 46.8, 32.1, 29.9, 29.8, 29.6, 29.5, 26.4, 22.9, 14.3.

$^{135}\text{DEPT}$ (101 MHz, CDCl_3): δ = 124.4, 111.9, 110.9, 110.6, 69.8, 46.8, 32.1, 29.9, 29.9, 29.8, 29.7, 29.6, 29.5, 26.4, 22.9, 14.3.

Maldi-TOF MS: m/z = 654.633 (M^+).

2,6-Bis((S)-(-)-alpha-methoxy-alpha-(trifluoromethyl)phenylacetyl)-13,16-bis(dodecyloxy)-triptycene (49)



To a stirred solution of (S)-(-)-alpha-methoxy-alpha-(trifluoromethyl)phenylacetic acid (87.2 mg, 373 μmol , 2.03 equiv.), DCC (85.5 mg, 410 μmol , 2.24 equiv.), DMAP (9.10 mg, 074.5 μmol) in DCM (2 mL) was added a solution of 2,6-dihydroxy-13,16-bis(dodecyloxy)-triptycene (**48**, 120 mg, 183 μmol , 1.00 equiv.) in DCM (1 mL) and THF (0.5 mL) under argon atmosphere. The mixture was stirred for further 5 hours at room temperature. The mixture was concentrated under reduced pressure, dissolved in AcOEt and filtered through a Celite pad. The filtrate was evaporated and subjected to column chromatography (SiO_2 ; EtOAc/cyclohexane, 1:8) to give the desired product as colorless oil (**49**, 183 mg, 0.168 mmol, 93%).

$^1\text{H NMR}$ (400 MHz, CDCl_3): δ = 7.64 – 7.57 (m, 4H), 7.48 – 7.41 (m, 6H), 7.37 (dd, $^3J_{\text{H,H}} = 8.0$, $^4J_{\text{H,H}} = 2.8$ Hz, 2H), 7.20 (dd, $^4J_{\text{H,H}} = 2.3$, $^4J_{\text{H,H}} = 1.2$ Hz, 2H), 6.76 (dd, $^3J_{\text{H,H}} = 8.0$, $^4J_{\text{H,H}} = 2.3$ Hz, 2H), 6.50 (d, $^4J_{\text{H,H}} = 3.1$ Hz, 2H), 5.87 (s, 2H), 3.99 – 3.85 (m, 4H), 3.65 (s, 6H), 1.89 – 1.76 (m, 4H), 1.58 – 1.45 (m, 4H), 1.45 – 1.20 (m, 32H), 0.95 – 0.83 (m, 6H).

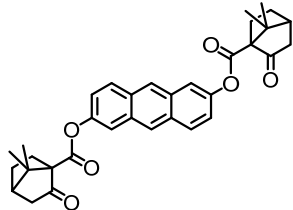
$^{13}\text{C NMR}$ (101 MHz, CDCl_3): δ = 165.1, 148.3, 147.4, 147.1, 146.5, 143.6, 132.0, 129.8, 128.6, 127.3, 124.5, 117.0, 116.9, 110.8, 69.5, 55.6, 46.8, 31.9, 29.7, 29.7, 29.5, 29.4, 26.2, 22.7, 14.1.

$^{135}\text{DEPT}$ (101 MHz, CDCl_3): δ = $^{13}\text{C NMR}$ (101 MHz, CDCl_3) δ 129.8, 128.6, 127.3, 124.5, 117.0, 117.0, 110.8, 69.5, 55.6, 46.8, 31.9, 29.7, 29.7, 29.5, 29.4, 26.2, 26.2, 22.7, 14.1.

$^{19}\text{F NMR}$ (376 MHz, CDCl_3): δ = -71.6, -71.6.

Maldi-TOF MS: m/z = 1086.232 (M^+).

Anthracene-2,6-diyl bis((1S)-7,7-dimethyl-2-oxobicyclo[2.2.1]heptane-1-carboxylate) (56)



To a stirred solution of (1S)-(+)-ketopinic acid (2.75 g, 15.1 mmol, 2.03 equiv.), DCC (3.47 g, 16.7 mmol, 2.24 equiv.), DMAP (369 mg, 3.02 mmol, 0.80 equiv.) in THF (50 mL) was added a solution of 2,6-dihydroxyanthracene (**3**, 1.56 g, 7.43 mmol, 1.00 equiv.) in THF (25 mL) under argon atmosphere. The mixture was stirred for further 18 hours at room temperature. The mixture was concentrated under reduced pressure, dissolved in ethyl acetate and filtered through a Celite pad. The filtrate was evaporated and subjected to column chromatography (SiO₂; EtOAc/cyclohexane, 1:4). Due to further impurities it was subjected a second time to column chromatography (SiO₂; Toluene/cyclohexane, 10:1) and recrystallised in EtOAc. The desired product was obtained as colorless crystalline compound (**56**, 800 mg, 1.484 mmol, **20%**). As a byproduct the monofunctionalized anthracene derivative **57** was isolated as a colorless solid (**57**, 1.05 g, 2.81 mmol, **37.8%**).

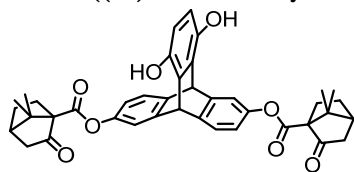
¹H NMR (400 MHz, CDCl₃): δ = 8.38 (s, 2H), 8.00 (d, $^3J_{\text{H,H}} = 9.1$ Hz, 2H), 7.75 (d, $^4J_{\text{H,H}} = 2.2$ Hz, 2H), 7.29 (dd, $^3J_{\text{H,H}} = 9.1$, $^4J_{\text{H,H}} = 2.3$ Hz, 2H), 2.73 – 2.49 (m, 4H), 2.22 (t, $^3J_{\text{H,H}} = 4.4$ Hz, 2H), 2.20 – 1.95 (m, 6H), 1.52 (ddd, $J^2J_{\text{H,H}} = 12.9$, $^3J_{\text{H,H}} = 9.2$, $^4J_{\text{H,H}} = 3.9$ Hz, 2H), 1.33 (s, 6H), 1.26 (s, 6H).

¹³C NMR (101 MHz, CDCl₃): δ = 210.5, 169.0, 148.0, 131.6, 130.3, 129.8, 126.3, 122.4, 118.3, 68.3, 49.8, 44.7, 44.2, 26.7, 26.6, 21.6, 20.1.

¹³⁵DEPT (101 MHz, CDCl₃): δ = 129.8, 126.3, 122.4, 118.3, 44.7, 44.2, 26.7, 26.6, 21.6, 20.1.

HRMS (ESI) calcd for C₃₄H₃₄NaO₄ [M+H]⁺: 561.2248 found 561.2254.

2,6-Bis((1S)-7,7-dimethyl-2-oxobicyclo[2.2.1]heptane-1-carboxylate)-13,16-dihydroxy-triptycene (58)



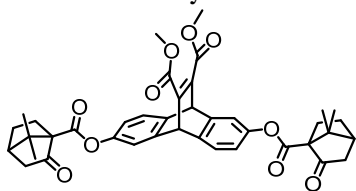
To an oven dried round bottom glass anthracene-2,6-diyl bis((1S)-7,7-dimethyl-2-oxobicyclo[2.2.1]heptane-1-carboxylate) (**56**, 340 mg, 631 μ mol, 1.00 equiv.) and p-benzopuinone (137 mg, 1.27 mmol, 2.01 equiv.) were dissolved in toluene (15 mL). The reaction mixture was heated to reflux and stirred overnight. Toluene (150 mL) was added and the solution was washed with water (3x50 mL). The solvent was removed under reduced pressure and the crude product was purified by column chromatography (SiO₂; EtOAc/cyclohexane, 1:4). To remove remaining impurities another column chromatography (*reversed*-phase - C₁₈; water/acetonitrile, 2:8) was performed to yield the target compound as colorless glasslike compound (**58**, 150 mg, 0.631 mmol, **37%**). The Diels – Alder product **59** was isolated only in 14% as diastereomers.

¹H NMR (500 MHz, DMSO-d₆): δ = 8.92 (s, 2H), 7.42 (d, ³J_{H,H} = 8.1, Hz, 2H), 7.17 (d, ⁴J_{H,H} = 2.0 Hz, 2H), 6.70 (dd, ³J_{H,H} = 7.9, ⁴J_{H,H} = 2.2 Hz, 2H), 6.35 (br, 2H), 5.87 (s, 2H), 2.62 – 2.54 (m, 2H), 2.43 – 2.33 (m, J = 12.7 Hz, 2H), 2.17 – 2.12 (m, 2H), 2.08 – 1.93 (m, 4H), 1.79 – 1.71 (m, 2H), 1.51 – 1.42 (m, 2H), 1.13 (s, 3H), 1.11 (s, 3H).

¹³C NMR (101 MHz, CDCl₃): δ = 147.6, 145.7, 143.5, 131.7, 124.8, 118.1, 117.9, 113.9, 46.3, 44.3, 43.7, 26.4, 26.0, 21.5, 19.9.

DART MS (550 °C, +): m/z (%) 500 (25), 664.3.6 (M+NH₄⁺, 100), 665.3 (49), 828.4 (42), 1310 (M+NH₄⁺, 11.5).

2,6-Bis((1S)-7,7-dimethyl-2-oxobicyclo[2.2.1]heptane-1-carboxylate)-9,10-dihydro-11,12-dicarbomethoxyethenanthracene (60)



To a degassed stirred solution of (1S)-(+)-ketopinic acid (186 mg, 937 μmol , 2.20 equiv.), DCC (200 mg, 959 μmol , 2.25 equiv.), DMAP (52.0 mg, 341 μmol , 0.80 equiv.) in DCM (6 mL) was added a solution of 2,6-dihydroxy-9,10-dihydro-11,12-dicarbomethoxyethenanthracene (**21**, 150 mg, 426 μmol , 1.00 equiv.) in DCM (1.5 mL) under argon atmosphere. The mixture was stirred for further 18 hours at room temperature. The reaction mixture was diluted in ethyl acetate and filtered. The mixture was concentrated under reduced pressure and subjected to column chromatography (SiO_2 ; tBME/cyclohexane, 2:3) to yield the target compound as white crystalline compound (**60**, 240 mg, 345 μmol , **81%**).

$^1\text{H NMR}$ (400 MHz, CDCl_3): δ = 7.34 (dd, $^3J_{\text{H,H}} = 8.0$, $^4J_{\text{H,H}} = 2.2$ Hz, 2H), 7.20 (d, $^4J_{\text{H,H}} = 2.1$ Hz, 2H), 6.78 (dd, $^3J_{\text{H,H}} = 7.9$, $^4J_{\text{H,H}} = 2.2$ Hz, 2H), 5.43 (s, 2H), 3.78 (s, 6H), 2.67 – 2.53 (m, 2H), 2.53 – 2.37 (m, 2H), 2.21 – 1.84 (m, 8H), 1.48 – 1.40 (m, 2H), 1.22 (s, 6H), 1.17 (s, 6H).

$^{13}\text{C NMR}$ (101 MHz, CDCl_3): δ = 210.4, 168.7, 165.7, 148.1, 147.0, 145.3, 141.0, 124.6, 118.4, 118.1, 68.2, 52.6, 51.9, 49.7, 44.7, 44.1, 26.5, 21.5, 20.0.

$^{135}\text{DEPT}$ (101 MHz, CDCl_3): δ = 124.6, 118.4, 118.1, 52.6, 51.9, 44.7, 44.1, 26.5, 26.5, 21.5, 20.0.

HRMS (ESI) calcd for $\text{C}_{40}\text{H}_{41}\text{O}_{10}$ $[\text{M}+\text{H}]^+$: 681.294 found 681.2692.

References

- [1] M.-F. Yu, B. S. Files, S. Arepalli, R. S. Ruoff, *Phys. Rev. Lett.* **2000**, *84*, 5552–5555.
- [2] Q. Cao, H. Kim, N. Pimparkar, J. P. Kulkarni, C. Wang, M. Shim, K. Roy, M. A. Alam, J. A. Rogers, *Nature* **2008**, *454*, 495–500.
- [3] D. D. Tune, B. S. Flavel, R. Krupke, J. G. Shapter, *Adv. Energy Mater.* **2012**, *2*, 1043–1055.
- [4] Y.-L. Zhao, J. F. Stoddart, *Acc. Chem. Res.* **2009**, *42*, 1161–1171.
- [5] S. Koltzenburg, M. Maskos, O. Nuyken, *Polymere: Synthese, Eigenschaften und Anwendungen*, Springer Berlin Heidelberg, Berlin, Heidelberg, **2014**.
- [6] L. H. Sperling, *Introduction to Physical Polymer Science*, Wiley, Hoboken, N.J., **2006**.
- [7] P. C. Painter, M. M. Coleman, *Fundamentals of Polymer Science: An Introductory Text*, Technomic Pub. Co, Lancaster, Pa, **1997**.
- [8] R. F. T. Stepto, *Pure Appl. Chem.* **2009**, *81*, DOI 10.1351/PAC-REC-08-05-02.
- [9] M. F. L. De Volder, S. H. Tawfick, R. H. Baughman, A. J. Hart, *Science* **2013**, *339*, 535–539.
- [10] B. Peng, M. Locascio, P. Zapol, S. Li, S. L. Mielke, G. C. Schatz, H. D. Espinosa, *Nat. Nanotechnol.* **2008**, *3*, 626–631.
- [11] E. Pop, D. Mann, Q. Wang, K. Goodson, H. Dai, *Nano Lett.* **2006**, *6*, 96–100.
- [12] A. Oberlin, M. Endo, T. Koyama, *J. Cryst. Growth* **1976**, *32*, 335–349.
- [13] S. Iijima, *Nature* **1991**, *354*, 56–58.
- [14] D. S. Bethune, C. H. Kiang, M. S. de Vries, G. Gorman, R. Savoy, J. Vazquez, R. Beyers, *Nature* **1993**, *363*, 605–607.
- [15] A. Jorio, G. Dresselhaus, M. S. Dresselhaus, Eds. , *Carbon Nanotubes: Advanced Topics in the Synthesis, Structure, Properties, and Applications*, Springer, Berlin ; New York, **2008**.
- [16] Q. Cao, J. A. Rogers, *Adv. Mater.* **2009**, *21*, 29–53.
- [17] D. Sun, M. Y. Timmermans, Y. Tian, A. G. Nasibulin, E. I. Kauppinen, S. Kishimoto, T. Mizutani, Y. Ohno, *Nat. Nanotechnol.* **2011**, *6*, 156–161.
- [18] T. Zhang, S. Mubeen, B. Yoo, N. V. Myung, M. A. Deshusses, *Nanotechnology* **2009**, *20*, 255501.
- [19] W. Yang, K. R. Ratinac, S. P. Ringer, P. Thordarson, J. J. Gooding, F. Braet, *Angew. Chem. Int. Ed.* **2010**, *49*, 2114–2138.
- [20] Z. Chen, X. Zhang, R. Yang, Z. Zhu, Y. Chen, W. Tan, *Nanoscale* **2011**, *3*, 1949.
- [21] D. A. Heller, H. Jin, B. M. Martinez, D. Patel, B. M. Miller, T.-K. Yeung, P. V. Jena, C. Höbartner, T. Ha, S. K. Silverman, et al., *Nat. Nanotechnol.* **2009**, *4*, 114–120.
- [22] T. Hasan, Z. Sun, F. Wang, F. Bonaccorso, P. H. Tan, A. G. Rozhin, A. C. Ferrari, *Adv. Mater.* **2009**, *21*, 3874–3899.
- [23] E. Gaufrès, N. Iazard, X. Le Roux, D. Marris-Morini, S. Kazaoui, E. Cassan, L. Vivien, *Appl. Phys. Lett.* **2010**, *96*, 231105.
- [24] V. Scardaci, Z. Sun, F. Wang, A. G. Rozhin, T. Hasan, F. Hennrich, I. H. White, W. I. Milne, A. C. Ferrari, *Adv. Mater.* **2008**, *20*, 4040–4043.
- [25] Y.-W. Song, S. Yamashita, C. S. Goh, S. Y. Set, *Opt. Lett.* **2007**, *32*, 430.
- [26] W. Zhang, P. Sherrell, A. I. Minett, J. M. Razal, J. Chen, *Energy Environ. Sci.* **2010**, *3*, 1286.
- [27] W. Zhang, J. Chen, G. F. Swiegers, Z.-F. Ma, G. G. Wallace, *Nanoscale* **2010**, *2*, 282–286.
- [28] B. Cornelio, G. A. Rance, M. Laronze-Cochard, A. Fontana, J. Sapi, A. N. Khlobystov, *J. Mater. Chem. A* **2013**, *1*, 8737.
- [29] Z. P. Guo, S. H. Ng, J. Z. Wang, Z. G. Huang, H. K. Liu, C. O. Too, G. G. Wallace, *J. Nanosci. Nanotechnol.* **2006**, *6*, 713–718.
- [30] A. Facchetti, T. J. Marks, Eds. , *Transparent Electronics: From Synthesis to Applications*, Wiley, Chichester, U.K, **2010**.
- [31] R. Saito, G. Dresselhaus, M. S. Dresselhaus, *Physical Properties of Carbon Nanotubes*, Imperial College Press, London, **1998**.
- [32] A. Di Crescenzo, V. Ettore, A. Fontana, *Beilstein J. Nanotechnol.* **2014**, *5*, 1675–1690.
- [33] S. Niyogi, M. A. Hamon, H. Hu, B. Zhao, P. Bhowmik, R. Sen, M. E. Itkis, R. C. Haddon, *Acc. Chem. Res.* **2002**, *35*, 1105–1113.
- [34] D. A. Britz, A. N. Khlobystov, *Chem. Soc. Rev.* **2006**, *35*, 637.
- [35] L.-C. Qin, *Phys Chem Chem Phys* **2007**, *9*, 31–48.
- [36] E. A. Laird, F. Kuemmeth, G. A. Steele, K. Grove-Rasmussen, J. Nygård, K. Flensberg, L. P. Kouwenhoven, *Rev. Mod. Phys.* **2015**, *87*, 703–764.
- [37] J.-C. Charlier, *Acc. Chem. Res.* **2002**, *35*, 1063–1069.

- [38] M. Rickhaus, M. Mayor, M. Juríček, *Chem Soc Rev* **2017**, *46*, 1643–1660.
- [39] M. Endo, T. Hayashi, Y.-A. Kim, *Pure Appl. Chem.* **2006**, *78*, DOI 10.1351/pac200678091703.
- [40] M. Endo, *Jpn. J. Appl. Phys.* **2012**, *51*, 40001.
- [41] N. Arora, N. N. Sharma, *Diam. Relat. Mater.* **2014**, *50*, 135–150.
- [42] J. Prasek, J. Drbohlavova, J. Chomoucka, J. Hubalek, O. Jasek, V. Adam, R. Kizek, *J. Mater. Chem.* **2011**, *21*, 15872.
- [43] H. Wang, Z. Bao, *Nano Today* **2015**, *10*, 737–758.
- [44] J. R. Sanchez-Valencia, T. Dienel, O. Gröning, I. Shorubalko, A. Mueller, M. Jansen, K. Amsharov, P. Ruffieux, R. Fasel, *Nature* **2014**, *512*, 61–64.
- [45] B. Liu, F. Wu, H. Gui, M. Zheng, C. Zhou, *ACS Nano* **2017**, *11*, 31–53.
- [46] L. A. Girifalco, M. Hodak, R. S. Lee, *Phys. Rev. B* **2000**, *62*, 13104–13110.
- [47] A. Thess, R. Lee, P. Nikolaev, H. Dai, P. Petit, J. Robert, C. Xu, Y. H. Lee, S. G. Kim, A. G. Rinzler, et al., *Science* **1996**, *273*, 483–487.
- [48] K. D. Ausman, R. Piner, O. Lourie, R. S. Ruoff, M. Korobov, *J. Phys. Chem. B* **2000**, *104*, 8911–8915.
- [49] J. L. Bahr, E. T. Mickelson, M. J. Bronikowski, R. E. Smalley, J. M. Tour, *Chem. Commun.* **2001**, 193–194.
- [50] C. A. Furtado, U. J. Kim, H. R. Gutierrez, L. Pan, E. C. Dickey, P. C. Eklund, *J. Am. Chem. Soc.* **2004**, *126*, 6095–6105.
- [51] S. Giordani, S. Bergin, V. Nicolosi, S. Lebedkin, W. J. Blau, J. N. Coleman, *Phys. Status Solidi B* **2006**, *243*, 3058–3062.
- [52] B. J. Landi, H. J. Ruf, J. J. Worman, R. P. Raffaele, *J. Phys. Chem. B* **2004**, *108*, 17089–17095.
- [53] M. S. Arnold, S. I. Stupp, M. C. Hersam, *Nano Lett.* **2005**, *5*, 713–718.
- [54] M. S. Arnold, A. A. Green, J. F. Hulvat, S. I. Stupp, M. C. Hersam, *Nat. Nanotechnol.* **2006**, *1*, 60–65.
- [55] T. Tanaka, H. Jin, Y. Miyata, H. Kataura, *Appl. Phys. Express* **2008**, *1*, 114001.
- [56] C. Y. Khripin, J. A. Fagan, M. Zheng, *J. Am. Chem. Soc.* **2013**, *135*, 6822–6825.
- [57] J. A. Fagan, C. Y. Khripin, C. A. Silvera Batista, J. R. Simpson, E. H. Hároz, A. R. Hight Walker, M. Zheng, *Adv. Mater.* **2014**, *26*, 2800–2804.
- [58] H. Liu, D. Nishide, T. Tanaka, H. Kataura, *Nat. Commun.* **2011**, *2*, 309.
- [59] X. Wei, T. Tanaka, N. Akizuki, Y. Miyauchi, K. Matsuda, M. Ohfuchi, H. Kataura, *J. Phys. Chem. C* **2016**, *120*, 10705–10710.
- [60] B. S. Flavel, M. M. Kappes, R. Krupke, F. Hennrich, *ACS Nano* **2013**, *7*, 3557–3564.
- [61] N. Nakashima, T. Fujigaya, *Chem. Lett.* **2007**, *36*, 692–697.
- [62] J. Chen, *Science* **1998**, *282*, 95–98.
- [63] J. Chen, A. M. Rao, S. Lyuksyutov, M. E. Itkis, M. A. Hamon, H. Hu, R. W. Cohn, P. C. Eklund, D. T. Colbert, R. E. Smalley, et al., *J. Phys. Chem. B* **2001**, *105*, 2525–2528.
- [64] J. Liu, *Science* **1998**, *280*, 1253–1256.
- [65] N. I. Kovtyukhova, T. E. Mallouk, L. Pan, E. C. Dickey, *J. Am. Chem. Soc.* **2003**, *125*, 9761–9769.
- [66] P. K. Rai, R. A. Pinnick, A. N. G. Parra-Vasquez, V. A. Davis, H. K. Schmidt, R. H. Hauge, R. E. Smalley, M. Pasquali, *J. Am. Chem. Soc.* **2006**, *128*, 591–595.
- [67] E. Dujardin, T. W. Ebbesen, A. Krishnan, M. M. J. Treacy, *Adv. Mater.* **1998**, *10*, 611–613.
- [68] W. Zhao, C. Song, P. E. Pehrsson, *J. Am. Chem. Soc.* **2002**, *124*, 12418–12419.
- [69] D. Tasis, N. Tagmatarchis, A. Bianco, M. Prato, *Chem. Rev.* **2006**, *106*, 1105–1136.
- [70] J. N. Coleman, U. Khan, W. J. Blau, Y. K. Gun'ko, *Carbon* **2006**, *44*, 1624–1652.
- [71] J. N. Coleman, U. Khan, Y. K. Gun'ko, *Adv. Mater.* **2006**, *18*, 689–706.
- [72] R. Yerushalmi-Rozen, I. Szleifer, *Soft Matter* **2006**, *2*, 24–28.
- [73] C. Alberto, P. Gonzalez-Morones, C. Jos Espinoza-Gonzalez, J. Guillermo, M. G. Neira-Velzquez, A. Senz-Galindo, L. Itzel Lopez-Lpez, in *Synth. Appl. Carbon Nanotub. Their Compos.* (Ed.: S. Suzuki), InTech, **2013**.
- [74] V. Skákalová, A. B. Kaiser, U. Dettlaff-Weglikowska, K. Hrnčariková, S. Roth, *J. Phys. Chem. B* **2005**, *109*, 7174–7181.
- [75] E. B. Bekyarova, S. Niyogi, S. Sarkar, X. Tian, M. Chen, M. L. Moser, K. Ayub, R. H. Mitchell, R. C. Haddon, *Synth. Met.* **2015**, *210*, 80–84.
- [76] A. Hirsch, *Angew. Chem. Int. Ed.* **2002**, *41*, 1853.
- [77] T. Fujigaya, N. Nakashima, *Sci. Technol. Adv. Mater.* **2015**, *16*, 24802.
- [78] M. S. Strano, V. C. Moore, M. K. Miller, M. J. Allen, E. H. Haroz, C. Kittrell, R. H. Hauge, R. E. Smalley, *J. Nanosci. Nanotechnol.* **2003**, *3*, 81–86.
- [79] Y. Noguchi, T. Fujigaya, Y. Niidome, N. Nakashima, *Chem. Phys. Lett.* **2008**, *455*, 249–251.

- [80] A. Ishibashi, N. Nakashima, *Bull. Chem. Soc. Jpn.* **2006**, *79*, 357–359.
- [81] A. Star, J. F. Stoddart, D. Steuerman, M. Diehl, A. Boukai, E. W. Wong, X. Yang, S.-W. Chung, H. Choi, J. R. Heath, *Angew. Chem. Int. Ed.* **2001**, *40*, 1721–1725.
- [82] D. W. Steuerman, A. Star, R. Narizzano, H. Choi, R. S. Ries, C. Nicolini, J. F. Stoddart, J. R. Heath, *J. Phys. Chem. B* **2002**, *106*, 3124–3130.
- [83] M. Zheng, A. Jagota, E. D. Semke, B. A. Diner, R. S. Mclean, S. R. Lustig, R. E. Richardson, N. G. Tassi, *Nat. Mater.* **2003**, *2*, 338–342.
- [84] X. Tu, S. Manohar, A. Jagota, M. Zheng, *Nature* **2009**, *460*, 250–253.
- [85] M. Zheng, E. D. Semke, *J. Am. Chem. Soc.* **2007**, *129*, 6084–6085.
- [86] A. Nish, J.-Y. Hwang, J. Doig, R. J. Nicholas, *Nat. Nanotechnol.* **2007**, *2*, 640–646.
- [87] J.-Y. Hwang, A. Nish, J. Doig, S. Douven, C.-W. Chen, L.-C. Chen, R. J. Nicholas, *J. Am. Chem. Soc.* **2008**, *130*, 3543–3553.
- [88] F. Chen, B. Wang, Y. Chen, L.-J. Li, *Nano Lett.* **2007**, *7*, 3013–3017.
- [89] H. W. Lee, Y. Yoon, S. Park, J. H. Oh, S. Hong, L. S. Liyanage, H. Wang, S. Morishita, N. Patil, Y. J. Park, et al., *Nat. Commun.* **2011**, *2*, 541.
- [90] H. Wang, J. Mei, P. Liu, K. Schmidt, G. Jiménez-Osés, S. Osuna, L. Fang, C. J. Tassone, A. P. Zoombelt, A. N. Sokolov, et al., *ACS Nano* **2013**, *7*, 2659–2668.
- [91] F. A. Lemasson, T. Strunk, P. Gerstel, F. Hennrich, S. Lebedkin, C. Barner-Kowollik, W. Wenzel, M. M. Kappes, M. Mayor, *J. Am. Chem. Soc.* **2011**, *133*, 652–655.
- [92] H. Ozawa, N. Ide, T. Fujigaya, Y. Niidome, N. Nakashima, *Chem. Lett.* **2011**, *40*, 239–241.
- [93] H. Ozawa, T. Fujigaya, Y. Niidome, N. Hotta, M. Fujiki, N. Nakashima, *J. Am. Chem. Soc.* **2011**, *133*, 2651–2657.
- [94] H. Ozawa, T. Fujigaya, Y. Niidome, N. Nakashima, *Chem. - Asian J.* **2011**, *6*, 3281–3285.
- [95] W. Gomulya, G. D. Costanzo, E. J. F. de Carvalho, S. Z. Bisri, V. Derenskyi, M. Fritsch, N. Fröhlich, S. Allard, P. Gordiichuk, A. Herrmann, et al., *Adv. Mater.* **2013**, *25*, 2948–2956.
- [96] N. Stürzl, F. Hennrich, S. Lebedkin, M. M. Kappes, *J. Phys. Chem. C* **2009**, *113*, 14628–14632.
- [97] H. Wang, G. I. Koleilat, P. Liu, G. Jiménez-Osés, Y.-C. Lai, M. Vosgueritchian, Y. Fang, S. Park, K. N. Houk, Z. Bao, *ACS Nano* **2014**, *8*, 2609–2617.
- [98] A. Adronov, D. Fong, *Chem Sci* **2017**, DOI 10.1039/C7SC02942J.
- [99] N. A. Rice, A. V. Subrahmanyam, S. E. Laengert, A. Adronov, *J. Polym. Sci. Part Polym. Chem.* **2015**, *53*, 2510–2516.
- [100] N. A. Rice, A. Adronov, *Macromolecules* **2013**, *46*, 3850–3860.
- [101] N. A. Rice, A. Adronov, *J. Polym. Sci. Part Polym. Chem.* **2014**, *52*, 2738–2747.
- [102] F. Lemasson, N. Berton, J. Tittmann, F. Hennrich, M. M. Kappes, M. Mayor, *Macromolecules* **2012**, *45*, 713–722.
- [103] M. Tange, T. Okazaki, S. Iijima, *ACS Appl. Mater. Interfaces* **2012**, *4*, 6458–6462.
- [104] M. Tange, T. Okazaki, S. Iijima, *J. Am. Chem. Soc.* **2011**, *133*, 11908–11911.
- [105] N. Berton, F. Lemasson, J. Tittmann, N. Stürzl, F. Hennrich, M. M. Kappes, M. Mayor, *Chem. Mater.* **2011**, *23*, 2237–2249.
- [106] K. S. Mistry, B. A. Larsen, J. L. Blackburn, *ACS Nano* **2013**, *7*, 2231–2239.
- [107] S. Liang, A. V. Subrahmanyam, M. Khadem, Y. Zhao, A. Adronov, *RSC Adv* **2016**, *6*, 25733–25740.
- [108] X. Zhang, J. Zhao, M. Tange, W. Xu, W. Xu, K. Zhang, W. Guo, T. Okazaki, Z. Cui, *Carbon* **2015**, *94*, 903–910.
- [109] H. Li, F. Zhang, S. Qiu, N. Lv, Z. Zhao, Q. Li, Z. Cui, *Chem. Commun.* **2013**, *49*, 10492.
- [110] N. Berton, F. Lemasson, A. Poschlad, V. Meded, F. Tristram, W. Wenzel, F. Hennrich, M. M. Kappes, M. Mayor, *Small* **2014**, *10*, 360–367.
- [111] N. Berton, F. Lemasson, F. Hennrich, M. M. Kappes, M. Mayor, *Chem. Commun.* **2012**, *48*, 2516.
- [112] P. Imin, F. Cheng, A. Adronov, *Polym. Chem.* **2011**, *2*, 1404.
- [113] J. Ding, Z. Li, J. Lefebvre, F. Cheng, G. Dubey, S. Zou, P. Finnie, A. Hrdina, L. Scoles, G. P. Lopinski, et al., *Nanoscale* **2014**, *6*, 2328.
- [114] S. P. Schießl, N. Fröhlich, M. Held, F. Gannott, M. Schweiger, M. Forster, U. Scherf, J. Zaumseil, *ACS Appl. Mater. Interfaces* **2015**, *7*, 682–689.
- [115] P. Gerstel, S. Klumpp, F. Hennrich, O. Altintas, T. R. Eaton, M. Mayor, C. Barner-Kowollik, M. M. Kappes, *Polym. Chem.* **2012**, *3*, 1966.
- [116] T. Lei, Y.-C. Lai, G. Hong, H. Wang, P. Hayoz, R. T. Weitz, C. Chen, H. Dai, Z. Bao, *Small* **2015**, *11*, 2946–2954.

- [117] S. Park, H. W. Lee, H. Wang, S. Selvarasah, M. R. Dokmeci, Y. J. Park, S. N. Cha, J. M. Kim, Z. Bao, *ACS Nano* **2012**, *6*, 2487–2496.
- [118] T. Lei, G. Pitner, X. Chen, G. Hong, S. Park, P. Hayoz, R. T. Weitz, H.-S. P. Wong, Z. Bao, *Adv. Electron. Mater.* **2016**, *2*, 1500299.
- [119] N. A. Rice, A. V. Subrahmanyam, B. R. Coleman, A. Adronov, *Macromolecules* **2015**, *48*, 5155–5161.
- [120] D. Fong, W. J. Bodnaryk, N. A. Rice, S. Saem, J. M. Moran-Mirabal, A. Adronov, *Chem. - Eur. J.* **2016**, *22*, 14560–14566.
- [121] S. D. Stranks, A. M. R. Baker, J. A. Alexander-Webber, B. Dirks, R. J. Nicholas, *Small* **2013**, *9*, 2245–2249.
- [122] S. D. Stranks, S. N. Habisreutinger, B. Dirks, R. J. Nicholas, *Adv. Mater.* **2013**, *25*, 4365–4371.
- [123] H. Wang, B. Hsieh, G. Jiménez-Osés, P. Liu, C. J. Tassone, Y. Diao, T. Lei, K. N. Houk, Z. Bao, *Small* **2015**, *11*, 126–133.
- [124] T. Lei, I. Pochorovski, Z. Bao, *Acc. Chem. Res.* **2017**, *50*, 1096–1104.
- [125] F. Jakubka, S. P. Schießl, S. Martin, J. M. Englert, F. Hauke, A. Hirsch, J. Zaumseil, *ACS Macro Lett.* **2012**, *1*, 815–819.
- [126] L. Qian, W. Xu, X. Fan, C. Wang, J. Zhang, J. Zhao, Z. Cui, *J. Phys. Chem. C* **2013**, *117*, 18243–18250.
- [127] K. Akazaki, F. Toshimitsu, H. Ozawa, T. Fujigaya, N. Nakashima, *J. Am. Chem. Soc.* **2012**, *134*, 12700–12707.
- [128] P. Deria, C. D. Von Bargaen, J.-H. Olivier, A. S. Kumbhar, J. G. Saven, M. J. Therien, *J. Am. Chem. Soc.* **2013**, *135*, 16220–16234.
- [129] Y. Joo, G. J. Brady, M. J. Shea, M. B. Oviedo, C. Kanimozhi, S. K. Schmitt, B. M. Wong, M. S. Arnold, P. Gopalan, *ACS Nano* **2015**, *9*, 10203–10213.
- [130] F. Toshimitsu, N. Nakashima, *Nat. Commun.* **2014**, *5*, 5041.
- [131] T. Lei, X. Chen, G. Pitner, H.-S. P. Wong, Z. Bao, *J. Am. Chem. Soc.* **2016**, *138*, 802–805.
- [132] I. Pochorovski, H. Wang, J. I. Feldblyum, X. Zhang, A. L. Antaris, Z. Bao, *J. Am. Chem. Soc.* **2015**, *137*, 4328–4331.
- [133] F. Lemasson, J. Tittmann, F. Hennrich, N. Stürzl, S. Malik, M. M. Kappes, M. Mayor, *Chem. Commun.* **2011**, *47*, 7428.
- [134] J. Ding, Z. Li, J. Lefebvre, X. Du, P. R. L. Malenfant, *J. Phys. Chem. C* **2016**, *120*, 21946–21954.
- [135] M. C. Hersam, *Nat. Nanotechnol.* **2008**, *3*, 387–394.
- [136] P. Hammershøj, P. H. H. Bomans, R. Lakshminarayanan, J. Fock, S. H. Jensen, T. S. Jespersen, T. Brock-Nannestad, T. Hassenkam, J. Nygård, N. A. J. M. Sommerdijk, et al., *Chem. – Eur. J.* **2012**, *18*, 8716–8723.
- [137] M. A. Petti, T. J. Shepodd, R. E. Barrans, D. A. Dougherty, *J. Am. Chem. Soc.* **1988**, *110*, 6825–6840.
- [138] P. Corbett, J. M. Sanders, S. Otto, *Chem. - Eur. J.* **2008**, *14*, 2153–2166.
- [139] P. Hodge, G. A. Power, M. A. Rabjohns, *Chem. Commun.* **1997**, 73–74.
- [140] O. Geiseler, M. Müller, J. Podlech, *Tetrahedron* **2013**, *69*, 3683–3689.
- [141] E. Krasnokutskaya, N. Semenischeva, V. Filimonov, P. Knochel, *Synthesis* **2007**, *2007*, 81–84.
- [142] X. Liu, Z. J. Weinert, M. Sharafi, C. Liao, J. Li, S. T. Schneebeli, *Angew. Chem. Int. Ed.* **2015**, *54*, 12772–12776.
- [143] X. Liu, Z. J. Weinert, M. Sharafi, C. Liao, J. Li, S. T. Schneebeli, *Angew. Chem. Int. Ed.* **2015**, *54*, 12772–12776.
- [144] C. Zhang, C.-F. Chen, *J. Org. Chem.* **2006**, *71*, 6626–6629.

Curriculum Vitae

Ina Bodoky



Personal

Date of birth January 29, 1988, in Basel, Switzerland
Citizenship Swiss, Hungarian
Civil status Single, no children
Address Schlettstadterstrasse 9, 4055 Basel, Schweiz
Phone number +41 76 529 5214
E-Mail address ina@bodoky.ch

Education and Professional Experience

- 2013–11/2017 **PhD in organic Chemistry**, University of Basel, Switzerland
Setting the Hook for Specific Single Walled Carbon Nanotubes (SWCNT)
Advisor: Prof. Dr. M. Mayor.
Presented at scientific meetings and conferences in Europe and the USA (talks, posters)
- 2011–2012 **Master of Science in Chemistry**, University of Basel, Switzerland
Structural Diversity by Lewis Acid Catalyzed Domino-Type Inverse Electron Demand Diels-Alder Processes
Advisor: PD Dr. Hermann A. Wegner.
Results published in a high impact journal.
- 2011 **Academic internship in Chemistry**, University of Irvine, United States
Influence of Second Coordination-Sphere Ligands for Organometallic Catalysis
Advisor: Prof. Dr. A. S. Borovik.
- 2007–2011 **Bachelor of Science in Chemistry**, University of Basel, Switzerland
- 2001–2006 **Matura**, Gymnasium Bäumlhof, Basel, Switzerland
Swiss high school degree, with majors in Mathematics and Applied Sciences

Scientific Contributions

Trainings and Certificates

- 2016 *HPLC training including method development under LABSolution* (course with certificate), Shimadzu, Germany, 3 days
- 2016 *Training LC-MS/MS-8040 Triple Quadrupole* (course with certificate), Shimadzu, Switzerland, 1 day
- 2016 *Einführung in die HPLC TR09* (course with certificate), Schweizerische Chemische Gesellschaft and Division für Analytische Wissenschaft, Switzerland, 2 days

Awards

- 2015 *Best Poster Presentation* (Runner-up), 13th Swiss Snow Symposium 2014, Saas Fee, Switzerland.
- 2014 *Clariant CleanTech Award 2014*, Awarded for outstanding, environmentally friendly, renewable research. Awarded by Clariant, the University of Basel and the University of Applied Science and Arts Northwestern Switzerland (second prize, CHF 2'500.-).

Publications

- 2017 *Configurational Stability of [5]Helicenes*
P. Ravat, R. Hinkelmann, D. Steinebrunner, A. Prescimone, I. Bodoky, M. Juriček,
Org. Lett., 2017, 19 (14), 3707–3710.
- 2016 *Bidentate Lewis Acid Catalyzed Domino Diels–Alder Reaction of Phthalazine for the Synthesis of Bridged Oligocyclic Tetrahydronaphthalenes*
L. Schweighauser, I. Bodoky, S. N. Kessler, D. Häusinger, C. Donsbach, H. A. Wegner,
Org. Lett., 2016, 18, 1330.
- 2012 *Bidentate Lewis Acid Catalyzed Inverse-Electron-Demand Diels–Alder Reaction for the Selective Functionalization of Aldehydes*

L. Schweighauser, I. Bodoky, S. N. Kessler, D. Häusinger, H. A. Wegner, *Synthesis*, 2012, 44, 2195.

Oral Presentations

- 2014 *Fischen nach molekularen Drähten, Selektive Dispersion von einwandigen CNTs*
representative of the organic chemistry department in front of the deanery of the University of Basel, Switzerland.
- 2014 *Setting the Hook for Specific Single Walled Carbon Nanotubes*
Swiss Chemical Society, Fall Meeting 2014, ETH and University of Zürich, Switzerland

Posters Presentations

- 2015–2016 *Setting the Hook for Specific Single Walled Carbon Nanotubes*,
ISNA 16, Madrid, Spain, and Chirality 2015, Boston, USA
- 2013–2016 *Setting the Hook for Specific Single Walled Carbon Nanotubes*,
12th, 13th, 14th Swiss Snow Symposium and Swiss Chemical Society Fall Meeting, Switzerland
- 2013–2015 *Fishing for Specific Single Walled Carbon Nanotubes*,
32nd, 34th, 35th Regio-Symposium, France, Germany and Switzerland
- 2012 *Bidentate Lewis Acid Catalysis*, 32nd Regio-Symposium, Rheinfelden, Germany

Leadership and Teamwork

- Leadership **Tuition** of undergraduates in practical skills (3rd semester Chemistry, Pharmaceutical-Science and Nano-Science students)
Preparation, Supervision and correction of examinations (undergraduate level)
Supervising Tutor of a Master Student (3 month practical) and *Kids at Science* (Schweizer Jugend Forscht, 5 days)
- Organization Member of the **organization team** of the annual *department symposium* (2013 / 2014).
- Teaching **Substitute teacher** in Chemistry and Mathematics (high school level and undergraduate level)
Teacher for the *Freies Gymnasium*, Basel, Switzerland, for the school's Lernfit-program in Chemistry and Mathematics (freelance)

Extra-Curricular Activities & International Experience

- 2008–2016 **Service-assistant** for *Albrecht Catering* and Restaurant *L'Unique*, Basel, Switzerland
- 2007 Two month **English school** and living with a local family in Melbourne, Australia.
- 2006 Two months **internship** as editor at the *Medical Tribune*, Basel, Switzerland
- 2006 One month **internship** in a photographic studio, Mészáros László Photography, Budapest, Hungary

Language Skills

German (native), **English** (proficient), **Hungarian** (oral proficient, written basic), **French** (basic)

Personal Interest

- Hobbies Traveling, Snowboarding, Fitness, Haute Cuisine
- Extended Travels Backpacking through Australia, Argentina, USA, Brazil and Southeast Asia

Referenzen

- Prof. Dr. M. Mayor** University of Basel, Switzerland, marcel.mayor@unibas.ch, +41 61 207 10 06
- Prof. Dr. H. A. Wegner** Justus-Liebig University Giessen, Germany, Hermann.A.Wegner@org.Chemie.uni-giessen.de, +49 641 99-34330

